Petrography, Mineral Chemistry and Microstructures of Gabbros from the Mid-Cayman Rise Spreading Center

A thesis presented to the Faculty
of the State University of New York
at Albany
in partial fulfillment of the requirements
for the degree of
Master of Science

College of Science and Mathematics
Department of Geological Sciences

Frieda L. Malcolm
1979

Petrography, Mineral Chemistry and Microstructures of Gabbros from the Mid-Cayman Rise Spreading Center

Abstract of
a thesis presented to the Faculty
of the State University of New York
at Albany
in partial fulfillment of the requirements
for the degree of
Master of Science

College of Science and Mathematics
Department of Geological Sciences

Frieda L. Malcolm
1979

ABSTRACT

The suite of gabbroic rocks collected by the DSRV ALVIN in 1976 and 1977 from the walls of the Mid-Cayman Rise spreading center were studied in detail to provide the best available data on plutonic rocks sampled directly from the ocean floor. The rock types studied include variably deformed and altered gabbros, orthopyroxene gabbros, olivine gabbros and troctolites, and a few amphibolites. Mineral chemical analyses suggest that the various rock types are representative of a fractionation trend from magnesian troctolites through olivine and clinopyroxene gabbros to iron-enriched orthopyroxene gabbros. Within many individual samples, the primary mineral phases are apparently chemically homogeneous despite sometimes considerable alteration, which suggests reequilibration after original crystallization. Variation in mineral chemistry across the suite is larger than previously reported for ocean-floor gabbros; this may be due to the larger population of this study. The primary or secondary nature of plagioclase and amphibole must be distinguished in discussions of the igneous processes involved in the genesis of these rocks. In this suite, textural evidence is often inconclusive, and although sodic chemistry is assumed to indicate a secondary origin for plagioclase, no chemical indicator was found to apply to amphiboles. Many different deformation textures are observed in the samples, indicating considerable variation in the conditions of deformation within this slowly accreting ridge environment. Ductile features range from mechanical twins and bent crystals (low strain) to complete recrystallization with a well-developed foliation (high strain). Textures suggestive of cataclasis include zones .1-10 mm wide containing very fine, irregular grains;

kinked and cracked grains, usually very undulose; and crosscutting fractures. These textures may occur separately, or next to or overprinting each other. Of the variables controlling the formation of deformation features, temperature and water pressure are most easily estimated. Minimum temperature during deformation is suggested by minimum temperature of formation of mineral assemblages unaffected by this deformation. This temperature is greater than 550°C (epidote-amphibolite facies) for the majority of features observed, although sampling may have introduced a bias away from lower temperature features. Observations suggest enhanced recrystallization where the primary mineralogy has been hydrated to a greater extent. Theoretically, confining pressure for the gabbroic rocks in this suite may have varied from about .3-.9kb; fluid pressure should have been within these limits. Based on mineralogical evidence, cataclastic and ductile textures developed at both high and moderate temperatures. This suggests that strain rates and/or pressure vary considerably within regions where rocks are hot as well as where rocks are cooler, and that after high-temperature deformation some rocks cooled quickly enough to prevent significant recrystallization while others cooled more slowly. These interpretations indicate that the Cayman plutonics were raised to their present position by motions which varied from place to place and time to time, and suggests that the structural history of plutonic rocks formed at slowly accreting plate boundaries is highly variable and complex.

ACKNOWLEDGEMENTS

I wish to acknowledge the advise of Drs. S. E. DeLong, P. J. Fox, and A. Miyashiro as members of my committee. The captains and crews of the RV/KNORR, RV/LULU-DSRV/ALVIN, and RV/OCEANUS provided able assistance during the field programs. Financial support for the research conducted at Albany was provided by the National Science Foundation through grants OCE-7621882 and OCE-7720961. The microprobe analyses carried out at the Johnson Space Flight Center was done under the guidance of Dr. J. L. Warner and Mr. R. Brown and with the financial support of the Lunar and Planetary Institute. The drafted figures were drawn by R. Carosella and H. Sloan. D. Kelly and D. Paton typed the final manuscript.

Last but not least, the constant moral and spiritual support of my colleagues and friends throughout my graduate career is gratefully acknowledged.

TABLE OF CONTENTS

LIST OF FIGURES

LIST OF TABLES

CHAPTER 1: IGNEOUS PETROLOGY AND MINERAL CHEMISTRY

CHAPTER 1

The Mid-Cayman Rise (MCR) is a slowly spreading ridge segment about 100 km long that connects the Oriente and Swan Transforms (Fig. 1). This ridge shows the bilaterally symmetric variations in properties such as topography, sediment thickness and age (Holcombe and others, 1973), that are normally associated with mid-ocean ridges, but its axial valley sits 2-3 km deeper than usual. In 1976 and 1977, in situ sampling by the DSRV ALVIN on this spreading center (Fig. 2) revealed that gabbroic and ultramafic plutonic rocks are the dominant exposed rock types, at least in the two dive areas sampled (CAYTROUGH, 1979). The extensive exposure of plutonic rocks on the median valley walls is also anomalous compared to other spreading centers. This large collection of well-located plutonic samples from the rift valley walls provides the opportunity to study gabbroic rocks of varying types from a restricted geographic and geologic location. The purpose of this paper is to describe the petrography of the suite and the mineral chemistry of selected representative samples in order to constrain models for the generation and evolution of magmas in this area, and to provide a basis for comparison with other gabbroic suites, such as DSDP Site 334 (Hodges and Papike, 1976).

PETROGRAPHY

The gabbroic rocks recovered during the MCR diving program are coarse-grained and include troctolites, olivine gabbros, gabbros and orthopyroxene gabbros. Alteration has obscured the primary mineralogy in many samples, rendering classification difficult. Where possible, igneous terminology is applied according to the classification of the

Figure 1: Bathymetric map of the Mid-Cayman Rise (MCR) area. Dive Area 1 is on the eastern wall, Dive Area 2 on the western wall. Inset shows location of the MCR with respect to the North American (NOAM) Caribbean (CARI), South American (SOAM) and Cocos (COCO) plates.

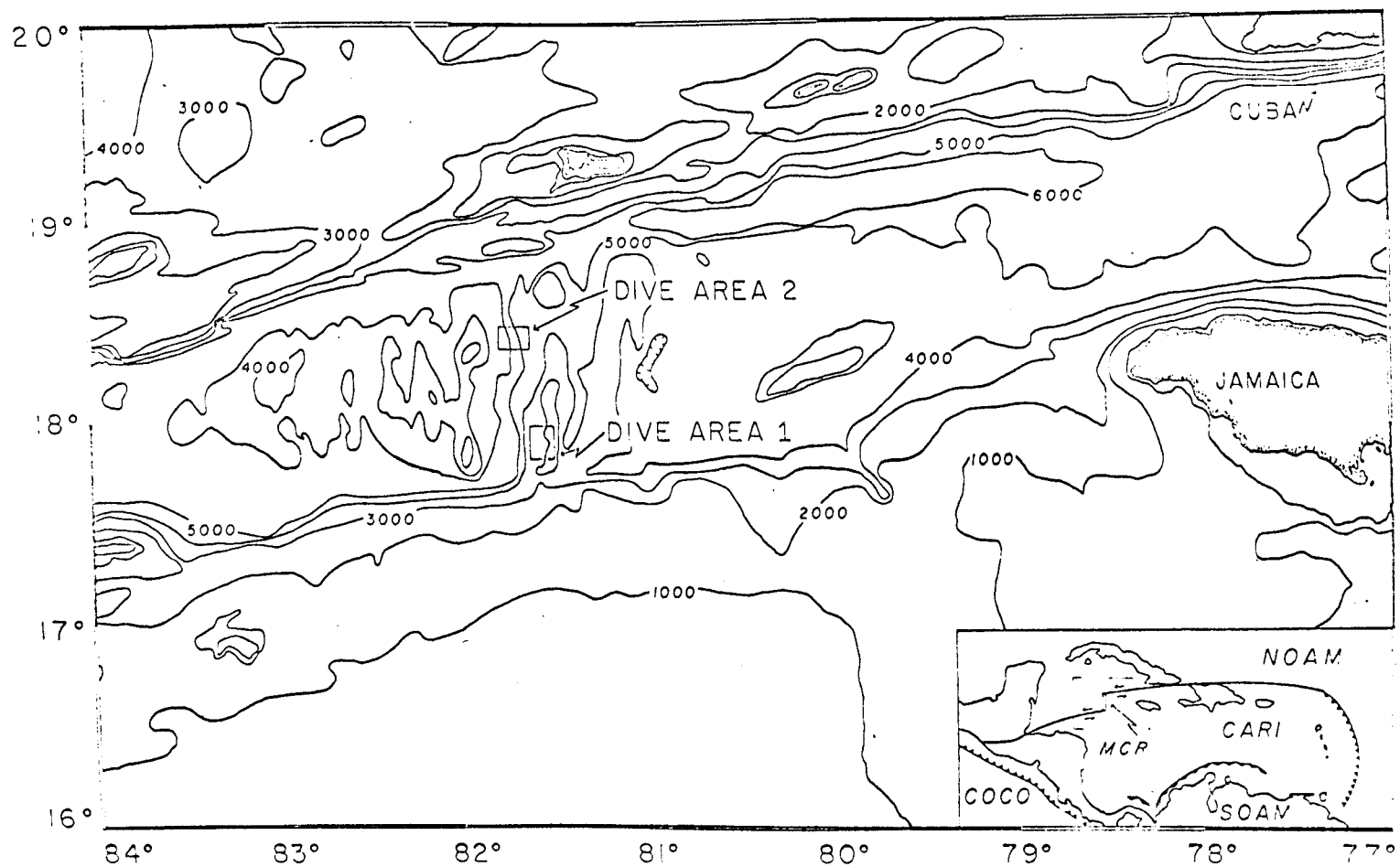
20°
19°
18°
17°
16°
84°
83°
82°
81°
80°
79°
78°
77°
3000
4000
2000
5000
6000
CUBAN
DIVE AREA 2
DIVE AREA 1
JAMAICA
1000
NOAM
MCR
CARI
COCO
SOAM

IUGS (Streckeisen, 1975). Where ambiguity exists, the term metagabbro or olivine-bearing metagabbro is applied. Amphibolite is used where amphibole is the only identifiable major mafic phase and plagioclase is the felsic mineral. Figure 2 shows the distribution of rock types within the dive areas. The distribution of rock types is not particularly systematic, but amphibolites are concentrated in the upper portions of Dive Area 1 and olivine-rich rocks are most abundant in the lower portions of both dive areas. It is unknown whether this distribution is indicative of systematic rock-type distribution in the crystallizing chamber, as the faulted nature of the topography does not allow structural reconstructions to be made.

Primary phases in these rocks, in order of decreasing overall abundance, are plagioclase (labradorite-bytownite), diopsidic augite, olivine, hornblende, opaques and hypersthene. Zircon is a rare accessory phase. Alteration phases include sodic plagioclase, hornblende, actinolite-tremolite, talc, some opaques, apatite, smectite, chlorite, sericite, serpentine and sphene. A few samples contain small amounts of epidote, clinozoisite, biotite, prehnite and/or hydrogrossular. The distinction between primary and secondary grains of the same mineral is made on the basis of textural relationships (such as relative grain size, grain shape, reaction rims, veins), although in many cases these criteria are not sufficient. The mafic phases are primarily anhedral and are interstitial to and poikilitic about lathlike plagioclase, often creating subophitic textures (Fig. 3). Olivine is usually rimmed by hornblende and rarely by orthopyroxene. Fifty-seven of the gabbroic rocks are olivine-bearing, nine of these are troctolites. Olivine often has irregular cuspate boundaries with plagioclase which suggest resorption of olivine (Fig. 4).

Figure 2: Bathymetric maps of the two dive areas. Dive traverses are annotated with sample locations and rock types collected. Rock types are: 1) altered gabbro, 2) altered orthopyroxene gabbro, 3) altered olivine gabbro, 4) altered troctolite, 5) micrometagabbro, 6) metagabbro, 7) olivine-bearing metagabbro, 8) weathered metagabbro, 9) amphibolite, 10) basalt, 11) greenstone, 12) ultramafic, 13) breccia. Underlined sample numbers indicate penetratively foliated samples.

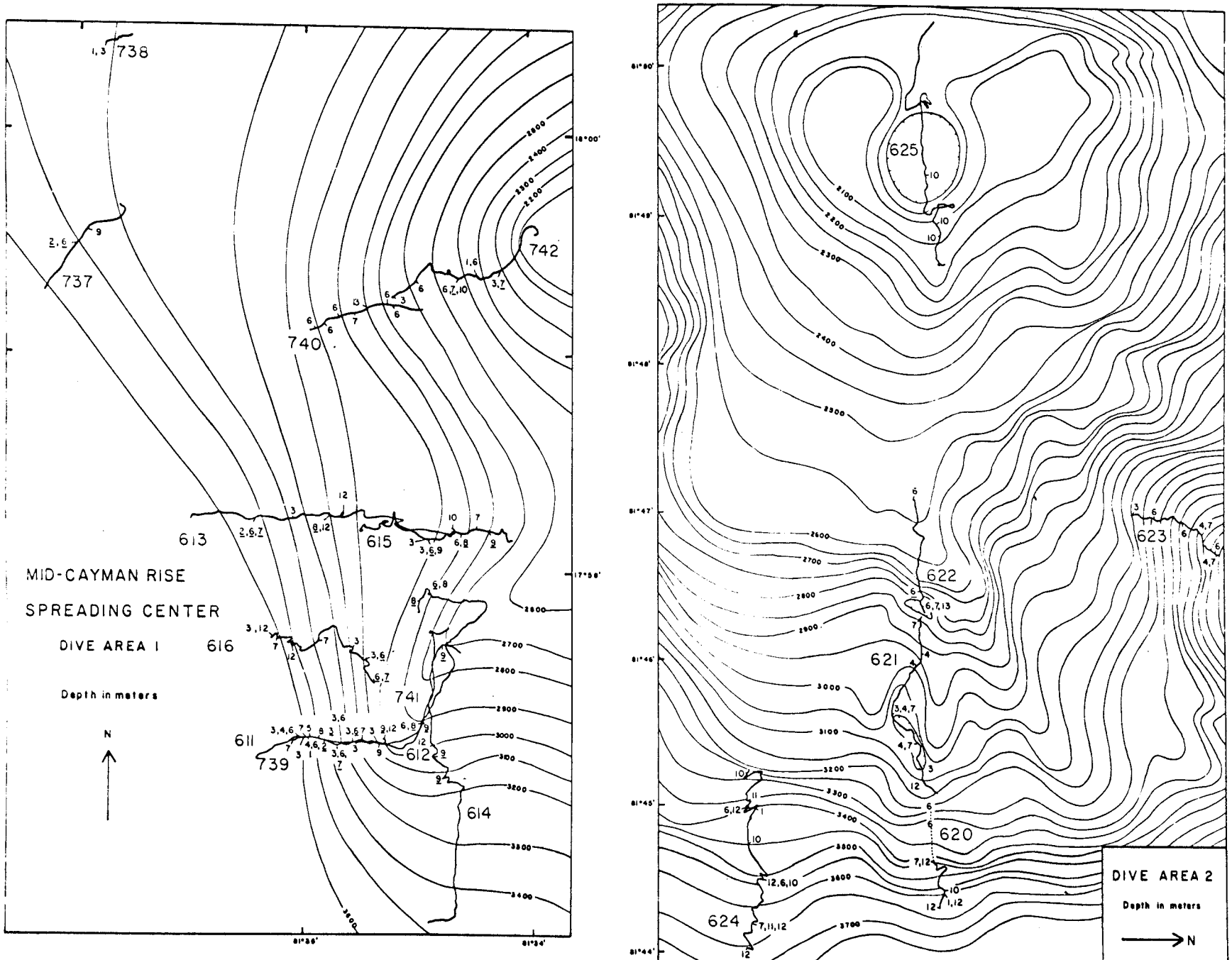
MID-CAYMAN RISE
SPREADING CENTER
DIVE AREA 1
Depth in meters
N
738
737
740
742
613
615
616
741
611
739
612
614
DIVE AREA 2
Depth in meters
N
625
622
623
621
620
624

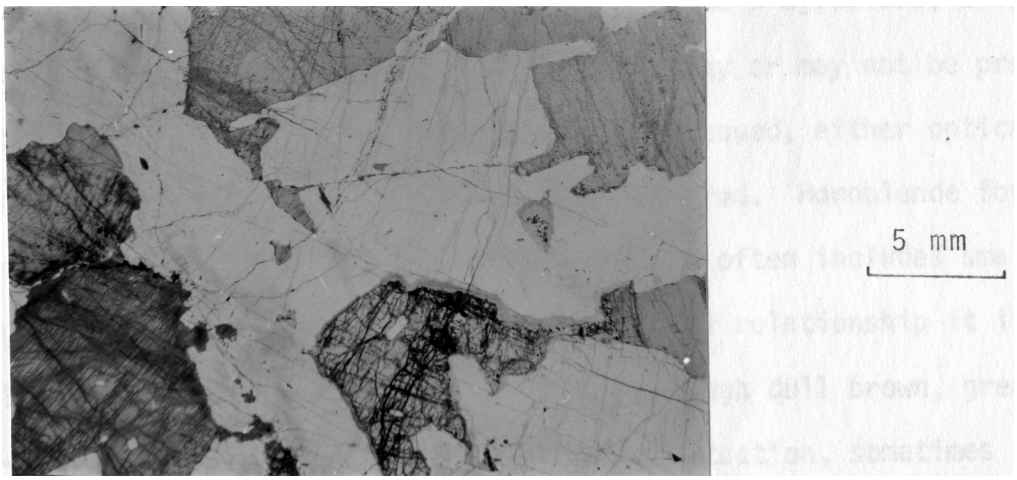

Figure 3: Subophitic texture in an altered olivine gabbro, sample 615-1-1. Plane light.

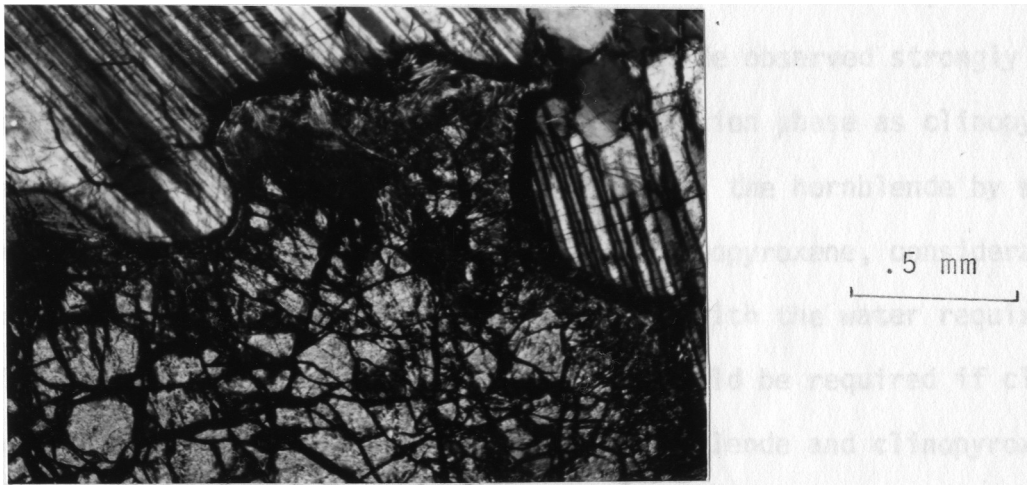

Figure 4: Cuspate boundaries between olivine and plagioclase suggests resorption of olivine. There is minor alteration of the olivine along the boundary to chlorite and tremolite. The plagioclase is polysynthetically twinned. Sample 621-3-2, olivine-bearing metagabbro; crossed polarizers.

In the few cases where orthopyroxene is a major primary phase, it is prismatic to subhedral and is not interstitial to plagioclase, although coexisting clinopyroxene usually is. Olivine may or may not be present in these samples. The major phases are rarely zoned, either optically or chemically, unless some alteration has occurred. Hornblende forms narrow rims around the major mafic minerals and often includes small, irregular to euhedral opaques. In this textural relationship it is usually red-brown and apparently primary, although dull brown, green, and blue-green hornblende also occur in the same situation, sometimes in optical continuity with the red-brown hornblende, and these other-colored hornblendes are usually considered secondary.

A variety of exsolution textures are observed in clinopyroxene, some of which are similar to those illustrated by Hodges and Papike (1976). Although red-brown hornblende and opaques are the most common phases in elongate, crystallographically controlled lamellae, these may or may not be primary. The volume of hornblende observed strongly suggests that the hornblende must be an alteration phase as clinopyroxene is unlikely to contain enough water to form all the hornblende by simple exsolution. If the original lamellae were orthopyroxene, considerable Ca and Ti would have to enter the grain along with the water required to form hornblende. Less element migration would be required if clinopyroxene were the original phase, because hornblende and clinopyroxene are much closer in composition. Both clinopyroxene and orthopyroxene are observed as unaltered exsolution lamellae. Clinopyroxene may also be intergrown with clinopyroxene (Fig. 5), although not in the vermicular fashion described by Cann (1971). In a few samples clinopyroxene textures suggest some intragrain compositional variation by the irregularity (patchy nature) of some exsolution textures (Fig. 6). This

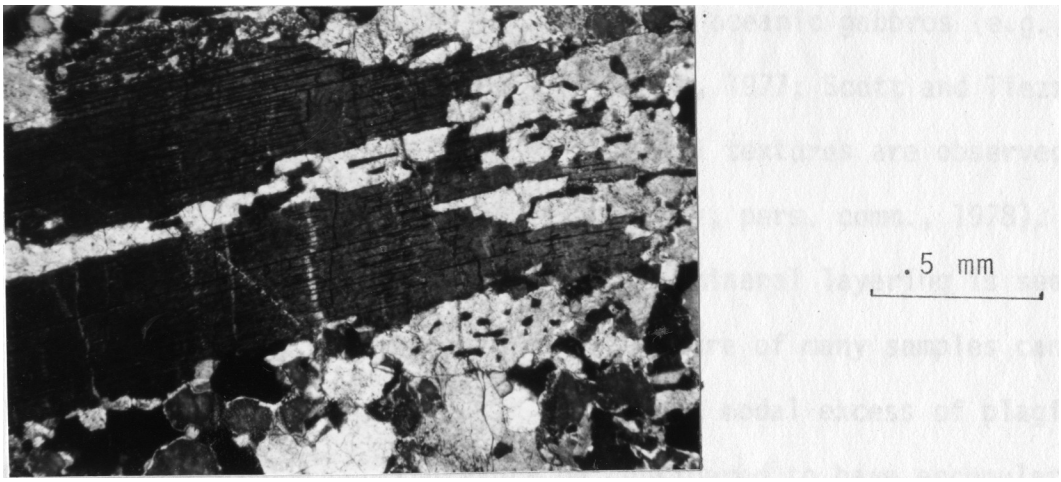

Figure 5: Example of intergrown clinopyroxene texture, modified on perimeter by recrystallization. Sample 741-2-2, altered olivine gabbro; crossed polarizers.

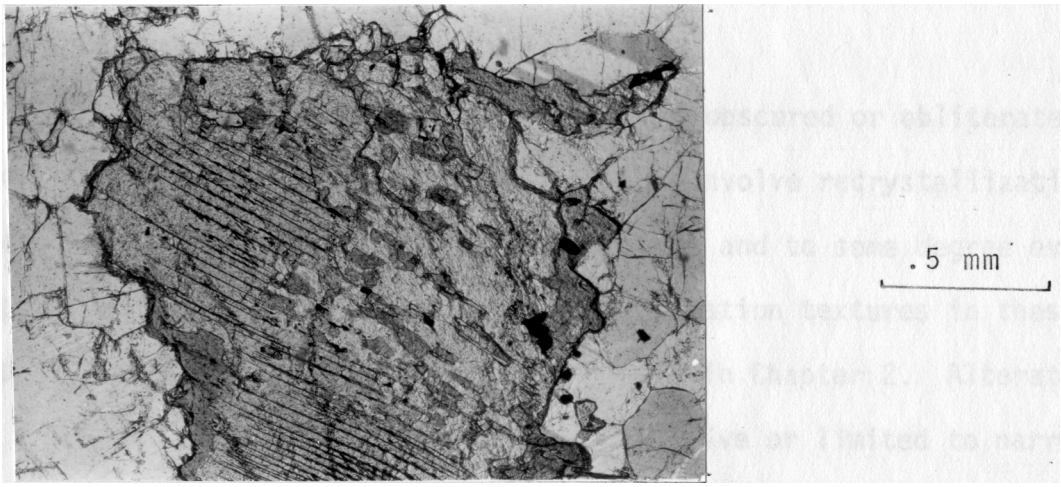

Figure 6: Moderately aligned inclusions of red-brown hornblende in a clinopyroxene are found in a "patch" without cleavage. Sample 739-1-1, altered olivine gabbro; plane light.

variation has not been confirmed analytically.

Cumulate textures have been described in oceanic gabbros (e.g., Hodges and Papike, 1976; Helmstaedt and Allen, 1977; Scott and Tiezzi, 1976); it is apparent, however, that identical textures are observed in non-cumulate rocks (McBirney, in review; Casey, pers. comm., 1978). In thin section and in hand specimen no primary mineral layering is seen in the MCR samples, so the possible cumulate nature of many samples cannot be verified. A few samples do have a distinct modal excess of plagioclase (greater than 75%) and can therefore be considered to have accumulated plagioclase.

Coarse grain size has traditionally been considered an indicator of cooling rate, with increasing grain size correlated to slower cooling. However, it is now clear that many variables affect grain size, including nucleation rate, water content and degree of supercooling (Lofgren, 1978), so that the coarse textures of the MCR samples need not be the result of slow cooling.

In many samples the primary textures are obscured or obliterated by deformation and alteration. Deformation may involve recrystallization, fracture and/or the development of a foliation and to some degree every sample in the suite has been affected. Deformation textures in these samples are described and discussed in detail in Chapter 2. Alteration may be syntectonic or static and may be pervasive or limited to narrow zones. Most changes involve hydration reactions and are apparently initiated along fluid conduits opened by deformation. The nature of alteration and its relationship to deformation in the rocks will be discussed in a future manuscript.

MINERAL CHEMISTRY

Thirty-eight representative samples were selected from the gabbroic suite for microprobe analysis of the major silicate phases. Most of the analyses were performed with the automated MAC microprobe at the Johnson Space Center using a sample current of .02 μamps. Amphibole was analyzed with a sample current of .04 μamps. Feldspar analyses were made in three sweeps using the non-automated ARL microprobe at the Johnson Space Center with a sample current of about .02 μamps. A few samples were analyzed with the automated Etec microprobe at the University of Massachusetts, Amherst. All data reduction was done using the procedures of Bence and Albee (1968) with correction factors from Albee and Ray (1970). Representative analyses from samples of eight rock types are listed in Tables 1-4; a complete list of analyses is found in Appendix 3.

Olivine: Olivine was analyzed in 16 samples, and forsterite content ranges from 70 to 88 mole %. Variation within a single specimen is less than 3 mole % Fo, within analytical error. Zoning is absent within detectability limits and composition is apparently not affected by adjacent alteration, commonly talc + opaques, tremolite and/or serpentine. Although there is some scatter in the data, olivine is more forsteritic in troctolites than in clinopyroxene-rich rocks (Fig. 7). Olivine compositions and the range in composition reported here are comparable to those observed in oceanic basalts, for example, Fo_{80-90} for olivines in basalt cored on legs 2 and 3 of the DSDP (Frey and others, 1974), Fo_{70-86} for olivines in the basalt cores of DSDP Leg 34 (Mazzullo and Bence, 1976), and Fo_{83-89} for olivines in basalts collected by DSRV ALVIN from the FAMOUS area (Bryan and Moore, 1977). The olivine of the MCR rocks ranges to considerably more fayalitic compositions than the uniformly magnesian olivines (Fo_{86-87}) from the DSDP Site 334

TABLE 1

Representative Plagioclase Analyses

	613-1-1		611-5-1		739-2-2		611-3-1C			741-2-1		620-5-1	615-5-1	
	1-1	2-1	4	11	2-1	1-2	1-2	3-2	3-1	2-2	1-1	7	1	3
SiO_2	59.98	56.65	54.12	53.94	46.20	50.12	52.14	57.84	63.43	54.74	62.38	55.51	56.53	62.93
TiO_2	.02	.02	.00	.04	.01	.06	.05	.11	.04	.02	.00	.04	.05	.02
Al_2O_3	25.07	28.04	27.86	27.56	34.64	31.99	30.12	27.34	23.55	29.03	23.55	27.24	27.99	24.16
FeO	.38	.13	.11	.07	.14	.19	.37	.62	.32	.10	.16	.17	.02	.09
MnO	.00	.00	.00	.00	.01	.00	.01	.00	.00	.01	.02	.00	.00	.00
MgO	.00	.00	.00	.00	.01	.04	.19	.00	.00	.00	.00	.00	.00	.00
CaO	6.14	9.24	11.97	11.32	16.82	14.25	13.18	8.78	3.62	10.83	4.67	10.97	9.04	4.51
Na_2O	7.55	6.15	4.78	5.11	1.90	3.41	3.72	6.41	9.02	5.11	8.59	5.73	6.08	8.52
K_2O	.15	.07	.01	.02	.04	.06	.08	.07	.07	.16	.43	.04	.05	.12
TOTAL	99.29	100.29	98.85	98.06	99.77	100.13	99.85	101.16	100.06	100.00	99.79	99.70	99.77	100.34
Si	2.686	2.533	2.473	2.482	2.128	2.282	2.370	2.566	2.796	2.466	2.770	2.513	2.537	2.769
Ti	.001	.001	.000	.001	.000	.002	.002	.004	.001	.001	.000	.001	.002	.001
Al	1.323	1.478	1.501	1.495	1.881	1.717	1.614	1.429	1.224	1.541	1.233	1.454	1.481	1.253
Fe	.014	.005	.004	.003	.005	.007	.014	.023	.012	.004	.006	.006	.001	.003
Mn	.000	.000	.000	.000	.000	.000	.000	.000	.000	.000	.001	.000	.000	.000
Mg	.000	.000	.000	.000	.001	.002	.013	.000	.000	.000	.000	.000	.000	.000
Ca	.295	.443	.586	.558	.830	.695	.642	.417	.171	.523	.222	.532	.435	.213
Na	.655	.533	.423	.456	.170	.301	.328	.551	.771	.446	.739	.503	.529	.727
K	.008	.004	.001	.001	.002	.003	.004	.004	.004	.009	.024	.002	.003	.007
TOTAL	4.983	4.996	4.988	4.997	5.017	5.010	4.987	4.994	4.978	4.990	4.995	5.012	4.987	4.971
An	31	45	58	55	83	70	66	43	18	54	23	51	45	23

TABLE 2.

Representative Olivine Analyses

	611-5-1	739-2-2		620-5-1
	3	1	8	19
SiO_2	38.64	40.48	40.57	37.32
TiO_2	.01	.02	.03	.04
Al_2O_3	.00	.01	.01	.00
FeO	22.33	12.28	11.90	26.27
MnO	.23	.26	.23	.46
MgO	37.89	46.94	47.64	36.02
CaO	.00	.00	.02	.02
TOTAL	99.10	99.99	100.40	100.13
Si	1.013	1.003	.999	.990
Ti	.000	.000	.001	.001
Al	.000	.000	.000	.000
Fe	.490	.254	.245	.583
Mn	.005	.005	.005	.010
Mg	1.480	1.733	1.749	1.424
Ca	.000	.000	.001	.001
TOTAL	2.987	2.997	3.000	3.009
Fo	75	87	88	71

TABLE 3.

Representative Pyroxene Analyses

	613-1-1			611-5-1		739-2-2	611-3-1C		741-2-1			620-5-1	
	1	4	5	14	20	3	2-3	C	8	2	5	1	12
SiO_2	51.50	50.88	49.62	52.34	52.74	52.13	49.15	51.29	54.50	54.32	54.40	52.18	51.60
TiO_2	.49	.33	.35	.88	.67	.92	1.06	1.13	.40	.41	.30	.89	.86
Al_2O_3	1.23	.39	1.89	2.34	2.12	3.30	4.57	4.49	1.82	2.01	1.30	2.40	2.84
Cr_2O_3	.01	.03	.00	-----	-----	.41	.44	.63	.00	.00	.03	-----	-----
FeO	12.96	27.10	24.74	6.54	5.99	3.52	6.06	5.65	17.56	5.77	15.34	7.65	7.16
MnO	.53	.99	.96	.15	.15	.19	.13	.14	.46	.20	.40	.23	.28
MgO	12.53	18.64	18.12	16.74	16.10	16.25	16.18	16.81	23.90	15.52	20.40	16.78	14.42
CaO	19.98	1.67	3.48	19.78	21.68	23.29	20.36	20.06	.81	22.81	8.74	19.99	22.17
Na_2O	.39	.00	.06	.36	.34	.38	.29	.35	.00	.09	.17	.41	.49
K_2O	-----	-----	-----	.00	.00	-----	-----	-----	-----	-----	-----	.00	.00
TOTAL	99.62	100.03	99.22	99.13	99.79	100.38	98.24	100.54	99.45	101.13	101.08	100.53	99.82
Si	1.960	1.956	1.916	1.936	1.942	1.900	1.845	1.869	1.989	1.970	1.982	1.916	1.917
Ti	.014	.010	.010	.024	.019	.025	.030	.031	.011	.011	.008	.025	.024
Al	.055	.017	.086	.102	.092	.142	.202	.193	.078	.086	.056	.104	.124
Cr	.000	.001	.000	-----	-----	.012	.013	.018	.000	.000	.001	-----	-----
Fe	.413	.871	.799	.202	.185	.107	.190	.172	.536	.175	.467	.235	.223
Mn	.017	.032	.031	.005	.005	.006	.004	.004	.014	.006	.012	.007	.009
Mc	.711	1.069	1.043	.923	.884	.883	.905	.913	.300	.839	1.108	.919	.799
Ca	.815	.069	.144	.784	.855	.910	.819	.783	.032	.886	.341	.787	.883
Na	.029	.000	.004	.026	.024	.027	.021	.024	.000	.006	.012	.029	.035
K	-----	-----	-----	.000	.000	-----	-----	-----	-----	-----	-----	.000	.000
TOTAL	4.013	4.025	4.033	4.002	4.005	4.011	4.028	4.007	3.961	3.979	3.988	4.022	4.014
Wo	42	3	7	41	44	48	43	42	2	47	18	41	46
EN	37	53	53	48	46	47	47	49	70	44	58	47	42
FS	21	43	40	11	10	6	10	9	29	9	24	12	12

TABLE 4.

Representative Amphibole Analyses

	613-1-1			611-5-1		739-2-2		739-2-2	611-3-1C		741-2-1		620-5-1	615-5-1	
	1-3	3-8	3-10	2	13	2-6	1-1	2-8	2-1	3-3	3-11	2-7	14	1-5	2-1
SiO_2	52.01	53.63	47.72	44.20	43.84	44.34	49.34	56.34	48.18	51.61	52.01	50.81	42.18	49.58	49.96
Al_2O_3	2.95	.19	5.83	11.41	10.16	12.32	8.03	1.12	6.74	3.80	3.55	4.52	11.98	6.78	5.58
FeO	12.88	22.66	17.29	8.11	8.83	5.00	11.59	2.79	13.09	15.99	12.44	15.15	9.94	9.78	12.15
Fe_2O_3	.74	.00	.00	.00	.00	.00	.05	.00	.00	.00	.05	1.20	.00	.00	.00
MgO	15.44	17.30	12.08	15.14	16.17	17.72	14.45	23.67	14.85	15.77	16.58	12.33	13.98	16.87	15.75
MnO	.27	1.42	.43	.03	.07	.08	.33	.11	.14	.33	.25	.28	.12	.13	.12
TiO_2	.31	.06	1.12	2.52	2.22	2.94	.21	.00	1.59	.51	.78	.12	4.00	1.41	1.06
CaO	11.90	.97	10.68	11.71	11.20	12.36	12.58	10.76	11.51	8.24	11.18	12.61	11.54	11.94	11.37
Na_2O	.65	.04	1.85	2.54	2.71	2.48	1.20	.04	1.48	.95	.74	.27	2.89	1.84	1.95
K_2O	.10	.03	.27	.21	.22	.27	.07	.02	.27	.08	.17	.13	.31	.11	.17
TOTAL	97.25	96.30	97.27	95.87	95.42	97.51	97.85	94.85	97.85	97.28	97.75	97.42	96.94	98.44	98.11
Si	7.571	7.972	7.142	6.480	6.493	6.320	7.117	7.904	7.022	7.529	7.492	7.478	6.212	7.068	7.213
Al^{IV}	.429	.028	.858	1.520	1.507	1.680	.883	.096	.978	.471	.508	.523	1.788	.933	.787
Al^{VI}	.078	.006	.171	.452	.267	.390	.483	.089	.180	.182	.095	.262	.292	.207	.163
Fe^{+2}	1.568	2.817	2.164	.994	1.094	.596	1.398	.327	1.596	1.951	1.499	1.865	1.22	1.166	1.467
Fe^{+3}	.081	.000	.000	.000	.000	.000	.005	.000	.000	.000	.006	.133	.000	.000	.000
Mg	3.350	3.833	2.695	3.308	3.569	3.764	3.107	4.949	3.226	3.429	3.560	2.704	3.068	3.584	3.389
Mn	.033	.179	.055	.004	.009	.010	.040	.013	.017	.041	.031	.035	.015	.016	.015
Ti	.034	.007	.126	.278	.247	.315	.023	.000	.174	.056	.085	.013	.443	.151	.115
Ca	1.856	.155	1.713	1.840	1.777	1.888	1.945	1.618	1.798	1.288	1.726	1.989	1.821	1.824	1.759
Na_{M4}	.000	.004	.077	.125	.037	.037	.000	.004	.010	.053	.000	.000	.137	.053	.092
Na_A	.184	.007	.460	.598	.741	.648	.336	.007	.409	.215	.207	.077	.689	.456	.454
K	.019	.006	.052	.039	.042	.049	.013	.004	.050	.015	.031	.024	.058	.020	.031
A	.202	.013	.512	.637	.783	.697	.349	.011	.459	.230	.238	.102	.747	.476	.485
TOTAL	15.405	15.027	16.025	16.275	16.566	16.394	15.699	15.022	15.919	15.460	15.478	15.205	16.490	15.954	15.970
WO	27	2	26	30	28	30	30	23	27	19	25	30	30	28	27
EN	49	56	41	54	55	60	48	72	49	51	52	41	50	55	51
FS	23	41	33	16	17	10	22	5	24	29	22	28	20	18	22

Figure 7: Olivine forsterite content vs. Mg/Mg+Fe of the bulk rock fall close to the curve representing Roeder and Emslie's K_D of 0.33 for olivine and a coexisting liquid. Troctolites are more magnesium and have olivines that are more magnesian and have olivines that are more magnesiam than the majority of the samples, suggesting they crystallized from relatively unevolved liquids.

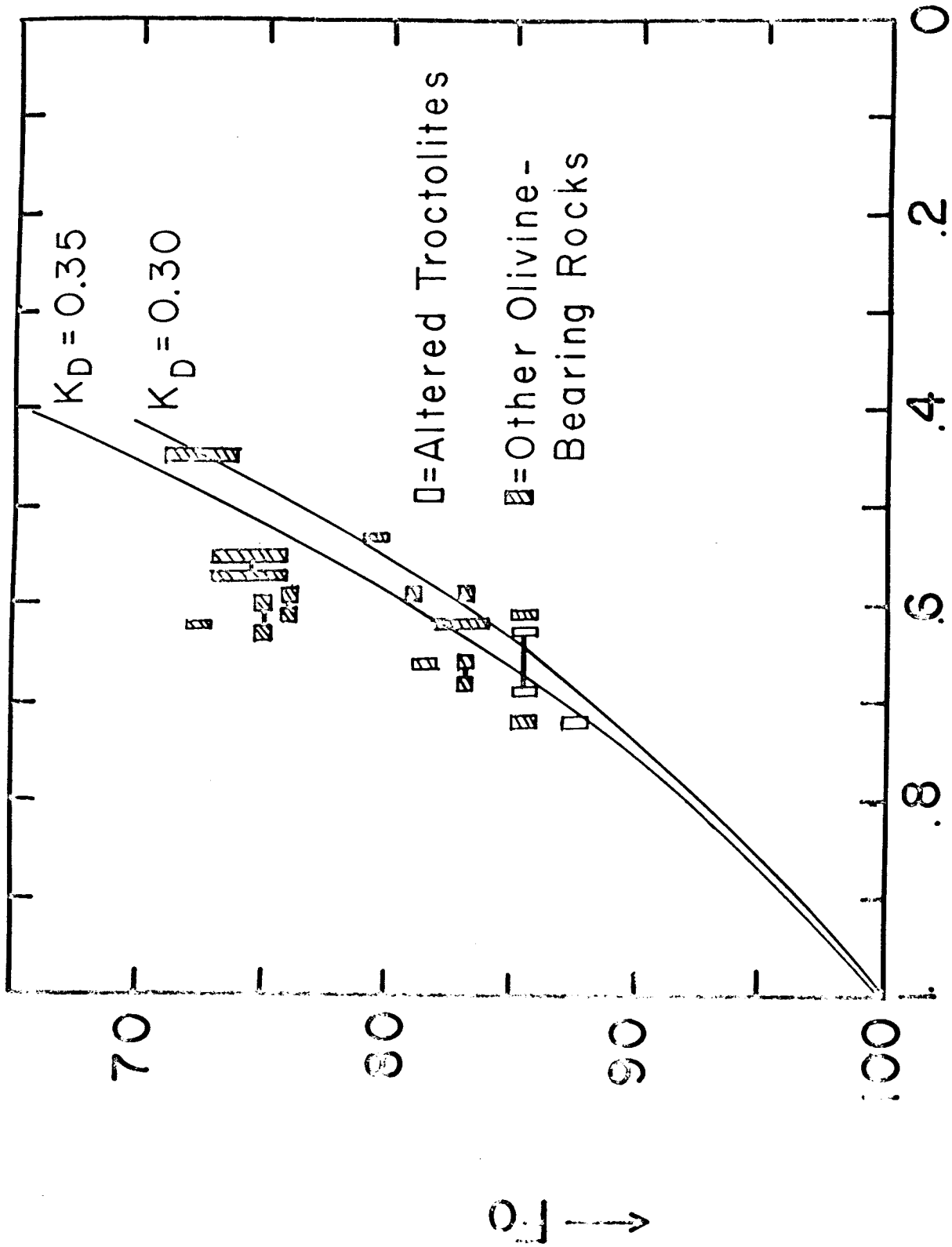

Mg / (Fe+Mg) Bulk rock

gabbroic samples (Hodges and Papike, 1976).

Roeder and Emslie (1970) and Walker and others (1976) investigated the distribution of Fe and Mg between olivine and coexisting basaltic liquid. Roeder and Emslie (1970) reported that K_D was approximately 0.30 over ranges in temperature (1150-1300°C) and oxygen fugacity ($10^{-0.68}$ to 10^{-12} atm.). Walker and others (1976) reported a K_D of 0.33 for lunar basalt composition and found no variation with temperature (1325-600°C), pressure (0-12 kb), or cooling rate (0.5-2000°C per hour). These results may be applied to natural systems to determine whether olivine crystallized in equilibrium with a liquid having a Mg/Mg+Fe ratio equal to that of the bulk rock in which it is found, or whether the bulk rock cannot represent an equilibrium liquid composition. A plot of Fo vs. Mg/Mg+Fe for specimens from the MCR suite indicates that the bulk Mg/Mg+Fe of many of these rocks is compatible with that of a probable liquid from which the olivine crystallized (Fig. 7). This may mean that the olivines crystallized in equilibrium with a liquid with the same Mg/Mg+Fe as the bulk rock. This interpretation necessitates that the Mg/Mg+Fe ratio of the bulk rock remains unchanged despite alteration. On the other hand, if secondary processes control the K_D of olivine that we have plotted (i.e. the olivine is secondary), then this plot indicates that the metamorphic olivine/bulk-rock distribution coefficient is equal to the olivine/liquid distribution coefficient. The deviation of some samples from the curves can be explained by alteration of the bulk rock Mg/Mg+Fe ratio after crystallization, relict olivine in a liquid of the bulk composition, or disequilibrium crystallization.

Pyroxenes: Almost all of the clinopyroxenes analyzed are diopside or diopsidic augite, and lie within the field $Wo_{40-50}En_{40-50}Fs_{5-10}$ (Fig. 8). There is a slight correlation between Mg/Mg+Fe of the

Figure 8: Quadrilateral plot of all pyroxene analyses from the MCR gabbros.

CAYMAN TROUGH PYROXENES

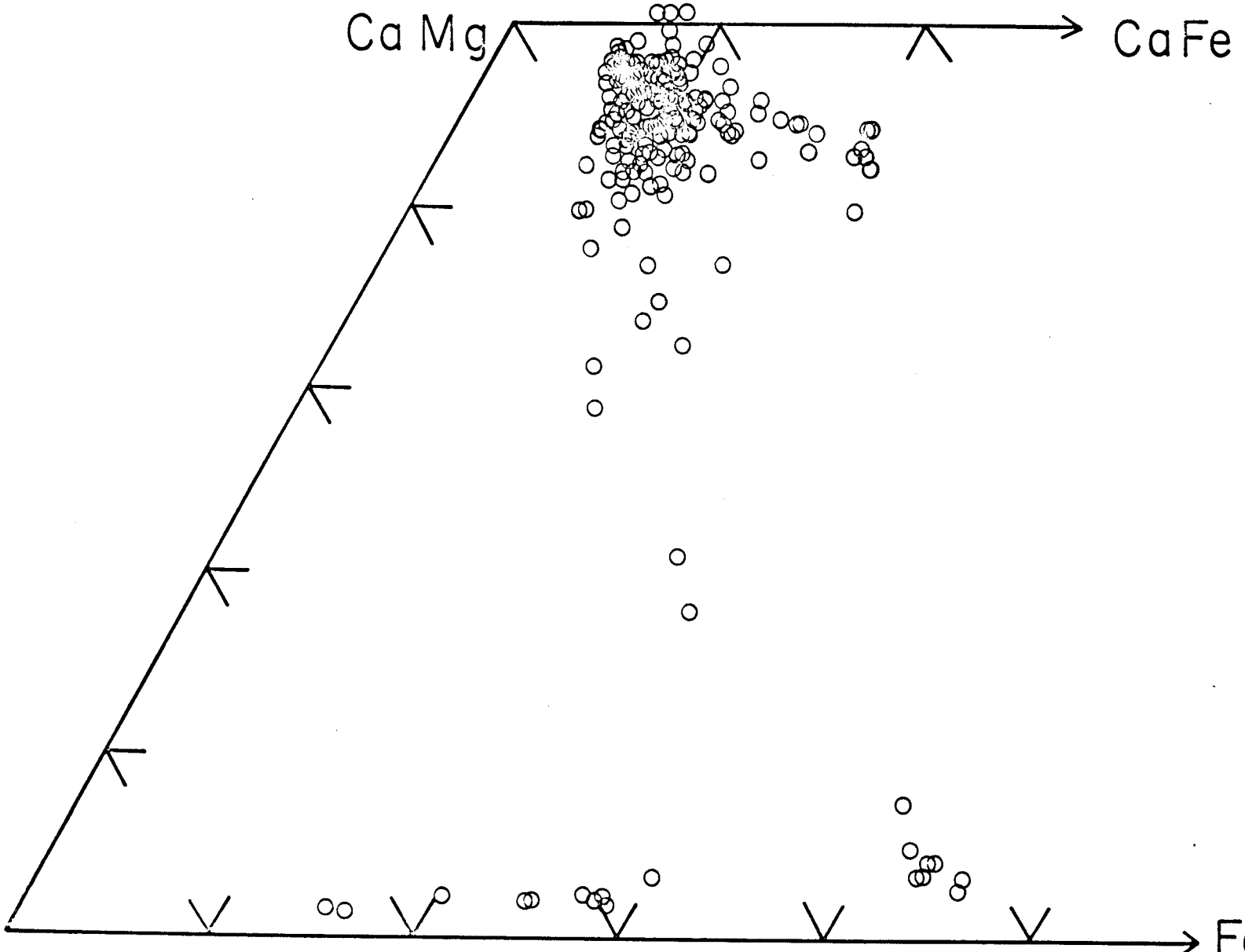

clinopyroxene and Mg/Mg+Fe of the bulk rock (Fig. 9). This trend is less pronounced than the comparable olivine trend at least in part because the variability of clinopyroxene composition within samples is quite large. The significance of this trend is questionable, because the distribution coefficient changes with pressure (Powell and Powell, 1974) and composition (Lindsley and others, 1974), and the effect of other variables is unknown. Ti and Cr contents are quite high in some clinopyroxenes, with up to .069 cations Ti and .035 Cr. However, there is little correlation between these two components within the group of analyses (Fig. 10). Low chrome contents are observed in gabbro, orthopyroxene gabbro and metagabbro clinopyroxenes. One sample each of troctolite and micrometagabbro have moderate chrome but high titanium contents in their clinopyroxenes. All other rock types show highly scattered values.

Orthopyroxene occurs in only a few of the analyzed samples and only very rarely as separate grains. Orthopyroxene is more ferrous than coexisting clinopyroxene, and this trend is enhanced with increasing iron content, as indicated by the tie lines on a quadrilateral plot (Fig. 11). This follows from experimentally determined and observed distribution coefficients for coexisting clino- and orthopyroxene (Kretz, 1963; Lindsley and others, 1974). Orthopyroxene-bearing rocks are among the most iron-rich and are the most evolved if an olivine tholeiite parental magma is assumed. Calcium contents place both pyroxenes near the 810°C solvus of Lindsley and others (1974), suggesting low-temperature equilibration. This equilibration is likely a re-equilibration in some samples, where exsolution or recrystallization is observed, but may be primary where these textures are absent.

Additional evidence for equilibration is provided by Ti/Al ratios.

Figure 9: Clinopyroxene Mg/Mg+Fe vs. bulk rock Mg/Mg+Fe. Fe is total Fe. Solid lines connect points for samples with two, differing bulk analyses; dashed lines connect coexisting clino- and orthopyroxenes.

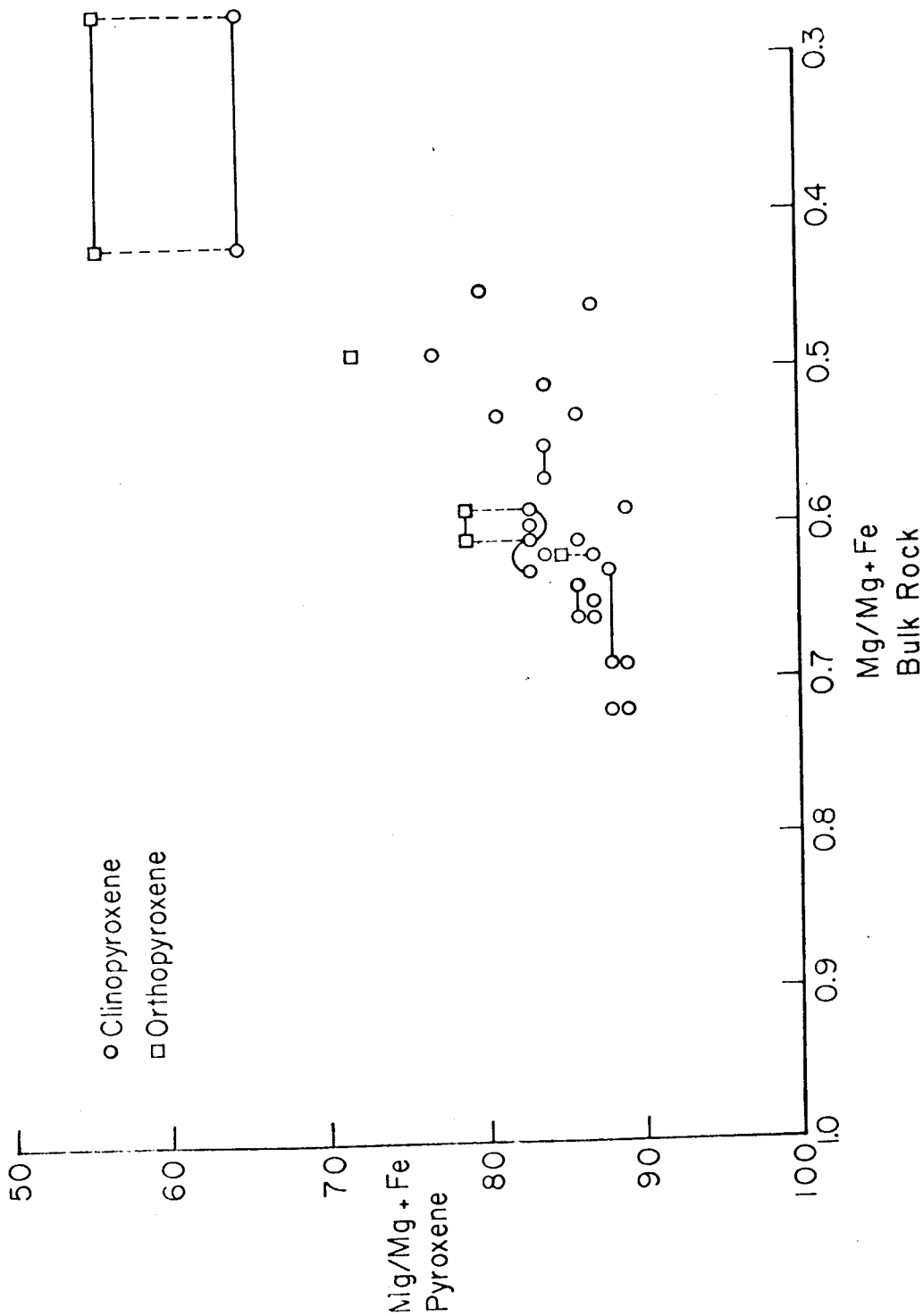
o Clinopyroxene
□ Orthopyroxene
Mg/Mg + Fe
Pyroxene
50
60
70
80
90
100
1.0
0.9
0.8
0.7
0.6
0.5
0.4
0.3
Mg/Mg+Fe
Bulk Rock

Figure 10: Ti vs. Cr plot for clinopyroxenes show the lack of a clear correlation between these two elements.

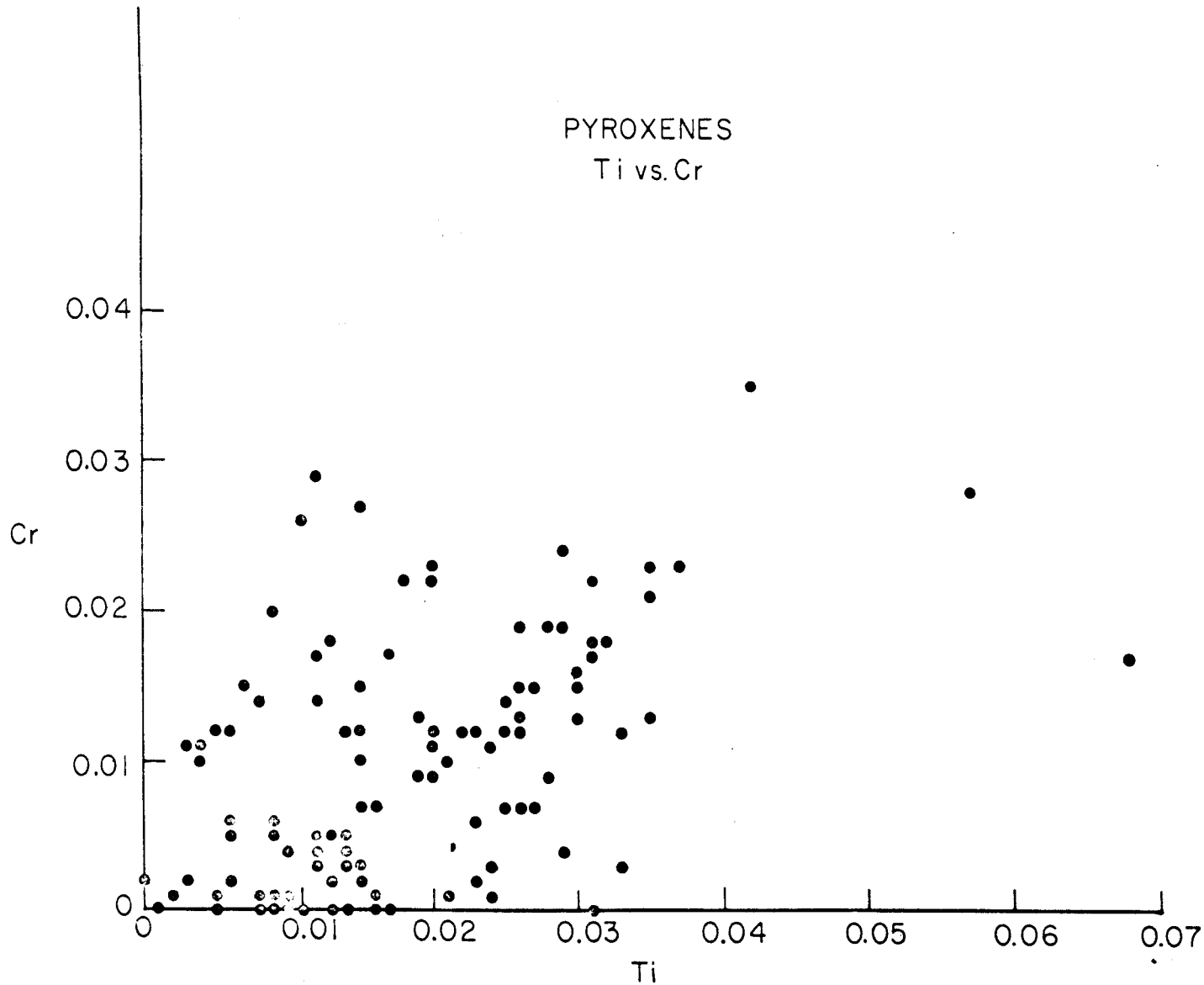
PYROXENES
Ti vs. Cr
Cr
0.04
0.03
0.02
0.01
0
0
0.01
0.02
0.03
0.04
0.05
0.06
0.07
Ti

Figure 11: A plot of coexisting clino- and orthopyroxenes indicates that orthopyroxenes become progressively more iron-rich than the clinopyroxenes in same sample with increasing iron content. Lindsley and others (1974) 810° solvus is approximated by the dotted area.

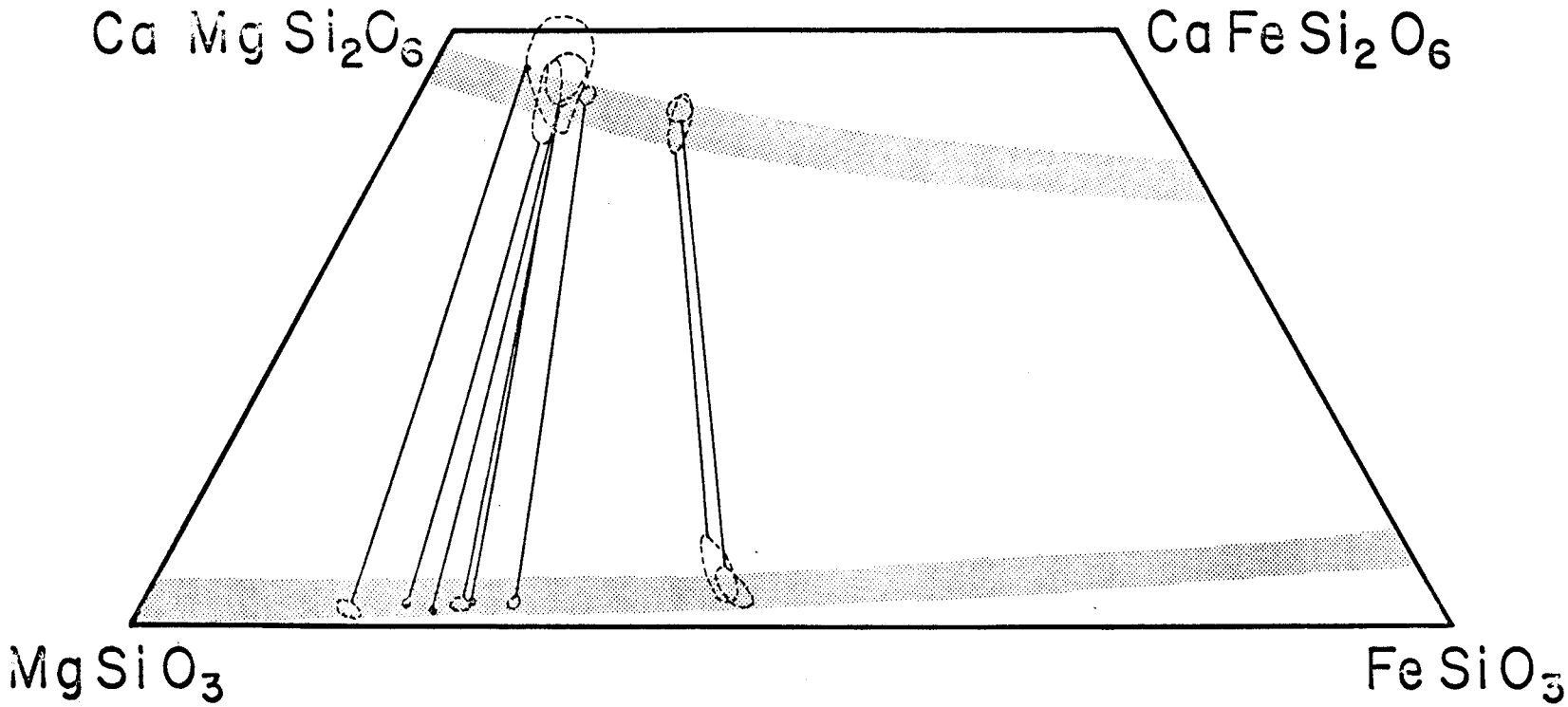

COEXISTING OPX and CPX

Walker and others (1976) found that Ti/Al ratios decrease with slower cooling and that very low Ti and Al contents are apparently indicative of very slow cooling. The larger concentrations in basaltic pyroxenes compared with gabbroic pyroxenes apparently result from the trapping of incompatible elements during the more rapid crystallization of the basalts. While recrystallization textures indicate that many of the Cayman pyroxene compositions do not reflect initial cooling conditions, low Ti/Al ratios and low Ti and Al contents (Fig. 12) may indicate equilibrium was achieved during recrystallization.

Plagioclase: There is an extreme range in anorthite content in the plagioclases analyzed, from 6 to 84 mole %. This range reflects the preservation of some primary calcic plagioclase and alteration to albite of other plagioclase. Those grains with An less than 50% are usually clearly secondary in nature. They are often small, and have granoblastic textures or follow cracks or grain boundaries in an irregular fashion around relict plagioclase. Many of the calcic plagioclase analyses are in the 55-75% An range, in contrast to only rare analyses less than 80% An in the DSDP Site 334 gabbroic rocks (Hodges and Papike, 1976). The considerably lower An contents of the Cayman plagioclases may be due in part to pervasive, optically undetected alteration in these rocks because secondary plagioclase is more albitic, occurs commonly in these samples and is often not optically distinct from much more calcic plagioclase. On the other hand, a correlation between rock type and the anorthite content of the most calcic plagioclases (Fig. 13) follows the fractionation trends predicted on the basis of the olivine and pyroxene chemistry: olivine-bearing rocks generally contain plagioclase that is more calcic than that in gabbros or orthopyroxene gabbros. There is considerable scatter in the data due to large compositional variation within rock

Figure 12: Ti vs Al of clinopyroxenes in the MCR gabbro plot in a larger field than the Oceanographer Fracture Zone (OFZ) gabbros but do not have as high Ti and Al contents as the OFZ basalts.

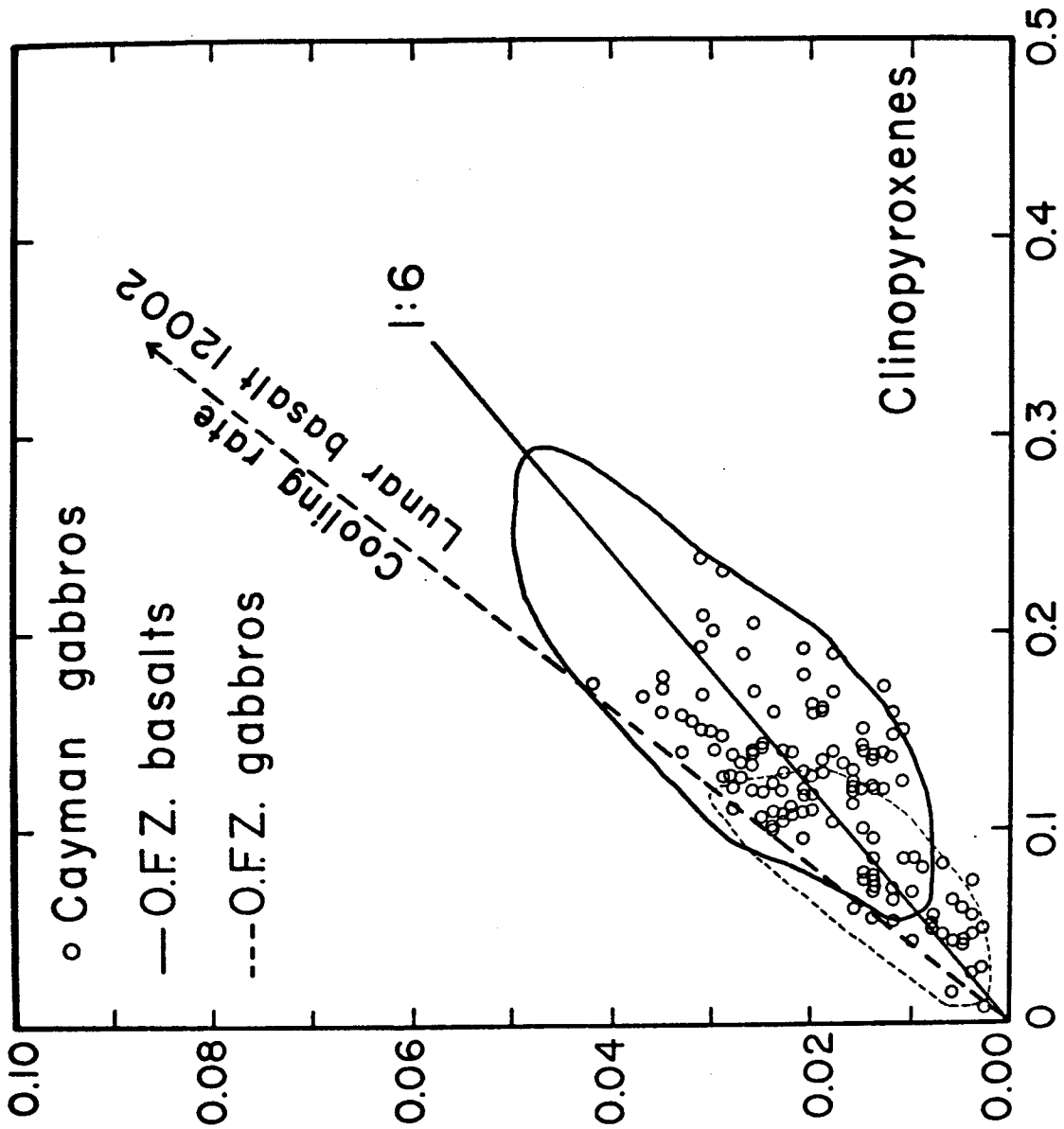
Ti/6 Oxygens
Al/6 Oxygens
0.10
0.08
0.06
0.04
0.02
0.00
0
0.1
0.2
0.3
0.4
0.5
Clinopyroxenes
9:1
Cooling rate
Lunar basalt 1200°
o Cayman gabbros
—O.F.Z. basalts
---O.F.Z. gabbros

Figure 13: Histograms of An content for each rock type indicate that maximum An content decreases with decreasing olivine content. The spread in values for each rock type is partly a function of total number of analyses and partly a reflection of the degree and chemistry of albitization of the plagioclase.

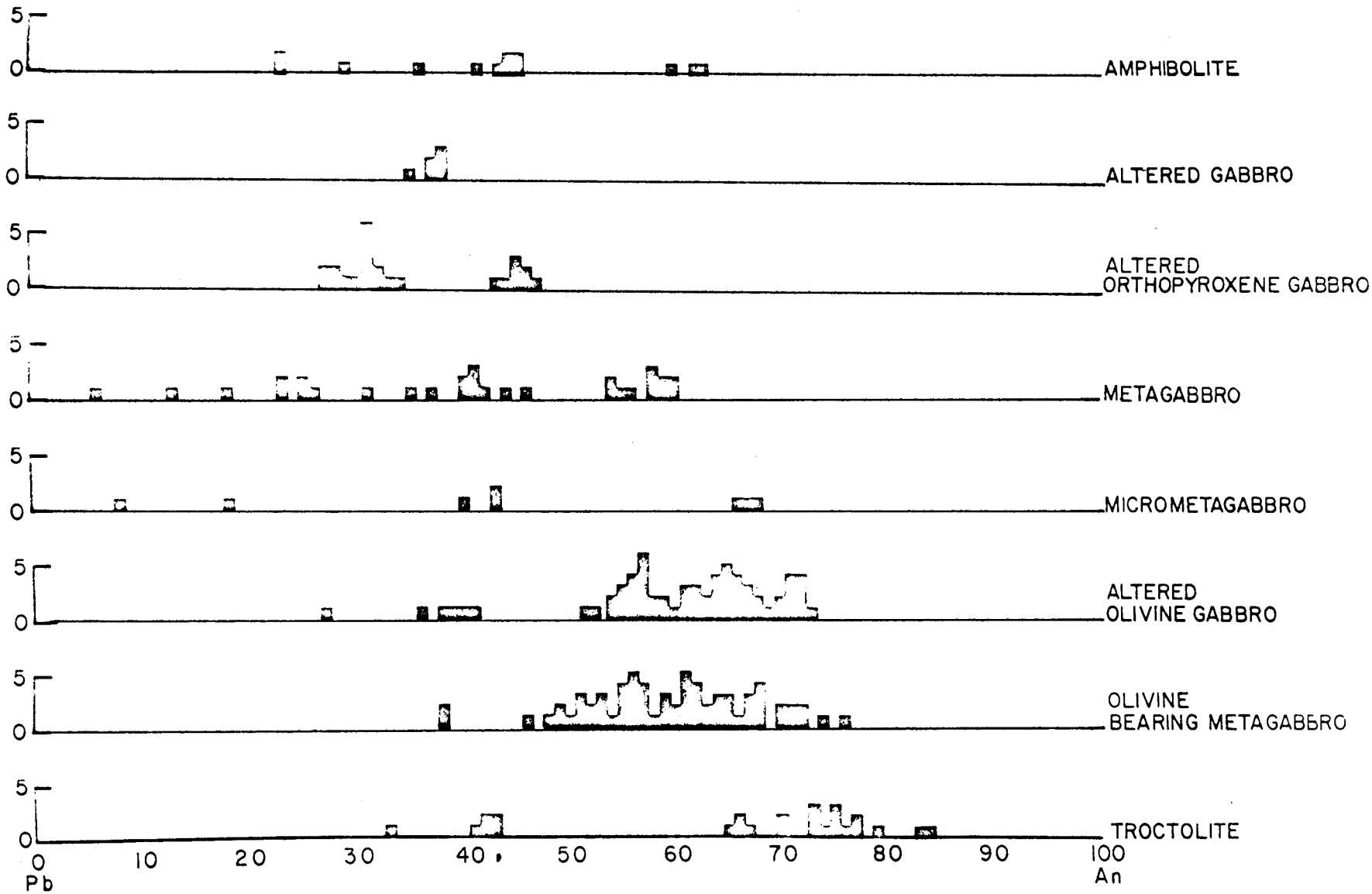
5
0
AMPHIBOLITE
ALTERED GABBRO
ALTERED
ORTHOPYROXENE GABBRO
METAGABBRO
MICROMETAGABBRO
ALTERED
OLIVINE GABBRO
OLIVINE
BEARING METAGABBRO
TROCTOLITE
0
10
20
30
40
50
60
70
80
90
100
Pb
An

types and to alteration effects (established on textural and chemical criteria), but the overall pattern is clear.

Large grains not optically zoned are also chemically unzoned, suggesting either equilibrium crystallization or reequilibration after crystallization was complete. Reequilibration may have lowered the anorthite contents slightly. Low Fe and Mg contents in the plagioclase are independent indicators of either relatively slow crystallization rates (Bryan, 1974) or reequilibration with removal of Fe (into oxides) and Mg (into alteration products or out of the rock), because these elements are incorporated in the feldspar crystal structure only during rapid crystal growth. Figure 14 shows that Fe and Mg are only rarely incorporated into plagioclase in these samples. This plot is a projection from the alkali feldspar components onto the ternary $(Fe, Mg)_2Si_3O_8$-$Ca_2Si_3O_8$-Al_4SiO_8 (Longhi, 1976). The calcic plagioclase cluster very close to the anorthite point, as expected in this projection for Fe- and Mg-poor compositions. Most other plagioclases are scattered in both the excess Al and Ca directions, but there are a few points that indicate considerable Fe and Mg substitution for Ca. This is unusual in comparison to ocean-floor basalts, where Fe and Mg clearly occupy tetrahedral sites (Bryan, 1974; Longhi, 1976; Shibata and others, 1979). This difference may be related to conditions of crystallization, but its significance is unknown.

A plot of maximum anorthite content vs. bulk Ca/Ca+Na indicates that there is more calcium in the rock than in the plagioclase (Fig. 15), which is contrary to the experimental relationships studied by Drake (1976). This trend is more pronounced with lower anorthite contents. Because decreasing anorthite content follows an increase in the modal content of other calcium-bearing minerals such as calcic clinopyroxene

Figure 14: Plot of all plagioclase analyses projected from the alkali feldspar components onto the ternary $(Fe, Mg)_2Si_3O_8$-$Ca_2Si_3O_8$-Al_4SiO_8 indicates very low Fe and Mg contents.

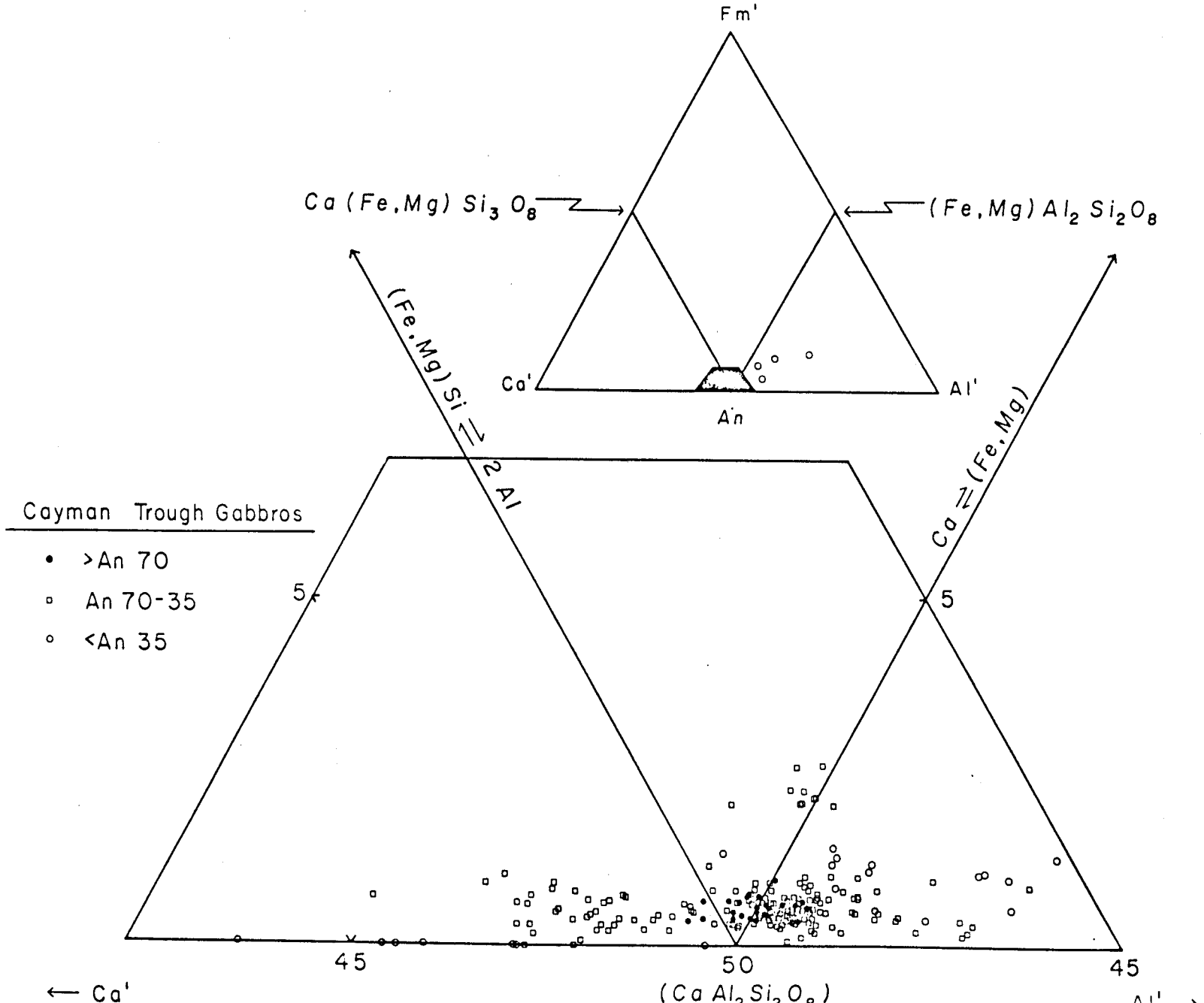
Fm'
Ca (Fe,Mg) Si3 O8
(Fe,Mg) Al2 Si2 O8
Ca'
Al'
An
(Fe,Mg) Si ⇄ 2 Al
Ca ⇄ (Fe,Mg)
Cayman Trough Gabbros
• >An 70
▫ An 70-35
◦ <An 35
5
5
45
50
45
← Ca'
(Ca Al2 Si2 O8)
Al' →

Figure 15: Plagioclase An content vs. Ca/Ca+Na of the bulk rock indicates relative calcium enrichment of the bulk rock.

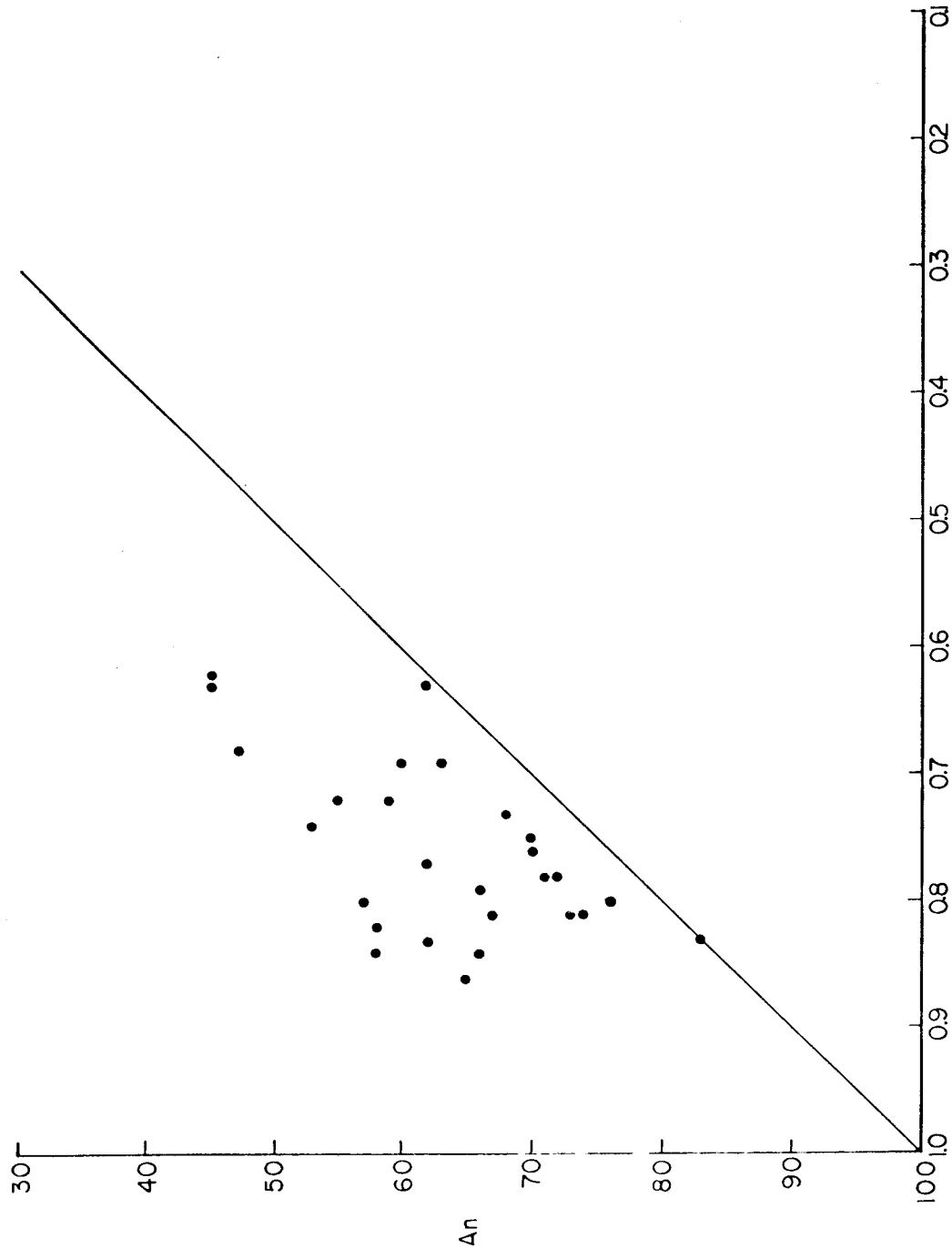
An
30
40
50
60
70
80
90
100
1.0
0.9
0.8
0.7
0.6
0.5
0.4
0.3
0.2
0.1
Bulk Rock Ca/Ca+Na

and amphibole, these minerals may affect the plagioclase/bulk-rock distribution coefficients and lower the An content of plagioclase. This would increase the Ca/Ca+Na ratio in the bulk rock in the direction observed in the MCR samples. In fact, Morse (1979) documents An depletion in plagioclases as a result of crystallization of augite.

Although anorthite contents in the plagioclases are lower in secondary grains, it is interesting to note that only three samples contain plagioclase more sodic than An_{20}, which defines the upper limit of the greenschist facies (Miyashiro, 1973). This supports the conclusion that much of the alteration and preceding deformation took place at high temperatures (see Chapter 2). Despite considerable evidence for Na enrichment of the altered plagioclase, it is not clear whether calcium is lost from the bulk rock during alteration. If loss does occur, it appears to be minimal. If loss does not occur, some calcic mineral must be formed from the calcium derived by alteration of both plagioclase and calcic clinopyroxene. It is possible that this mineral is tremolite, formed primarily as an alteration product of olivine or orthopyroxene. Epidote, another very calcic mineral, is frequently reported in similar rocks (e.g. Miyashiro and others, 1971; Bonatti and others, 1975), but is rare within the MCR suite. Calcite is also rare and very late in the alteration sequence, and can therefore not account for the bulk of the "lost" calcium.

Amphiboles: Both primary and secondary amphiboles are recognizable but the distinction is often difficult. The amphiboles in this suite vary in composition, both with respect to Fe/Mg ratios and aluminum contents. When plotted on a CaMg-CaFe-Fe-Mg quadrilateral (Fig. 16), they show greater variability in Mg/Mg+Fe than the other mafic silicates. Their Ca content is relatively uniform, however, and is always lower

Figure 16: Plot of all amphibole analyses on Mg-Fe-CaMg-CaFe quadrilateral shows considerable spread of Mg/Fe ratio but relatively constant Wo contents.

CAYMAN TROUGH AMPHIBOLES

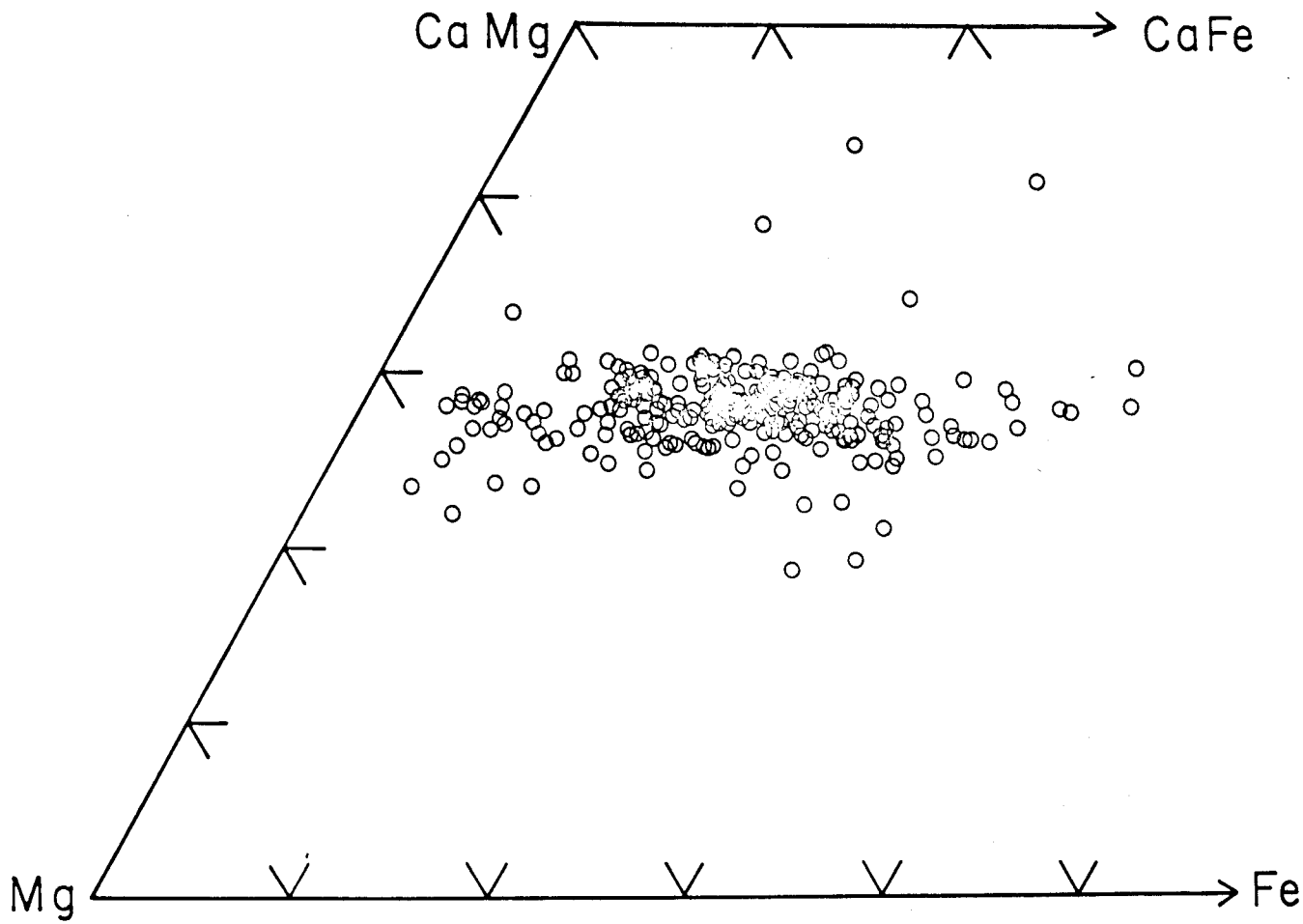

than that of coexisting clinopyroxenes. The most iron-rich amphiboles in a sample are more iron-rich than the coexisting clinopyroxenes and orthopyroxenes. This is consistent with the textural evidence that the amphiboles are very late in the crystallization sequence. There is good correlation among Si, Na+K and Ti contents within the amphiboles (Fig. 17), but we have found no other obvious chemical correlations despite an extensive search. It is interesting to note that Ti and Na are correlated with strongly colored grains, particularly reddish-brown hornblende, but there does not appear to be any other chemical indicator correlated with color.

The only clearcut textural correlation seen in these samples is that Al-poor, Mg-rich amphiboles are usually found in pseudomorphs of olivine. This is expected because olivine is also magnesian and other alteration products include opaques that probably act as a sink for some of the iron.

A plot of all points on an A-AL4-NAM4 "others" ternary diagram (Papike and others, 1974) shows a very strong clustering about 30% A (cations in the A site), with little NAM4 (Na in the M_4 site) (Fig. 18). This clustering is similar to that reported by Hodges and Papike (1976) for the DSDP Site 334 amphiboles. There are a few points that have a considerable amount of NAM4; these are predominantly fibrous amphiboles. There is more scatter in "others" components among amphiboles from more highly altered rocks, but no other rock-type correlation is evident.

Although red-brown hornblende is usually associated with only slightly altered rocks and texturally may indicate that it is either primary or very early in the alteration history within the strongly colored amphiboles color is not a reliable guide to time of formation and, by extension, relative temperature of formation. Color-zoned

Figure 17: Plots of Si vs. Na+K and Ti for the MCR amphiboles show good correlation among these elements.

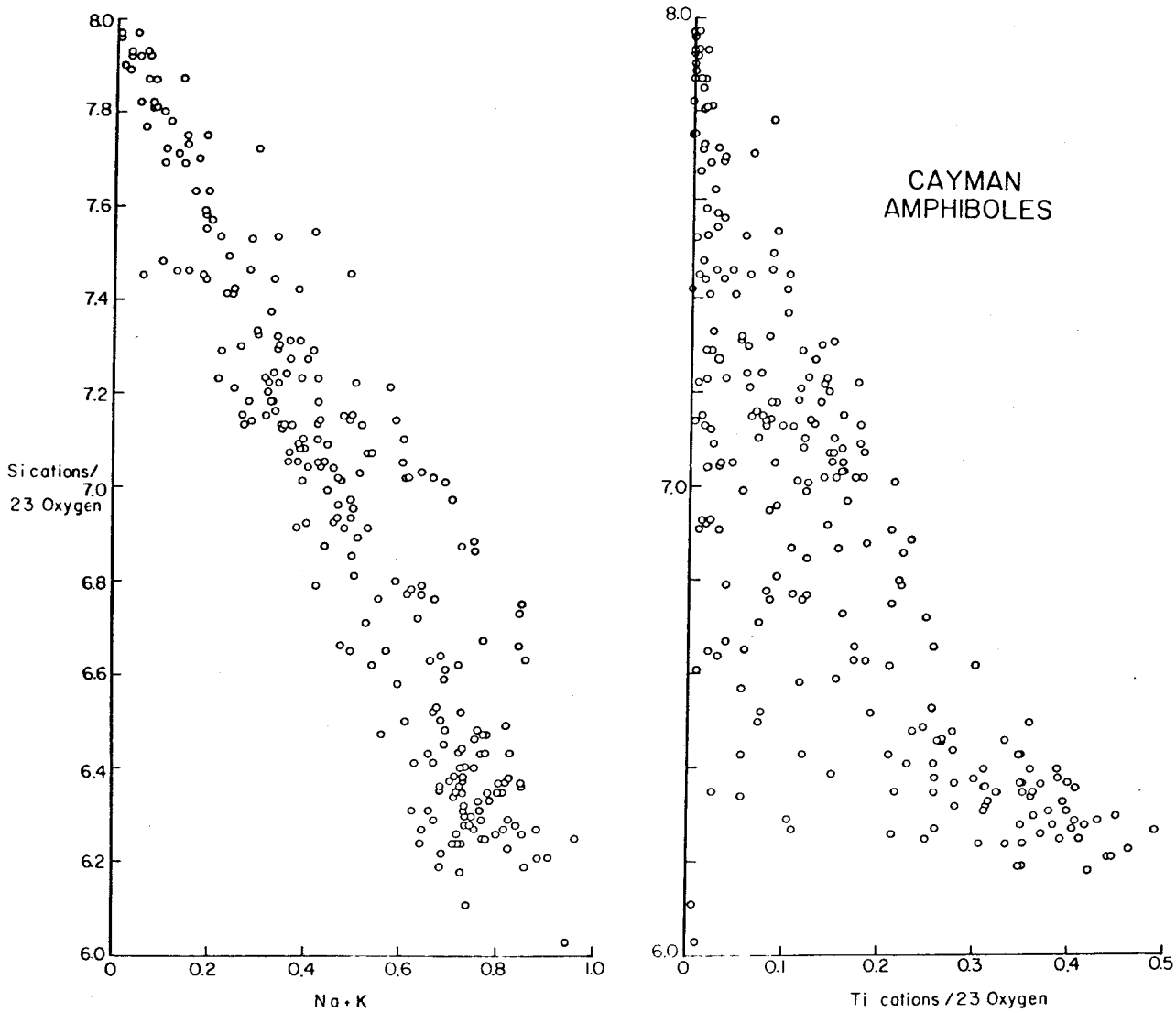
CAYMAN
AMPHIBOLES
Si cations/
23 Oxygen
Na + K
Ti cations / 23 Oxygen
8.0
7.8
7.6
7.4
7.2
7.0
6.8
6.6
6.4
6.2
6.0
0
0.2
0.4
0.6
0.8
1.0
0.1
0.3
0.5

Figure 18: Plot of all amphibole analyses on "others" ternary. A - cations in A site; NAM4 - cations in M_4 site; AL4 - tetrahedral Al. Fields for best "others" classification are 1) KATO, 2) ED, 3) PARG, HAST, KAER; 4) GL, RB; 5) TSCH, GED (Papike and others, 1974).

CAYMAN AMPHIBOLES

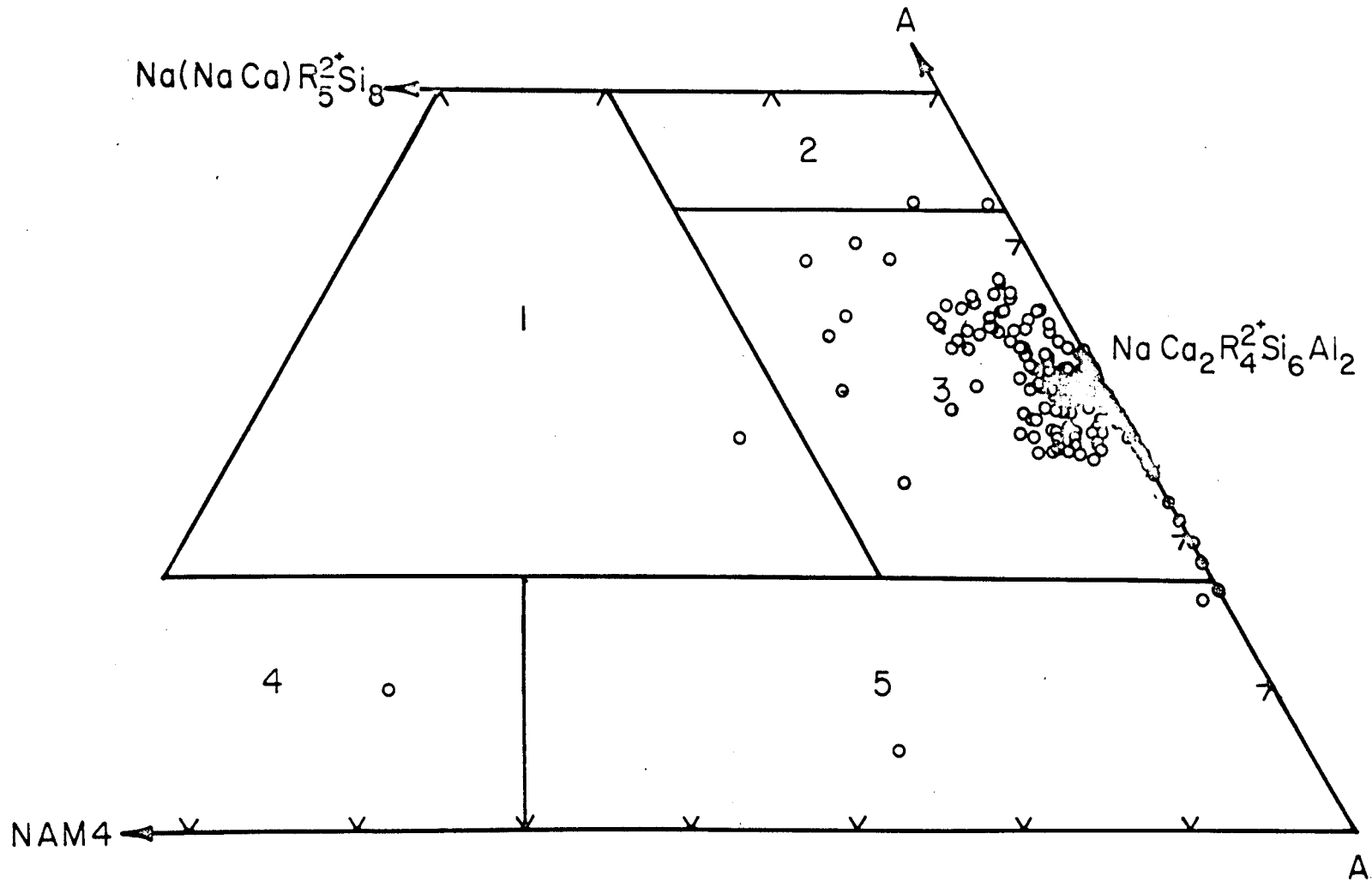

amphiboles are quite common, but the color zonation often does not follow a red-brown to brown to green to blue-green sequence, which is the sequence considered to correlate with decreasing temperature of formation (Miyashiro, 1973). Thus there are examples of grains with blue-green cores and red-brown rims, apparently optically continuous, and lateral variations in color with no systematic change are also common. These puzzling relationships are often present in samples where green or blue-green amphibole also clearly replaces clinopyroxene with a previously formed, dark amphibole rim. On the basis of these relationships we conclude that habit and textures must be the determining factors in recognizing a sequence of formation for the various amphiboles that may be present in a sample, and that color is an unreliable temperature guide in these rocks.

DISCUSSION

Inferences from phase diagrams: The primary mineralogy of the samples in the MCR suite indicates that some range in degree of fractionation of a parent olivine tholeiitic liquid is represented if accumulation of mafic minerals within these samples is assumed not to have occurred. Troctolites represent least fractionated and orthopyroxene gabbros most fractionated compositions. Some degree of magma mixing must also be involved to produce the olivine-free clinopyroxene gabbros, assuming the applicability of the 1-atm experimental results of Walker and others (1979, Figure 3). The geometric approach in the following discussion is similar to that of Irvine (1977). Figure 19 demonstrates how a plagioclase + clinopyroxene-saturated liquid can evolve from a combination of fractionation and magma mixing due to the curvature of the olivine-clinopyroxene-plagioclase cotectic. Liquids that are

Figure 19: Projection of plagioclase-saturated liquidus on the diopside-olivine-silica ternary, with theoretical mixing lines. Mixing of liquids on either end of these lines produces a third liquid which contains stable and unstable phases. See text for explanation of two examples. Liquids 1 + 2 yield liquid 3, which contains Ol + Pl + (Cpx) (unstable). Similarly, 2 + 4 = 5, containing CPX + Pl + (Ol); 2 + 7 = 6, containing Cpx + Pl + (Ol) + (Opx); 1 + 7 = 8, containing Ol + Pl + (Opx) + (Cpx); 1 + 9 = 10, containing Ol + Opx + Pl + (Cpx); and 1 + 9 = 11, containing Ol + Pl + (Opx) + (Cpx).

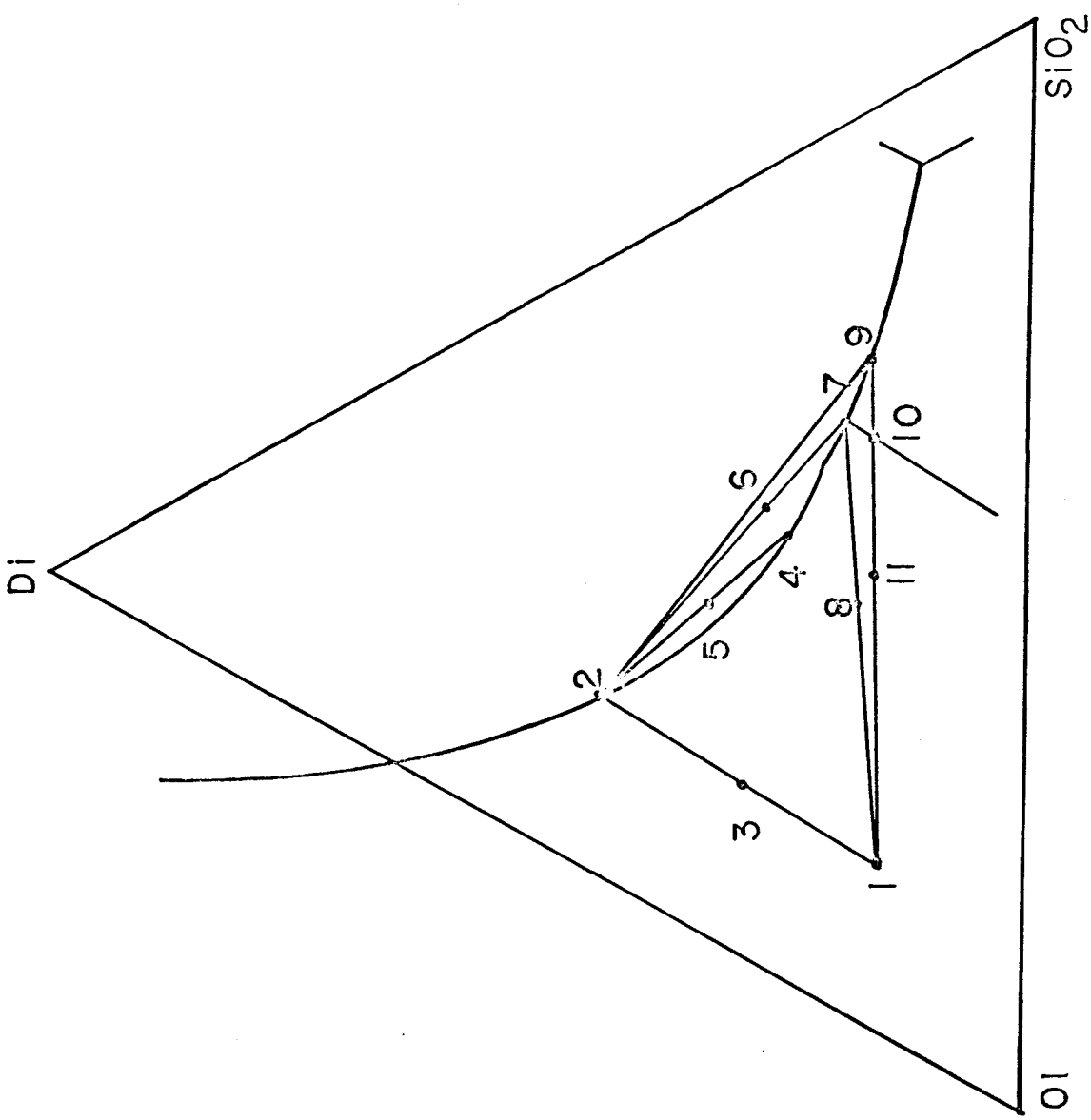
Di
SiO2
Ol
1
2
3
4
5
6
7
8
9
10
11

plagioclase + olivine-saturated and plagioclase + clinopyroxene-saturated will move toward the plagioclase-olivine-clinopyroxene cotectic as a result of fractionation. Fractionation along this cotectic has been suggested by Thompson and others (1979) for the fresh basalts recovered from the axial valley floor, so this process may still be operating within the magma chamber. Further fractionation will move these liquids toward, and possibly past, the peritectic point. Liquids that have evolved this far are saturated with plagioclase, clinopyroxene and orthopyroxene, producing orthopyroxene gabbros or clinopyroxene norites on crystallization.

Further permutations in the mineral assemblages of rocks crystallized from mixed magmas are possible if the two liquids mixed are not saturated with the same phases and/or the resulting liquid is saturated in a new phase, and if the disequilibrium phases are not totally resorbed after mixing. For example, if a liquid that is saturated with olivine + plagioclase (point 1 on Figure 19) is mixed with a liquid which has already reached three-phase saturation (point 2), the resulting liquid (point 3) will be saturated with olivine and plagioclase, but clinopyroxene will also be present as a relict phase. In addition, the compositions of the new plagioclase and olivine will be slightly different than the compositions of either phase in the two original magmas before mixing. The relict clinopyroxene would show indication of resorption if equilibrium were partially established in the new liquid or it might be armored by one of the new phases. A second possibility, which involves both resorption and the crystallization of a new phase, is the mix of two liquids on the olivine-clinopyroxene-plagioclase cotectic above the peritectic point (points 2 and 4). The resulting liquid

(point 5) is saturated with plagioclase and clinopyroxene, but might contain relict olivine of two compositions. These two examples illustrate how, in a setting where magma mixing occurs, solid-phase assemblages may be created that are not indicative of the liquids from which the individual phases crystallized. The composition of a mixture of any two liquids can be represented by a point on a straight line connecting the points representing the original liquid compositions, the phases that may be present in this new liquid include the phase(s) in each of the two original liquids and the phases(s) with which the mixed liquid is saturated. Additional examples of possible mixing lines are also shown on Figure 19, and phase assemblages possible for these lines are given in the figure caption. Textures that may be observed in relict phases may include resorption, armoring and subtle-to-prominent zoning. Repeated mixing, combined with fractionation, can lead to complex mineral assemblages and textures. In fact, the MCR gabbros do not, for the most part, exhibit complex resorption and armoring textures that might be expected in rocks that are products of repeated mixing and fractional crystallization. This may mean that the solid phase(s) have sufficient time to equilibrate with the new liquid composition after mixing before the next mixing episode is initiated, in which case the mineral assemblages do indicate the composition field of the coexisting liquid.

We have shown that olivine + plagioclase-saturated parent liquid may evolve to clinopyroxene + plagioclase-saturated liquids through a combination of fractionation and magma mixing. Although clinopyroxene gabbros may be evidence that fractionation and mixing have occurred within the Mid-Cayman Rise, the predominance of olivine-rich samples in the collection suggests that highly fractionated liquids are limited in

volumetric extent. The spatial distribution of these samples (Fig. 2) suggests that pockets of more evolved liquids may exist within a generally less evolved magma chamber, although this distribution may also be simply a function of the structures that expose these rocks.

Inferences from mineral chemistry: Inferences about the evolution of the magmas from which these samples crystallized that are based on the mineralogy of the rocks are compatible with inferences drawn from the trends of the chemistry of individual mineral phases. Olivines in troctolitic rocks are more forsteritic than olivines in gabbros, and clinopyroxenes in olivine gabbros are more magnesian than those in orthopyroxene gabbros. Olivine is absent in orthopyroxene gabbros. As described above, the maximum anorthite content of plagioclase is higher in the less evolved olivine-bearing rock types than in the gabbros and orthopyroxene gabbros.

If we compare the mineral chemistry of pairs of coexisting minerals to established equilibrium chemistry, it is apparent that igneous whole-rock equilibrium is not represented. For example, Walker and others (1979) have determined a series of mineral compositions of coexisting olivine and plagioclase equilibrated in tholeiitic liquids (Fig. 20). The chemistry of coexisting mineral pairs in the MCR gabbros does not coincide with the 1-atm experimental data; the plagioclase is too sodic for any given olivine composition. This suggests that the plagioclase and olivine compositions do not represent chemical equilibrium with a liquid (at least not at 1 atm), but may indicate that magma mixing has occurred without reequilibration or that some subsolidus chemical change, either reequilibration or disequilibrium alteration, has taken place. Exsolution of orthopyroxene in some olivine-clinopyroxene gabbros also indicates subsolidus reaction.

Figure 20: Maximum olivine Fo content vs coexisting maximum plagioclase An content. Curve represents equilibrium assemblages from experimental runs of Walker and others (1979); temperatures are experimental temperatures.

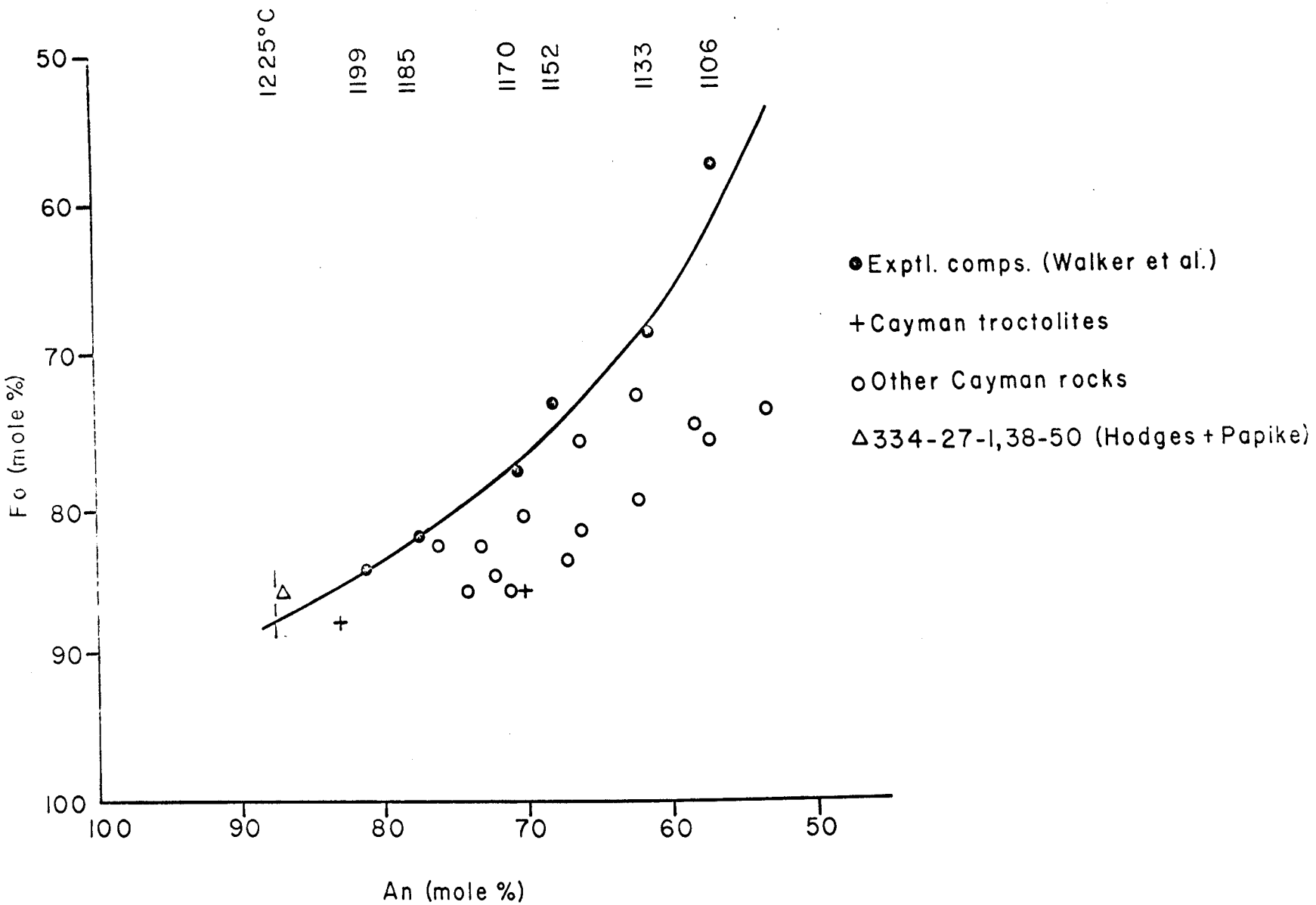
1225°C
1199
1185
1170
1152
1133
1106
50
60
70
80
90
100
Fo (mole %)
100
90
80
70
60
50
An (mole %)
Exptl. comps. (Walker et al.)
+Cayman troctolites
oOther Cayman rocks
Δ334-27-1,38-50 (Hodges + Papike)

Temperature calculations: Calculations of temperature of equilibration have been made for coexisting clinopyroxene-orthopyroxene pairs using Wells' (1977) procedure and for coexisting olivine-clinopyroxene pairs using Powell and Powell's (1974) method. For samples where more than one analysis of each phase was made, the compositions of the clinopyroxene and orthopyroxene with the highest En content were used in one calculation and those of the clino- and orthopyroxenes with the highest Fs content were used in a second calculation. Similarly, the composition of the most forsteritic olivine and of the clinopyroxene with the highest En content were paired, as were those of the least forsteritic olivine and of the clinopyroxene with the highest Fs content. The calculations for clinopyroxene-orthopyroxene pairs (all of which are separate grains, i.e., no host-lamellae pairs) yield maximum temperatures of 1193-1393°C and minimum temperatures of 1051-1260°C (Table 5). Temperatures from olivine-clinopyroxene pairs are considerably lower, 884-1018°C; 23 of 27 are 1000 ±10°C (Table 6). Pressure of 730 bars was used in the calculation; this is the equivalent of 6 km of water and 500 m of basaltic overburden. An additional 500 m of rock overburden adds only 1°C to the calculated temperatures. Both geothermometers could only be applied to two samples, 611-5-2A and 615-2-1, and the difference between the two methods is about 235°C. Temperatures estimated from the experiments of Walker and others (1979), based on plagioclase composition, yield temperatures between 1100 and 1150°C (from figure 20) for these two samples. The discrepancy between the results of the two-pyroxene and olivine-clinopyroxene calculations may be due to inaccuracies in one or both equations or may be due to lack of true equilibrium in the samples. The consistency in calculated temperatures from coexisting olivine-clinopyroxene pairs suggests that equilibrium between these two

Table 5. Temperatures calculated from coexisting orthopyroxene-clinopyroxene pairs

Sample No.	Temperature for pairs with highest En (°C)	Temperature for pairs with highest Fs (°C)
611-4-1AP	1193	1174
611-5-2A	1241	--
613-1-1	1334	1051
613-2-1	1254	1206
615-2-1	1242	--
737-1-2	1196	1190
741-1-1	1212	1201
741-2-1	1393	1260

Table 6. Temperatures calculated from coexisting olivine-clinopyroxene pairs*

Sample No.	Temperature for pairs of highest En and highest Fo (°C)	Temperature for pairs of highest Fs and lowest Fo (°C)
611-1-1	987	1006
611-5-1	991	--
611-5-2A	1009	1008
615-2-1	1006	999
615-4-1	999	995
620-5-1	999	996
621-3-1	1018	1015
621-3-2	1009	1010
739-1-1	1008	1015
739-2-2	1016	1016
739-3-1	1006	1005
739-6-1	1015	1009
741-3-1	1001	1009
742-5-2	884	1005

*Pressure assumed to be 730 bars.

was achieved at a temperature of 1000 ±10°C in these samples. If this is the case, there are several possible explanations of the two-pyroxene results: 1) the two pyroxenes are not in equilibrium with each other and therefore the calculations are meaningless. This may be the case in at least samples 613-1-1 and 741-2-1, where the calculations for the magnesian pairs in the samples yield temperatures that differ by 283° and 133°C, respectively, from the calculations for the ferrous pairs. Other calculations appear to have moderate internal consistency. 2) Clinopyroxene-orthopyroxene equilibrium was achieved at higher temperatures than olivine-clinopyroxene equilibrium. This is impossible because clinopyroxene is involved in both pairs and would therefore be out of equilibrium with orthopyroxene if it reequilibrated with olivine. 3) The calculations are not accurate and yield higher temperatures than actually prevailed. Because the mean deviation of all the experimental data Wells used to determine his equation is 64°C from the calculated temperatures and because he notes deviations of more than 100°C, this explanation is a real possibility. 4) Analytical error is sufficient to substantially affect the calculations. This possibility is considered unlikely because similar errors should also affect the olivine-clinopyroxene calculations. We conclude that the most reasonable explanations for the discrepancies in the calculated temperatures are 1) orthopyroxene and clinopyroxene may not have achieved equilibrium in some samples and 2) the Wells two-pyroxene geothermometer is inadequate. These temperature data, combined with textural evidence for alteration and recrystallization, imply that primary chemical relationships are masked by subsolidus reactions. Phase homogeneity is more likely to be the result of reequilibration than primary equilibrium crystallization,

and bulk composition need not represent a liquid composition.

CONCLUSIONS

The suite of plutonic rocks collected by DSRV ALVIN from the walls of the Mid-Cayman Rise spreading center are predominantly gabbroic. A fractionation trend from magnesian troctolites through olivine and clinopyroxene gabbros to iron-enriched orthopyroxene gabbros is suggested on the basis of mineral chemical analyses. Many of the primary minerals have apparently uniform chemistry despite sometimes considerable alteration. The homogeneous nature of many of those coarse-grained primary phases suggests reequilibration after original crystallization. Equilibrium crystallization is a possibility but is considered unlikely because the geologic setting favors rapid cooling and because comparison with experimental data suggests subsolidus equilibrium. The coarse grain size of the majority of the samples is thought to be unrelated to cooling rate, as recent experimental evidence shows that several other factors affect grain size (Lofgren, 1978).

Plagioclase and amphibole may be either primary or secondary. Textural evidence aids in distinguishing the two but may often be inconclusive. Sodic chemistry can be assumed to confirm a secondary origin for plagioclase, but no chemical criterion was found to distinguish primary and secondary amphiboles.

Bibliography - Chapter I

Albee, A.L. and Ray, L., 1970. Correction factors for electron probe microanalysis of silicates, oxides, carbonates, phosphates and sulfates, Anal. Chem., v. 42, p. 1408-1414.

Bence, A.E. and Albee, A.L., 1968. Empirical correction factors for the electron microanalysis of silicates and oxides, Jour. Geology, v. 76, p. 382-403.

Bonatti, E., Honnorez, J., Kirst, P. and Radicati, F., 1975. Metagabbros from the Mid-Atlantic Ridge at 06°N: Contact-hydrothermal-dynamic metamorphism beneath the axial valley, Jour. Geology, v. 83, p. 61-78.

Bryan, W.B., 1974. Fe-Mg relationships in sector-zoned submarine basalt plagioclase, Earth Planet. Sci. Lett., v. 24, p. 157-165.

Bryan, W.B. and Moore, J.G., 1977. Compositional variations of young basalts in the Mid-Atlantic Ridge rift valley near 36°49'N, Geol. Soc. America Bull., v. 88, p. 556-570.

Cann, J.R., 1971. Petrology of basement rocks from Palmer Ridge, N.E. Atlantic, Philos. Trans. Roy. Soc. London, Ser. A., v. 268, p. 605-617.

CAYTROUGH, 1979. Geological and geophysical investigation of the Mid-Cayman Rise spreading center: initial results and observations in Talwani, M., Harrison, C.G. and Hayes, D., eds., Deep drilling results in Atlantic Ocean: Ocean crust, Maurice Ewing Ser., v. 2.

Drake, M.J., 1976. Plagioclase-melt equilibria, Geochim. Cosmochim. Acta, v. 40, p. 457.

Frey, F.A., Bryan, W.B. and Thompson, G., 1974. Atlantic ocean floor: geochemistry and petrology of basalts from Legs 2 and 3 of the Deep-Sea Drilling Project, Jour. Geophys. Research, v. 79, p. 5507-5527.

Helmstaedt, H. and Allen, J.M., 1977. Metagabbronorite from DSDP hole 334: an example of high-temperature deformation and recrystallization near the Mid-Atlantic Ridge, Canadian Jour. Earth Sci., v. 14, p. 886-898.

Hodges, F.N. and Papike, J.J., 1976. DSDP Site 334: Magmatic cumulates from oceanic layer 3, Jour. Geophys. Research, v. 81, p. 4135-4151.

Holcombe, T.L., Vogt, P.R., Matthews, J.E. and Murchison, R.R., 1973. Evidence for sea-floor spreading in the Cayman Trough, Earth Planet. Sci. Lett., v. 20, p. 357-371.

Kretz, R., 1963. Distribution of magnesium and iron between orthopyroxene and calcic pyroxene in natural mineral assemblages, Jour. Geology, v. 71, p. 773-785.

Lindsley, D.H., King, H.E., Jr. and Turnock, A.C., 1974. Composition of synthetic augite and hypersthene coexisting at 810°C, Geophys. Res. Lett., v. 1, p. 134-136.

Lofgren, G.E., 1978. An experimental study of intersertal and subophitic texture (abs.), Trans. Amer. Geophys. Union, v. 59, p. 396.

Longhi, J., 1976. Iron, magnesium and silica in plagioclase, Ph.D. thesis, Harvard University.

Mazzullo, L.J. and Bence, A.E., 1976. Abyssal tholeiites from DSDP Leg 34: the Nazca Plate, Jour. Geophys. Research, v. 81, p. 4327-4351.

Miyashiro, A., 1973. Metamorphism and Metamorphic Belts, John Wiley and Sons, New York, 492 pp.

Miyashiro, A., Shido, F. and Ewing, M., 1971. Metamorphism in the Mid-Atlantic Ridge near 24° and 30°N, Philos. Trans. Roy. Soc. London, Ser. A, v. 268, p. 589-603.

Morse, S.A., 1979. Influence of augite on plagioclase fractionation, Jour. Geology, v. 87, p. 202-208.

Papike, J.J., Cameron, K.L. and Baldwin, K., 1974. Amphiboles and pyroxenes: characterization of other than quadrilateral components and estimates of ferric iron from microprobe data (abs.), Geol. Soc. America Abs. with Prog., v. 7, p. 1053.

Powell, M. and Powell, R., 1974. An olivine-clinopyroxene geothermometer, Contrib. Mineral. Petrol., v. 48, p. 249-263.

Roeder, P.L. and Emslie, R.F., 1970. Olivine-liquid equilibrium, Contrib. Mineral. Petrol., v. 29, p. 275-289.

Scott, R.B. and Tiezzi, L.J., 1976. Fractionation trends of a cumulate gabbro, Mid-Atlantic Ridge, 26°N (abs.), Trans. Amer. Geophys. Union, v. 57, p. 407.

Shibata, T., Walker, D. and DeLong, S.E., 1979. Petrology and fractionation of abyssal tholeiites from the Oceanographer Fracture zone (35°N, 35°W), Contrib. Mineral. Petrol. (in press).

Streckeisen, A., 1976. To each plutonic rock its proper name, Earth-Science Reviews, v. 12, p. 1-33.

Thompson, G., Bryan, W.B., Melson, W.G., 1979. Geological and geophysical investigation of the Mid-Cayman Rise spreading center: geochemical variation and petrogenesis of basalt glasses (in review).

Walker, D., Kirkpatrick, R.J., Longhi, J. and Hays, J.F., 1976. Crystallization history of lunar picritic basalt sample 12002: phase-equilibria and cooling-rate studies, Geol. Soc. America Bull., v. 87, p. 646-656.

Walker, D., Shibata, T. and DeLong, S.E., 1979. Abyssal tholeiites from the Oceanographer Fracture zone: II. phase equilibria and mixing. (in review).

Wells, P.R.A., 1977. Pyroxene thermometry in simple and complex systems, Contrib. Mineral. Petrol., v. 62, p. 129-139.

Winkler, H.G.F., 1976. Petrogenesis of Metamorphic Rocks, 4th ed., Springer-Verlag, New York, 334 pp.

CHAPTER 2: DEFORMATION

CHAPTER 2

The Mid-Cayman Rise spreading center is a slowly accreting boundary about 100 km long that connects the Oriente and the Swan Transforms. This ridge, with a full spreading rate of 20 mm/yr (Macdonald and Holcombe, 1978), has the bilaterally symmetric features associated with mid-oceanic ridges, such as topography, sediment thickness and age (Holcombe and others, 1973). Unlike typical slowly spreading ridges, however, the Mid-Cayman Rise axial valley floor lies at a depth of 6000 m, about 2-3 km deeper than usual. A multi-ship investigation of this area in 1976 and 1977 confirmed the actively spreading nature of the Rise (see CAYTROUGH, 1979, for a general outline of results), but also discovered extensive exposures of gabbroic and ultramafic rocks on the rift valley walls, which have not previously been associated with accreting plate boundaries.

One facet of the investigation involved the use of the DSRV ALVIN to study the microtopography, outcrop-scale structure and rock distribution on the rift valley walls. Two areas were studied in detail, one on the eastern wall near the intersection with the Swan Transform and one on the western wall to the north (see Fig. 21). In situ examination of the topography in the study areas indicates that the relief of the rift valley walls is created by numerous faults with throws of >500 m. Fault scarps are often nearly vertical and are connected by <45° slopes covered with pelagic carbonate and talus. The irregularity of many of the escarpment faces, the paucity of slickensides on these faces and the development of extensive talus fans suggest that many of the original fault planes have degraded by mass wasting. Samples collected

Figure 21: Bathymetric map of the Mid-Cayman Rise area. Dive Area 1 is on the eastern wall, Dive Area 2 on the western wall.

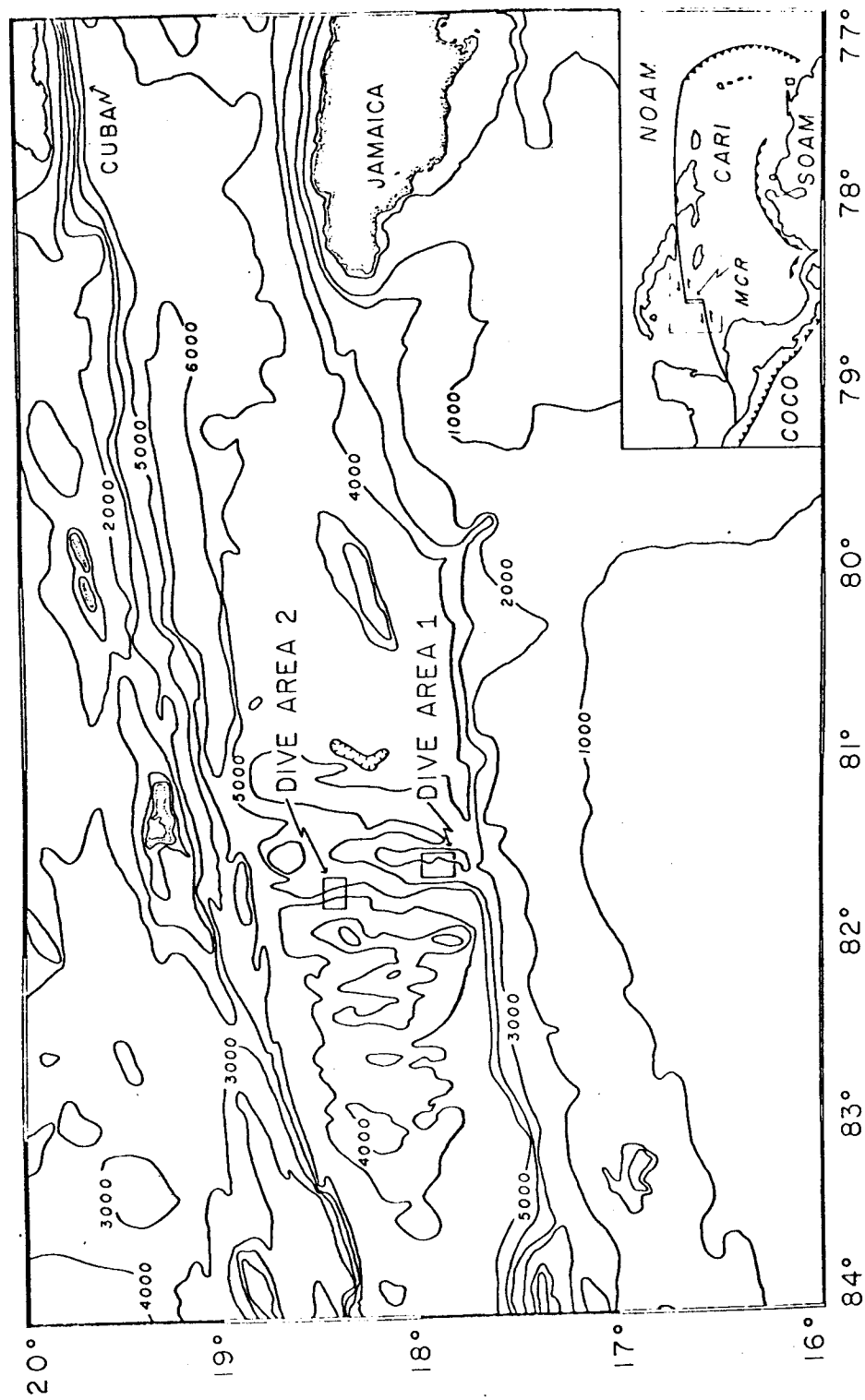
CUBA
JAMAICA
DIVE AREA 2
DIVE AREA 1
NOAM
CARI
MCR
COCO
SOAM
1000
2000
3000
4000
5000
6000
20°
19°
18°
17°
16°
84°
83°
82°
81°
80°
79°
78°
77°

were predominantly gabbroic, and rock-type distribution suggests that less than 500 m of basalt overlies the gabbroic layer in this area. The suite of plutonic rocks collected by the submersible is the only collection of gabbroic rocks acquired by direct sampling from an accreting plate boundary (CAYTROUGH, 1979). The size of the collection and the well-constrained sample locations allow us to characterize in detail the nature of the gabbroic rocks of this area. One hundred four samples have been described in detail (Appendix) and subsets have been analyzed for magnetic (Davis and others, 1979), seismic (Fox and others, in preparation), and chemical properties (DeLong and others, in preparation).

The purpose of this paper is to describe the variety of textures imposed on these rocks by deformation during their initial cooling. The textures and affected mineralogy will be interpreted in light of existing metamorphic and structural experimental data to aid in understanding the conditions experienced by rocks prior to their exposure at the sea floor. We will conclude with a discussion of the implications of the results of this study on our understanding of the nature of the oceanic crust and its evolution at accreting plate boundaries.

SAMPLE DESCRIPTIONS

The coarse-grained gabbroic rocks are highly variable with respect to mineralogy, textures and degrees of alteration and deformation. Primary rock types represented include troctolite, olivine gabbro, gabbro and orthopyroxene gabbro. Alteration has obscured the primary mineralogy in many samples; these are classified as metagabbro, olivine-bearing metagabbro, or amphibolite (where amphibole is presently the only major mafic phase). Where discernible, primary textures are

usually subophitic, and grain size ranges from 2 mm to 3-4 cm. No cumulate layering has been unequivocably identified although some samples have an apparent modal excess of plagioclase relative to reasonable liquid compositions. With respect to textures, mineralogy, and chemistry the Cayman Trough samples strongly resemble gabbroic rocks previously collected from the ocean floors, e.g. Melson and others (1968), Engel and Fisher (1975), Miyashiro and others (1971), and Bonatti and others (1975). The unique setting, however, suggests some caution in applying conclusions drawn from the study of the Cayman collection to samples from other localities.

STRAIN FEATURES

The spectrum of strain features observed within the collection is diverse, including microstructures developed within grains of primary silicate phases; recrystallized primary phases; veins and fractures; and the development of foliation. These features will be discussed individually, and then an attempt will be made to convey the many ways in which these features combine to create a broad range of rock textures.

Intragrain strain: Strained plagioclase is almost ubiquitous in the Cayman suite. Undulose extinction, intragranular cracks, some with very small offsets, mechanical twins (tapered and polysynthetic) which are sometimes kinked (Fig. 22), and irregular undulose extinction, which suggests the development of subgrain boundaries (Fig. 23), are observed. Mafic minerals exhibit some of these same features, though not as abundantly nor as often as plagioclase due to their greater resistance to deformation (Nicolas and Poirier, 1976). Olivine may have undulose extinction, kink bands and deformation lamellae. Strained pyroxene is broken or has bent cleavage. There is one exceptional

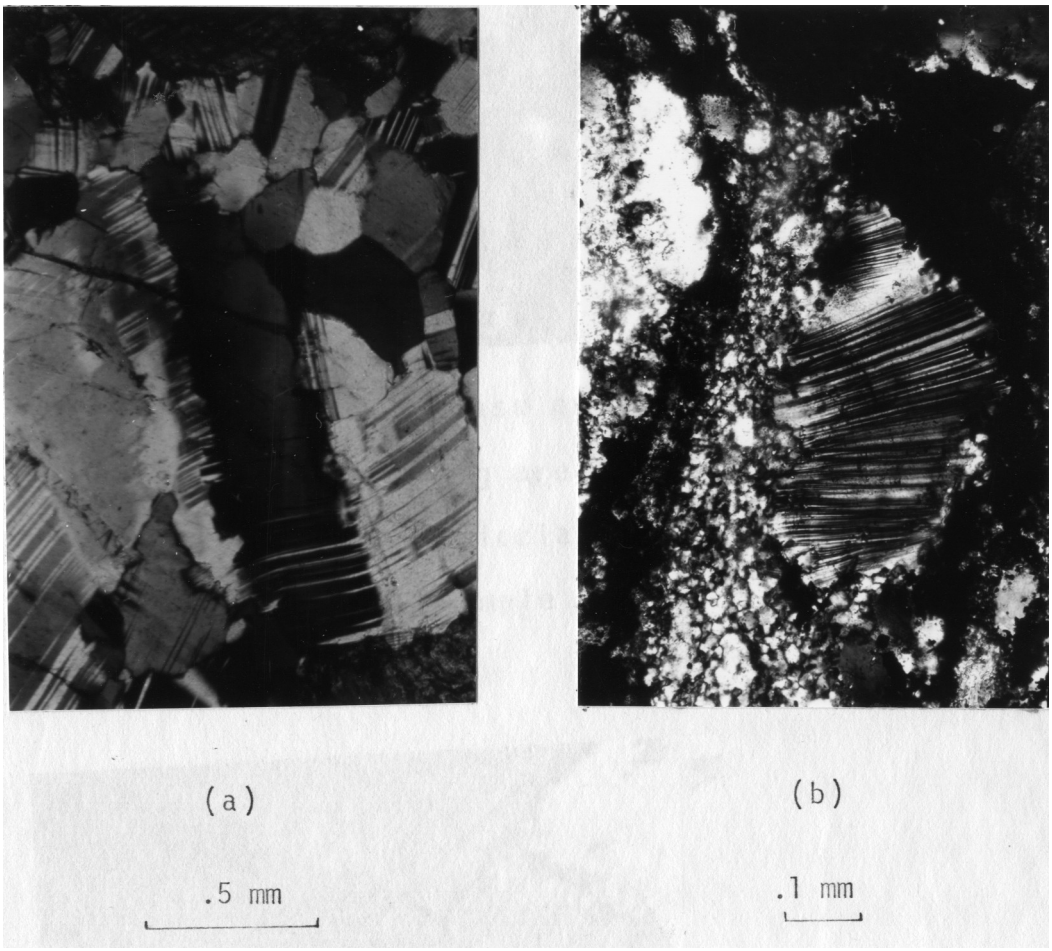

Figure 22: (a) Kinked plagioclase also has bent and tapered mechanical twins and has been partially recrystallized. Sample 611-5-2A, crossed polarizers. (b) Tapered mechanical twins radiate instead of being parallel as a result of bending. Porphyroclast of plagioclase in a fine-grained matrix of plagioclase and opaques. Sample 616-6-1, crossed polarizers.

Figure 23: Large plagioclase grain on the left shows irregular extinction, outlining areas which may become subgrains. Matrix is made up of plagioclase grains that probably developed in this manner. Sample 616-6-1, crossed polarizers.

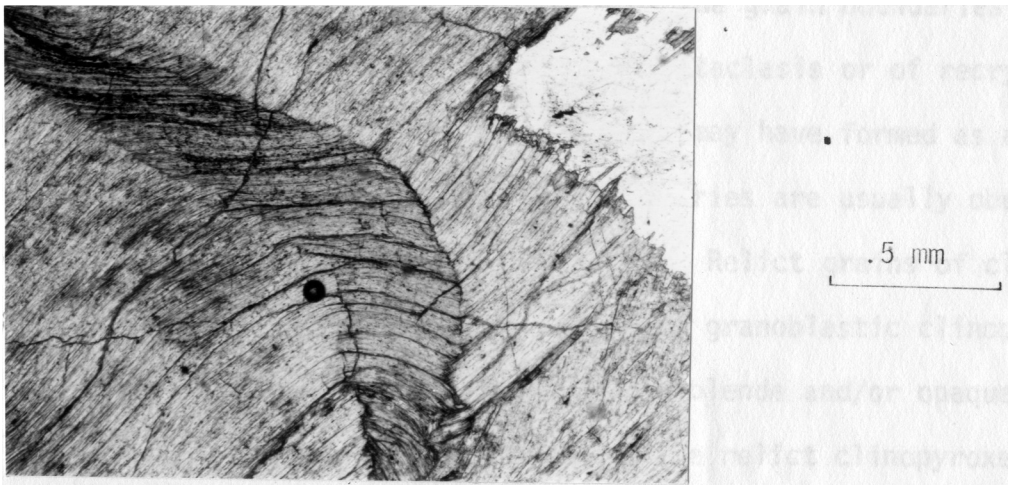

Figure 24: Sigmoidal kink band in amphibole pseudomorph of clinopyroxene. Sample 741-5-1, plane light.

example of a sigmoidal kink band in a clinopyroxene (partially replaced by amphibole) (Fig.24). Undulose extinction, bent cleavage, and kinks are observed in amphibole pseudomorphs, but it is unclear whether these features were created before or after alteration of the primary mineral.

Recrystallization: Recrystallization of plagioclase has produced features ranging from irregular or sutured grain boundaries to well-developed, equant, polygonal grains forming a granoblastic texture. Neoblasts vary from less than .5 mm to 5 mm in diameter (Fig.25), and occur in narrow elongate zones, as mortar around relict grains, or they may comprise almost all the plagioclase in a sample. In most samples, all but the smallest neoblasts show indications of internal strain, particularly mechanical twins and undulose extinction. In a few samples, extreme grain size reduction (to less than .25 mm) of both plagioclase and mafic minerals affects narrow zones or, more commonly, pervades the rock. It is not clear from the nature of the grain boundaries whether this grain size reduction is a result of cataclasis or of recrystallization. Medium-grained olivine aggregates may have formed as a result of recrystallization; however, grain boundaries are usually obscured by alteration so interpretation is difficult. Relict grains of clinopyroxene are commonly surrounded by rims of granoblastic clinopyroxene with interstitial orthopyroxene, brown hornblende and/or opaques, clearly products of recrystallization of the relict clinopyroxene (Fig. 26). In many cases recrystallization of primary mafic minerals does not occur; instead granoblastic metamorphic amphibole is formed. Growth of amphibole may be due to greater availability of water and/or lower temperature conditions during grain size reduction.

Foliation: Foliations are defined by planar or subplanar domains

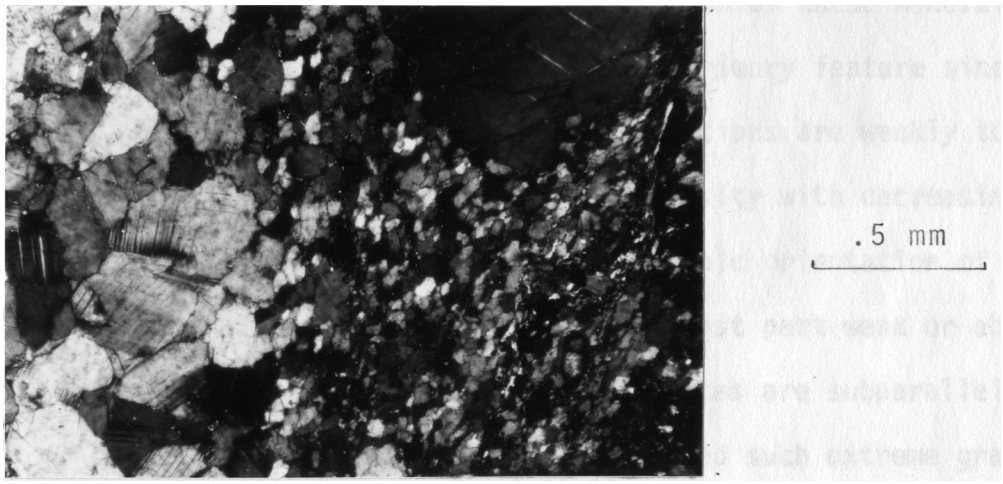

Figure 25: Plagioclase recrystallized grain size varies considerably, even in a single thin section. Grains on the right are <.05mm, those on the left are about .5 mm. Note that tapered twins and undulose extinction in grains on the right indicate continued strain. Sample 741-2-2, crossed polarizers.

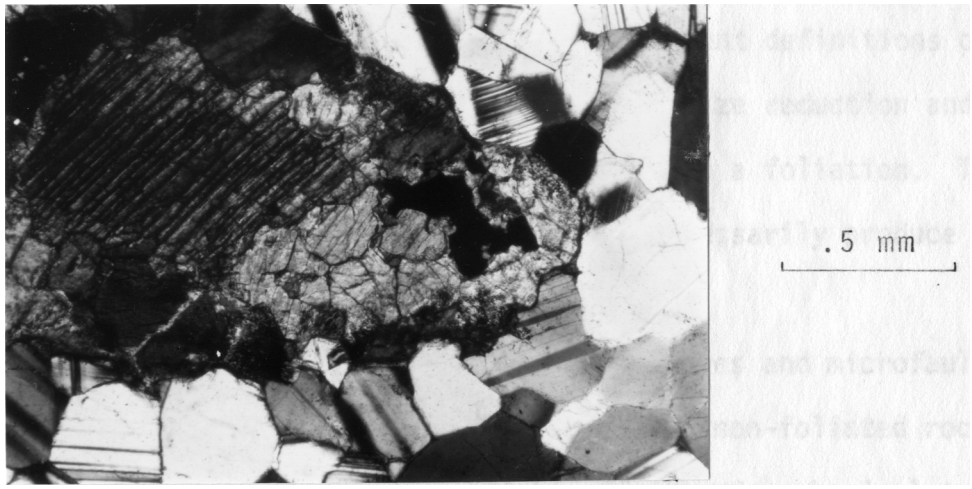

Figure 26: Granoblastic clinopyroxene rims relict grain. Red-brown hornblende appears at triple junctions. Plagioclase surrounding the pyroxene is coarsely recrystallized and shows some mechanical twinning as well as probably growth twins. Sample 613-1-2, crossed polarizers.

of plagioclase and mafic minerals. Segregation of these minerals into bands is apparently a secondary rather than primary feature since banding only occurs in deformed rocks. Foliations are weakly to very strongly defined, usually increasing in intensity with decreasing grain size. Preferred dimensional or crystallographic orientation of grains within single-mineral aggregates is for the most part weak or absent, but in rare cases c-axes in amphibole aggregates are subparallel to the foliation. Some foliated samples have suffered such extreme grain size reduction that the term "mylonitic" seems appropriate (Fig. 22b, 23). Relict grains within these samples may be as large as .5-1 cm, but the matrix is often of grains smaller than .25 mm. It is unclear, however, whether these samples truly represent cataclasis or whether they were formed by recrystallization under very rapid strain rates such that larger grain size could not be maintained. Bell and Etheridge (1973) define the term mylonite to include rocks produced by either origin; see Higgins (1971) and Zeck (1974) for different definitions of the term. A few samples show substantial grain size reduction and highly strained relict grains, yet have not developed a foliation. This relationship indicates high strain does not necessarily produce a foliation.

Fractures, microfaults and veins: Fractures and microfaults are scarce and are observed in weakly foliated or non-foliated rocks. Microfaults are usually observed as slight offsets of mechanical twins in plagioclase grains. In rare instances faults extend across a thin section and have offsets of more than 1 mm (Fig. 27).

In contrast to fractures, veins are very common. They are filled with various minerals, including clinopyroxene + brown hornblende; brown, green and/or blue-green hornblende; sodic to intermediate

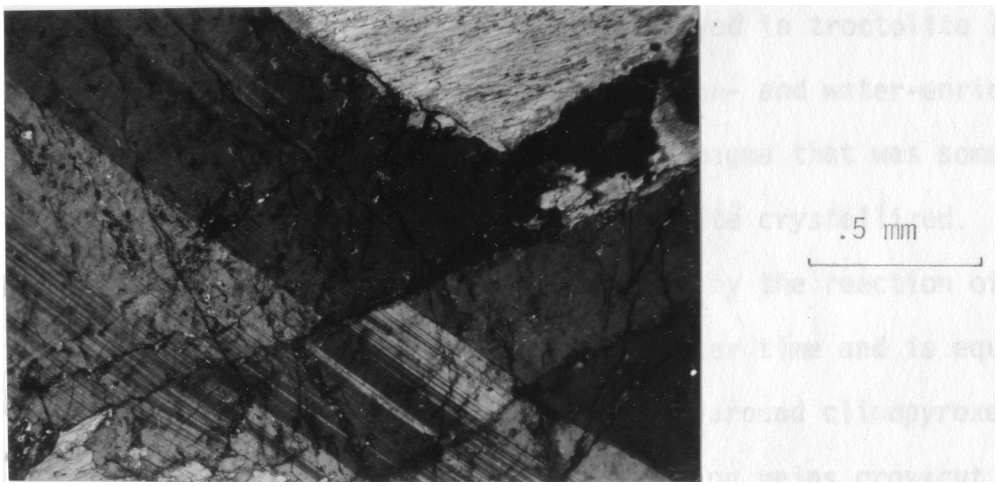

Figure 27: A microfault displaced this plagioclase grain after mechanical twins were developed. The fault does not appear to be filled with new minerals, but some healing may have occurred. Sample 615-2-1, crossed polarizers.

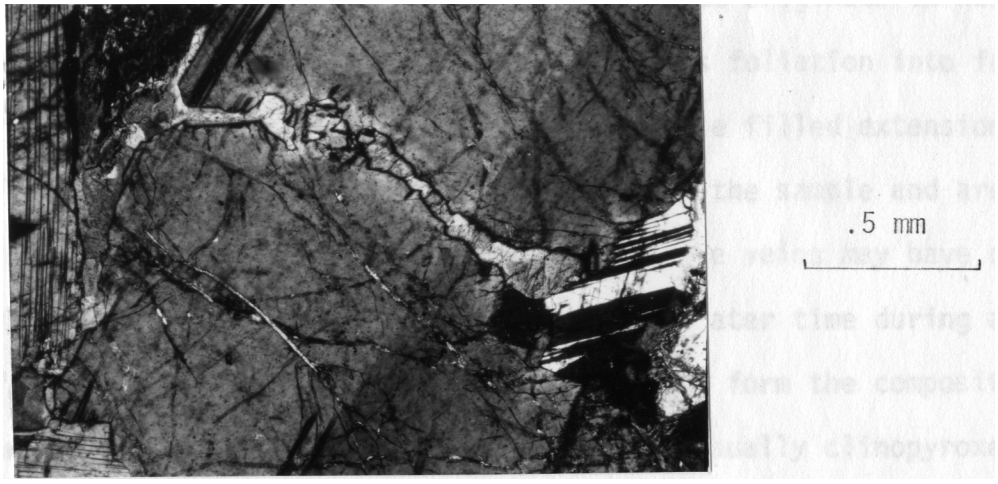

Figure 28: A vein of clinopyroxene and hornblende cuts across a single plagioclase grain. Irregular outlines and mineralogy suggest that the precipitating fluid was magmatic. Sample 739-2-2, crossed polarizers.

plagioclase; actinolite; chlorite; serpentine and other sheet silicates. Clinopyroxene + brown hornblende veins (observed in troctolite 739-2-2) do not represent very late-stage (silica-, iron- and water-enriched) primary fluid but possibly precipitated from magma that was somewhat more evolved than that from which the troctolite crystallized. It is probable that the brown hornblende was formed by the reaction of the clinopyroxene with a hydrous fluid at some later time and is equivalent to the brown hornblende rims typically formed around clinopyroxenes in the MCR suite (Fig.28). Many hornblende-bearing veins crosscut foliation or recrystallized textures, supporting the conclusions that earlier structures formed at high temperatures and that the subsequent brittle deformation related to formation of the veins took place at temperatures about or above 550°C, the lower limit of hornblende + plagioclase stability (Liou and others, 1974).

In two samples hornblende veins appear to originate in hornblende segregations and extend at high angles across foliation into felsic areas. In the first sample the veins resemble filled extension fractures (Fig. 29); in the second the veins cut across the sample and are not clearly related to extension (Fig. 30). These veins may have originated synchronously with the foliation or at some later time during alteration of the mafic minerals that were segregated to form the compositional banding. Grains of primary mafic minerals (usually clinopyroxene) are altered slightly to completely by reaction with fluids introduced along fractures later filled with amphibole. The degree to which mafic minerals adjacent to veins are altered varies among and within the samples, suggesting variability in the amount of altering fluids available. Where the surrounding material is only slightly altered, the fractures may have been shortlived and/or had a restricted amount

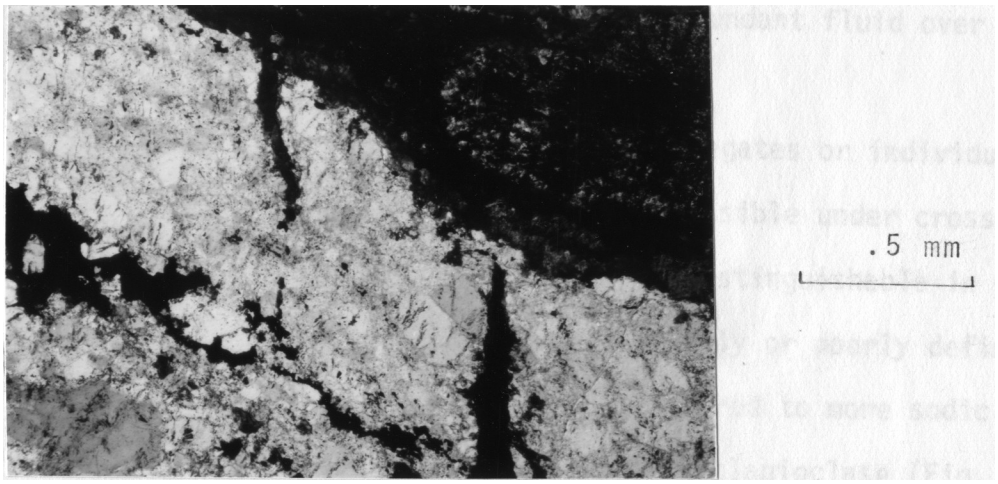

Figure 29: Hornblende-filled fractures are oblique to the foliation and are possible extension fractures. The mafic domains contain identical hornblende and opaques. Sample 615-2-3, plane light.

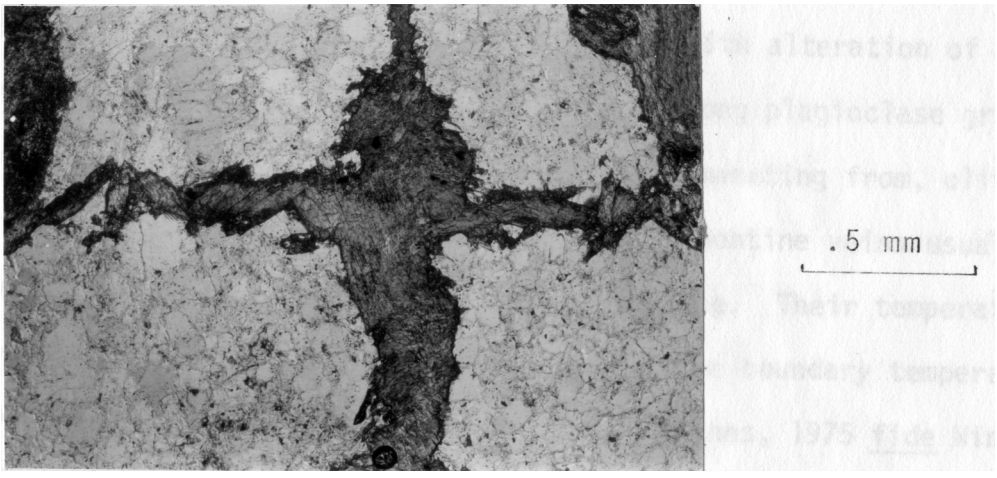

Figure 30: Green amphibole vein is irregular and does not clearly continue through dark foliation band of the same mineralogy. Foliation runs N-S, vein E-W. Note also the lack of preferred dimensional orientation in the foliation bands and in the vein. Sample 737-1-1, plane light.

of fluid passing through them. On the other hand, pervasive alteration suggests longer exposure to fluids or more abundant fluid over the same period of time.

Plagioclase veins are restricted to aggregates or individual grains of plagioclase. Often these veins are only visible under crossed polarizers; the vein and host materials are optically indistinguishable in plane light. Boundaries are usually ragged and may be sharply or poorly defined. In many cases the host grains were partially altered to more sodic plagioclase during the addition of the vein-filling plagioclase (Fig. 31). The sodic character of the vein material has been confirmed by microprobe analysis (Malcolm, 1978). Plagioclase veining often obliterates distinct grain boundaries by surrounding many individual grains, creating large, apparently continuous grains.

Veins crosscutting earlier hornblende and plagioclase veins include actinolite, chlorite, serpentine, and other sheet silicate veins. Chlorite $\pm$ actinolite veins are associated with alteration of mafic minerals. Chlorite alone commonly occurs along plagioclase grain boundaries. Serpentine veins occur within, and emanating from, olivine aggregates and pseudomorphs. Chlorite and serpentine veins usually crosscut preexisting talc alteration of the olivine. Their temperature of formation should be less than about 500°C, the boundary temperature between stability of talc and serpentine (Johannes, 1975 *fide* Winkler, 1976); supporting the interpretation that these veins formed at a lower temperature than amphibole veins. Veins filled with other unidentified sheet silicates are generally very late and confined to olivine and plagioclase areas.

Distribution in samples: The various strain features described above are distributed heterogeneously within samples and within the

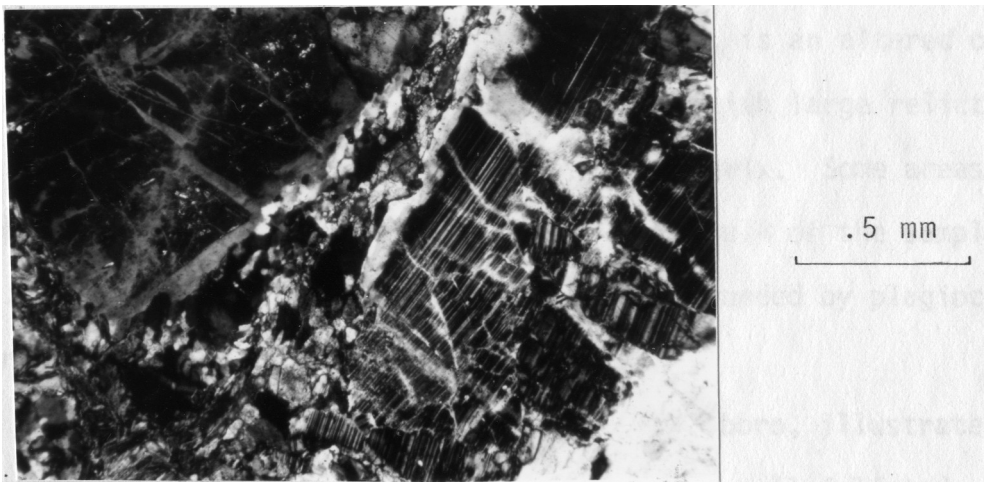

Figure 31: Mechanical twinning was followed by fracturing in the plagioclase grains. Areas surrounding the fractures and grain boundaries were subsequently altered and sealed with more sodic plagioclase (light streaks). Sample 741-5-1, crossed polarizers.

entire suite. Individual characteristics may be weakly to strongly developed and are found in some samples and not in others. All the samples exhibit some strain features.

In order to emphasize the heterogeneity of textures in the Cayman suite, three samples within which there are distinct textural variations will be described. The first sample, 611-4-1A, is an altered orthopyroxene gabbro. It is very weakly foliated, with large relict porphyroclasts in a very fine-grained plagioclase matrix. Some areas of the rock are considerably less disrupted than the bulk of the sample, and Fig. 32 shows plagioclase laths partially surrounded by plagioclase matrix.

Sample 612-3-1A, an olivine-bearing metagabbro, illustrates several features described above (Fig. 33). There is a well-foliated, very fine-grained zone that contains no primary mafic minerals and in which no relict textures are preserved (center). On the upper side of this zone (as pictured), coarse igneous textures are preserved despite some alteration and recrystallization and the development of a few narrow zones of very small grain size and crosscutting veins. On the other side of the mylonite zone, a moderate foliation has developed and grain size reduction is apparent (lower part of photograph). Relict large porphyroclasts are internally strained. Alteration of primary minerals is least in this portion, although crosscutting veins are observed. This sample represents a well-developed shear zone, but the typical sigmoidal pattern of foliation discussed by Ramsay and Graham (1970) is only apparent on the upper side of the zone.

The third example of heterogeneous textures on the thin section scale is sample 613-1-2. This non-foliated, olivine-bearing metagabbro

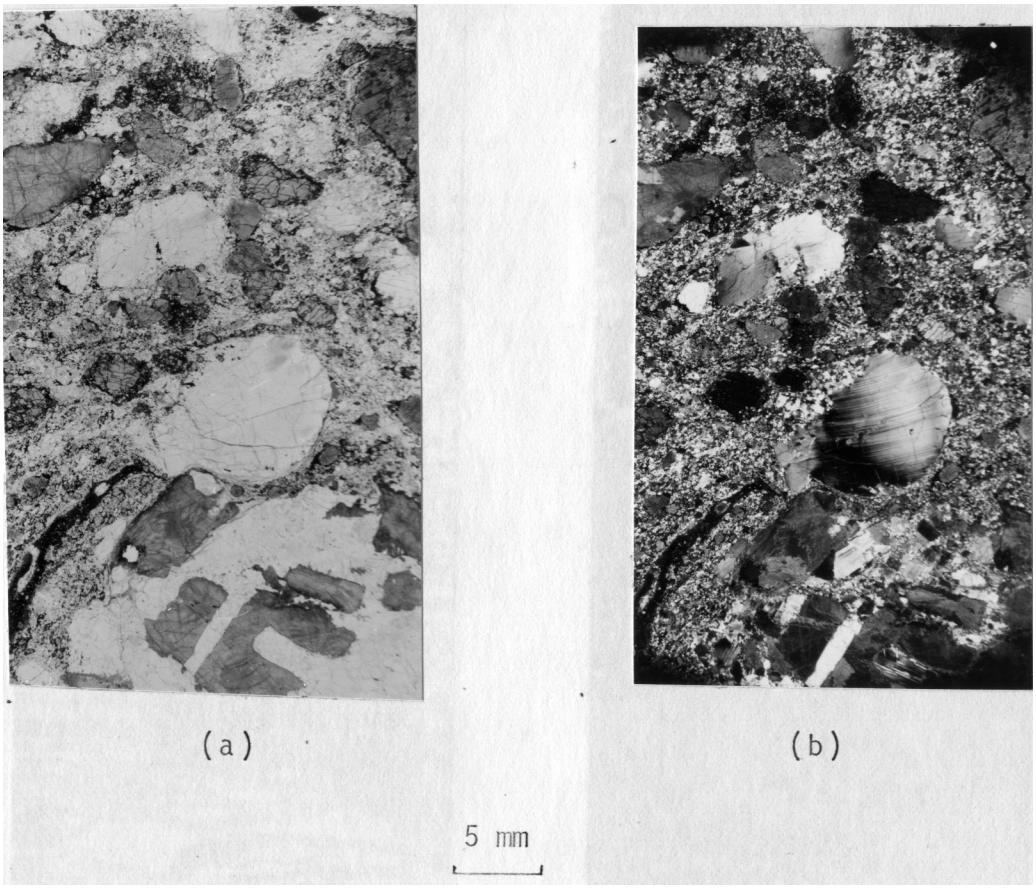

Figure 32: (a) Orthopyroxene gabbro 611-4-1A, which shows porphyroclasts in a fine-grained matrix of opaques and plagioclase. Subpoikilitic textures are still visible in lower part of photograph. Plane light. (b) Crossed polarized view emphasizes extent of grain size reduction and strained nature of porphyroclasts.

Figure 33: (a) Despite alteration and some recrystallization, igneous textures are still preserved in the upper portion of sample 612-3-1B. The transition from primary textures to a well-developed foliation in a fine-grained zone is quite abrupt. Several crosscutting veins are present. On the other side of the foliated zone, alteration is limited but there has been considerable recrystallization. A moderate foliation is also present which grades into the much stronger and finer-grained foliation above. Crosscutting veins have the same orientation as in the upper portion. (b) Crossed-polarized view shows that only a few large grains remain in the lower portion. These exhibit prominent undulose extinction.

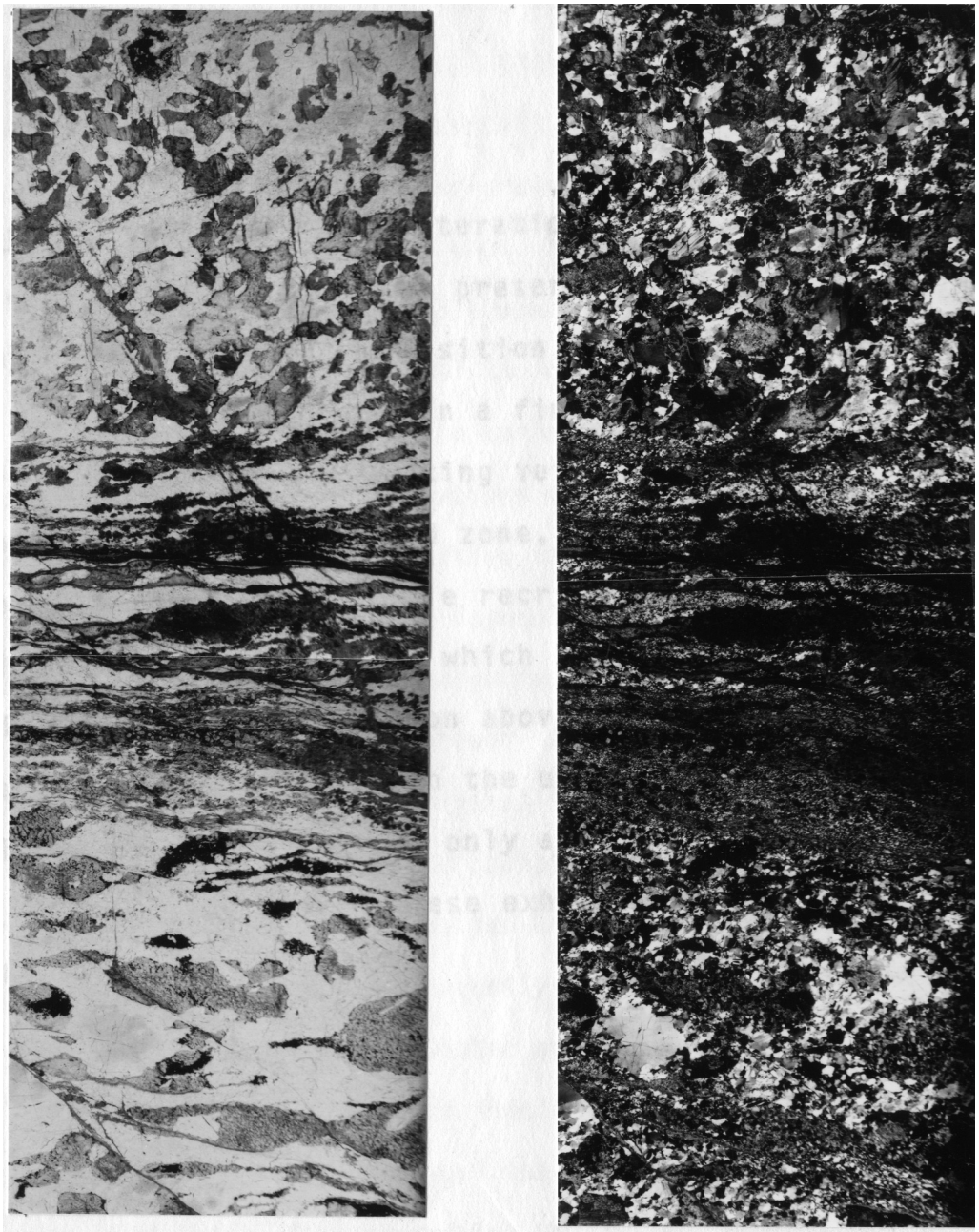

(a) (b)

5 mm

has a sharp curvilinear boundary which separates an area of finer-grained material with metasomatic alteration and irregular grain boundaries from an area of coarse grains, well-developed recrystallization textures and minimal alteration. Igneous textures are preserved in the coarse-grained area despite recrystallization of both plagioclase and clinopyroxene. The area of finer-grained material appears granulated, and the plagioclase grains are zoned. Figures 34 (a) and (b) show the macroscopic textural difference between the two portions; Figures 34 (c) and (d) are of a small segment of the boundary.

These samples illustrate the variability of textures within individual samples and show that textures may coexist but are not necessarily superimposed. With these properties in mind, let us now consider the distribution of textures in the Cayman suite. Table 7 presents a compilation under the following categories of the observed coexisting features which were described above: internally deformed plagioclase, internally deformed mafics, recrystallized plagioclase, recrystallized mafics and veins and fractures. Foliated and non-foliated rocks are distinguished. Samples with limited and almost exclusively low-temperature deformation are apparently almost exclusively non-foliated. No other difference between foliated and non-foliated rocks is apparent.

The mineralogy of veins and fractures is categorized in Table 8 because veins are found in many of the samples and create crosscutting relationships useful for determining timing and temperature of deformation. From this tabulation of the distribution and combinations of mineralogy, it is apparent that sheet silicate and hornblende veins are most common, both as the only veins and as coexisting veins. Most of the sheet silicate veins are of serpentine or chlorite; smectite,

Figure 34: (a) A curved but very sharp boundary separates coarse igneous textures (upper left) from finer-grained, disrupted textures (lower right). Sample 613-1-2, plane light. (b) Crossed polarizers. (c) Plane light and (d) crossed-polarized light photomicrographs illustrate a magnified section of the boundary between the two zones.

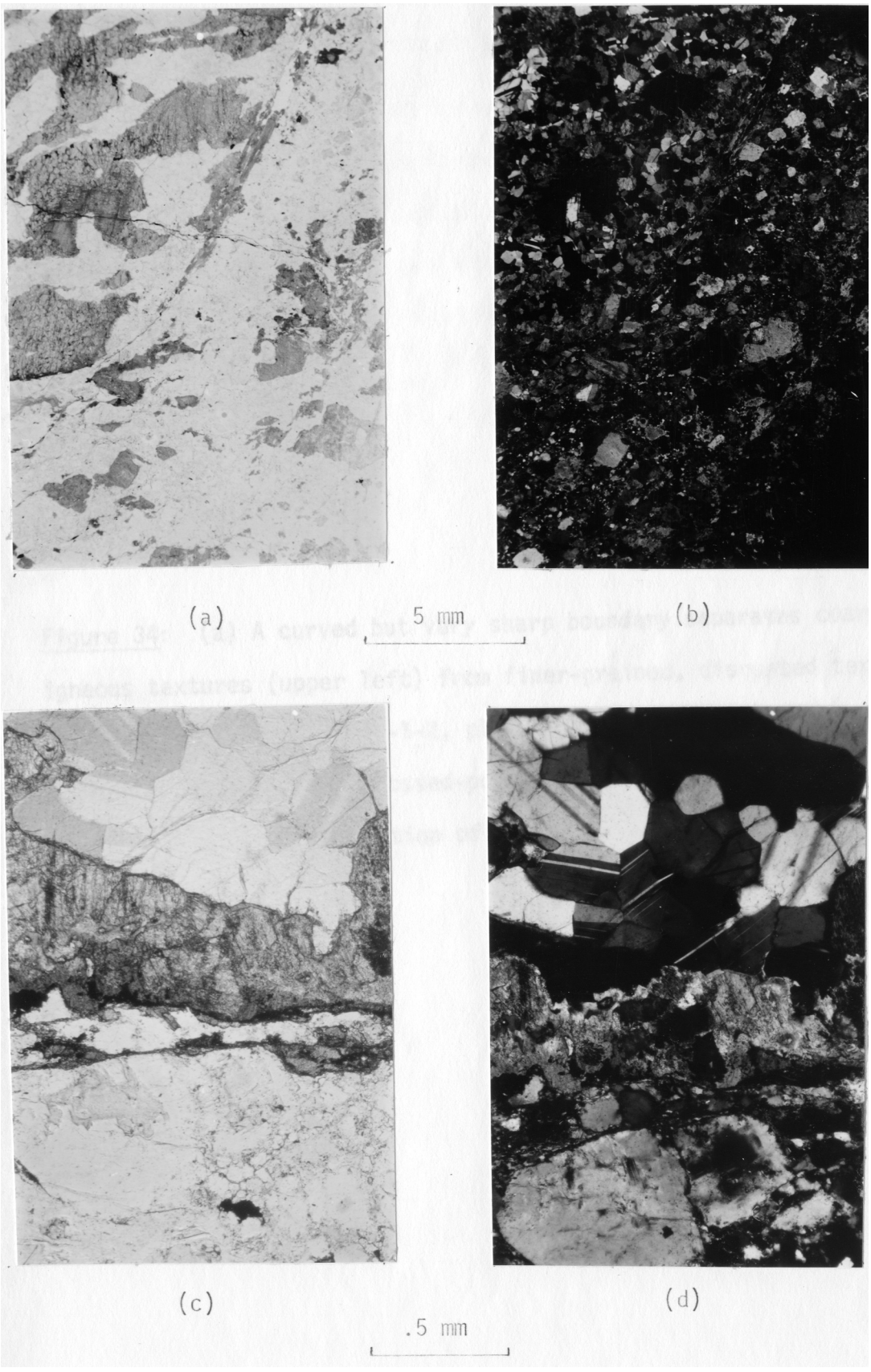
(a)
5 mm
(b)
(c)
.5 mm
(d)

Table 7. Textural Elements in Samples

I. Internally deformed plagioclase

II. Internally deformed mafics

III. Recrystallized plagioclase

IV. Recrystallized mafics

V. Veins and fractures

Combinations	Foliated Rocks	Non-foliated Rocks	Total
I	1	1	2
I,III	1	1	2
I,V	0	12	12
III,V	1	0	1
I,II,III	2	1	3
I,II,V	0	5	5
I,III,IV	3	0	3
I,III,V	4	14	18
I,IV,V	0	1	1
II,IV,V	0	1	1
I,II,III,V	2	7	9
I,II,IV,V	0	4	4
I,III,IV,V	7	8	15
II,III,IV,V	1	1	2
I,II,III,IV,V	8	18	26
TOTALS	30	74	104

Table 8. Veins and Fractures

I. Unfilled fractures only

II. Sheet silicate veins

III. Actinolite veins

IV. Hornblende veins

V. Plagioclase veins

Combinations	Foliated Rocks	Non-foliated Rocks
I	3	6
II	3	17
IV	5	8
V	3	4
II,III	0	5
II,IV	4	16
II,V	2	2
III,IV	0	1
IV,V	1	6
II,III,IV	0	2
II,IV,V	2	4
TOTAL	23	71

sericite and iddingsite (identified on the basis of optical properties only) are minor vein minerals and are last in crosscutting sequences.

The textures described above are not unique to the Cayman setting. Bogdanov and Ploshko (1967), Ploshko and others (1970), and Chernysheva (1970) have very briefly described granoblastic, cataclastic and bent-crystal textures in gabbroic rocks recovered from the Romanche Fracture Zone and the Indian Ocean. Bonatti and others (1975) describe veining, "mylonitic" veining and amphibolite banding in metagabbros from the Mid-Atlantic Ridge at 06°N. The most complete textural descriptions of deformed gabbroic rocks from the ocean floor are presented by Helmstaedt and Allen (1977). They describe several rocks from DSDP Site 334, which range from slightly deformed gabbros to a foliated metagabbronorite with recrystallized primary minerals. The deformation features they describe are remarkably similar to those seen in the Cayman rocks.

The spatial distribution of deformation features on the rift valley walls is complex, but a few generalities appear. Penetratively foliated rocks, of which many are amphibolites, occur predominantly in the upper portion of Dive Area 1; there are only two foliated gabbroic rocks from the west wall (Fig. 35). Fracturing occurs throughout both dive areas. The orientations of fractures and foliations were not accurately measured at the outcrop because of limitations of the submersible. Strike can only be measured by orienting the submersible parallel to the features in question and noting the heading, but this method is time-consuming and therefore not used often. Strike estimates can be made from photographs when the frame includes some indication of submersible orientation (either by digital display or from the compass on the sample basket), but corrections must be made because the cameras do not face straight forward. Dips are not measured because the submersible does not carry an inclinometer.

Figure 35: Rock distribution within the two dive areas in the Mid-Cayman Rise spreading center. Rock types are: (1) altered gabbro, (2) altered orthopyroxene gabbro, (3) altered olivine gabbro, (4) altered troctolite, (5) micrometagabbro, (6) metagabbro, (7) olivine-bearing metagabbro, (8) weathered metagabbro, (9) amphibolite, (10) basalt, (11) greenstone, (12) ultramafic, (13) breccia. Underlined sample numbers indicate penetratively foliated samples.

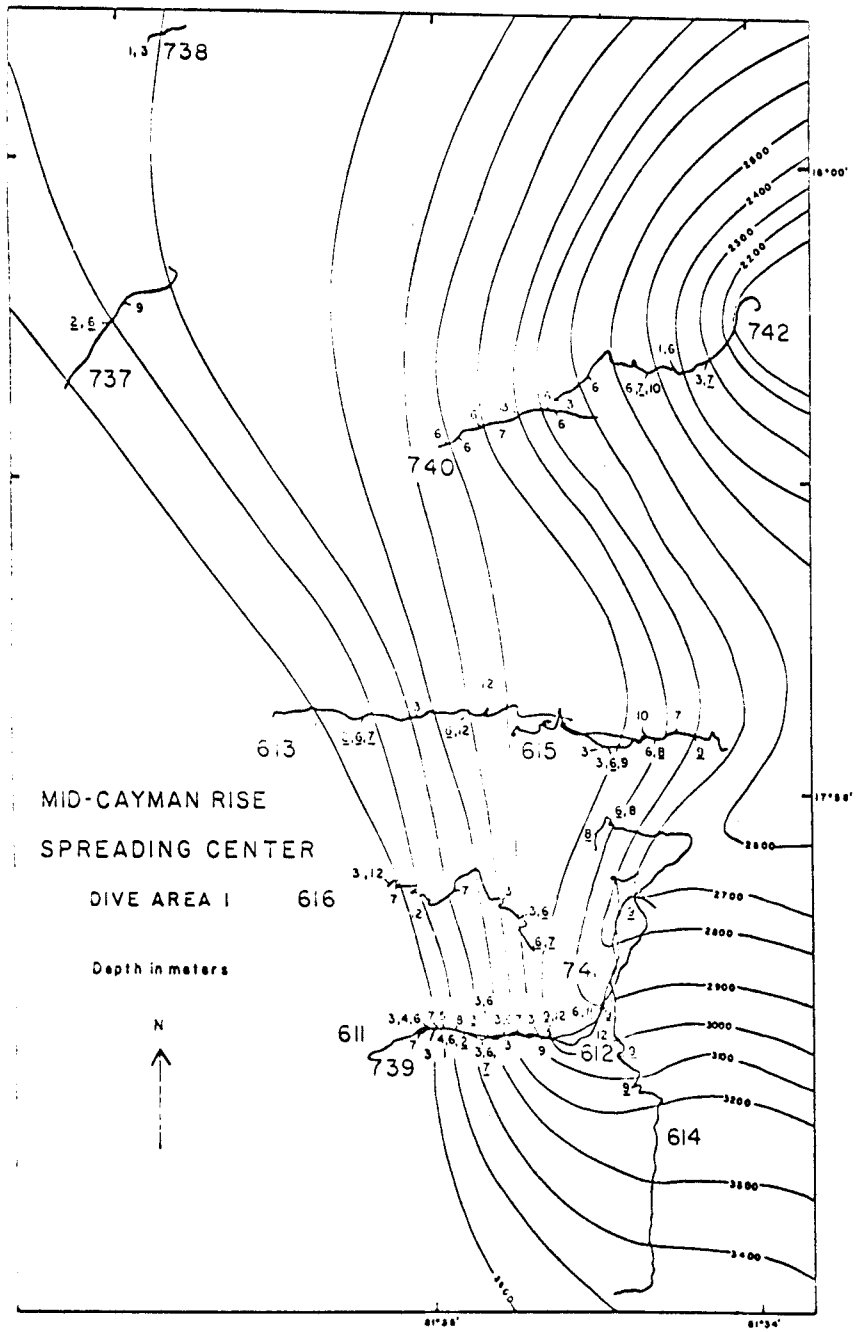
738
737
742
740
613
615
616
MID-CAYMAN RISE
SPREADING CENTER
DIVE AREA 1
Depth in meters
N
611
739
612
614

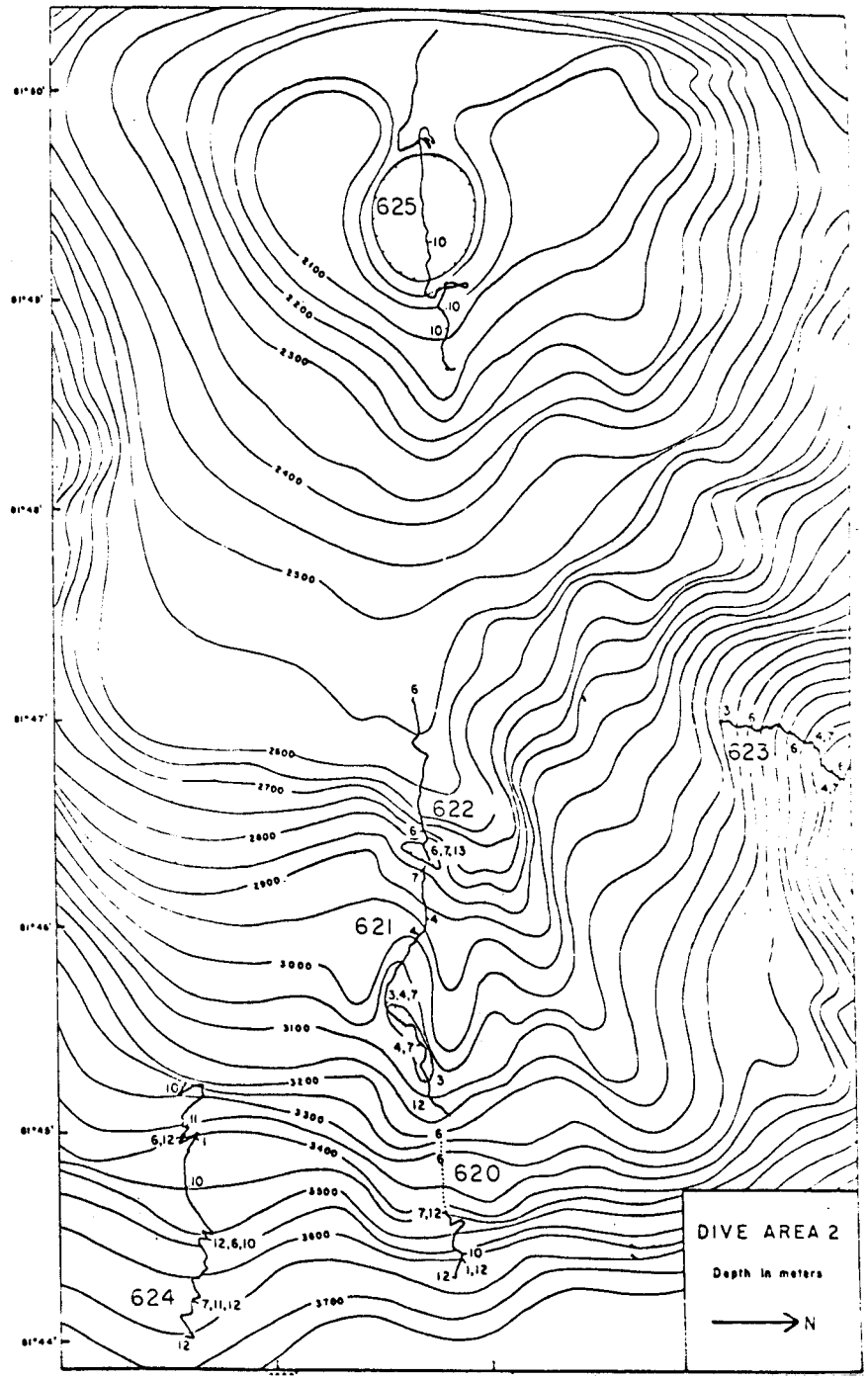
625
622
623
621
620
624
DIVE AREA 2
Depth in meters
N

Dip estimates, either on the bottom or from photographs are complicated by the fact that the submersible is not always horizontal and no record is available of its deviation from horizontal. A subhorizontal lineation in the rough surface is visible in some outcrops and may or may not be a textural manifestation of the described compositional banding. Outcrop fractures are usually nearly vertical and strike predominantly N-S and E-W, parallel and perpendicular to the ridge axis, but their relation to the hand-specimen fractures is unknown.

DISCUSSION

Many variables control the behavior of rocks during deformation and so determine the development of microstructures. Among the possible variables are temperature, confining pressure, strain rate and effective stress, fluid pressure, composition and mineralogy, and time. On the basis of our knowledge of the environment from which these rocks were collected and of the microstructures observed, we suggest that the rocks of the Cayman suite were deformed under the following conditions: 1) Temperatures were initially magmatic and fell continuously but irregularly to seawater temperatures. 2) Maximum confining pressure was less than 1 kb and decreased to about 0.3 kb as the rock body was raised to exposure on the sea floor. 3) Effective stresses and strain rates may have been highly variable in time and space. 4) Fluid pressure was also variable, probably lower than confining pressure at depth and equal to it at the sea floor. 5) Composition and mineralogy varied in space and time but were basically gabbroic. Plagioclase contents vary considerably, and mafic mineralogy varies from predominantly olivine to clinopyroxene to amphibole. 6) A maximum time span of less than 2.5 m.y., based on the magnetic anomaly identification of Macdonald and Holcombe (1978), has

been available to produce these deformation features.

Temperature: As a magma crystallizes, deformation can begin as soon as the crystalline material will support an applied deviatoric stress. Temperature limits on this upper threshold for deformation may be above or just at solidus temperatures (between 1000 and 1100°C for dry olivine tholeiite). Those samples than contain clinopyroxene + brown hornblende veins may represent cases in which some magmatic fluid remained at the initiation of deformation or in which magma was introduced along fractures into a rock at nearly solidus temperatures. Temperatures of formation of other structures are estimated as above or below about 550°C from mineral assemblages that are involved in the structure and from those that crosscut the structure. Temperatures at which slip, a dominant mechanism for ductile deformation, becomes significant have been investigated for the major phases found in these rocks (Nicolas and Poirier, 1976; Borg and Heard, 1970), but experimental conditions are limited to pressures or strain rates too high for direct application to these rocks, whose confining pressure never exceeded 1 kb. Temperature limits on the stability of secondary phases are also subject to debate. It is likely that hornblendes form at temperatures higher than 550°C (Liou and others, 1974), implying that structures containing or crosscut by hornblende have a minimum temperature of formation of 550°C. Any deformation that preceded the formation of talc from olivine by hydration occurred above 500°C; serpentine is the stable hydration product below 500°C (Johannes, 1975, fide Winkler, 1976). Chlorite is stable from diagenetic temperatures to about 800°C (Fawcett and Yoder, 1966) and is therefore unsatisfactory for temperature estimates on the basis of experimental data. It is one of the latest minerals to form in veins, however, and where it occurs with other

sheet silicates, such as smectite, is presumably a low-temperature phase. Most of the deformation observed involves hornblende and is therefore considered to be high-temperature deformation (greater than 550°C). Some brittle fracturing occurred later and highly localized, low-temperature deformation (much less than 500°C) probably occurred as the rocks were lifted to the sea floor by faulting.

Confining pressure: Maximum and minimum limits on hydrostatic pressure can be calculated, following a few assumptions. The rock types collected and the documented fault-related nature of the topography in the two dive areas suggest that gabbroic rocks are exposed by faults with throws of less than about 200 m. White and Stroup (1979) have proposed that rocks generated at depths greater than the apparent throw on the inward-facing faults may be exposed if there is outward-facing faulting. Quantitative estimates of the increased exposure are not possible because the density of outward-facing faults is obscured by talus and sediment and because the true throws on even the exposed faults cannot be measured. Given the density of inward-facing scarps and the overall slope of the rift valley wall, however, we assume that less than 500 m of basalt originally covered the gabbros, and that a maximum depth of generation for the exposed gabbros is 1 km. For pressure calculations, we also assume a crustal density of 3.00. Including the weight of an average of an average water column in the axial valley of 6 km, the maximum confining pressure experienced by these rocks should have been less than 0.88 kb. Minimum confining pressure calculated for the height of the water column at the sampling sites ranges from 0.26 to 0.35 kb.

Deviatoric stress and strain rate: Several authors have proposed using recrystallized grain size as a guide to paleo-stresses (e.g. Mercier

and others, 1977; Twiss, 1977). Such estimates are based on a combination of theory and some experimental data, and many simplifying assumptions are made in applying derived equations to naturally deformed material. These assumptions severely limit the applicability of the results (see White, 1979, for a comprehensive discussion of the limitations). As an example, we can calculate the deviatoric stress, σ, inferred from the grain size of recrystallized plagioclase, using Twiss' (1977) equation $\sigma=Bd^{-0.68}$, where B is a mineral constant (7.8 for anorthite) and d is the diameter of the recrystallized grains. For the Cayman rocks, d ranges from 0.01 to 5 mm, and σ therefore ranges from 178.7 to 2.6 MPa, respectively. Temperature and strain rate are known to affect these estimates but equations that take these effects into consideration have not been developed (White, 1979). Quantitative estimates of strain rate are precluded by the absence of adequate strain markers. On a qualitative level, high-temperature brittle deformation may have occurred at faster strain-rates than high-temperature ductile deformation, although the relationship between strain rate and ductile vs. brittle behavior is poorly understood and is complicated by other variables. Similarly, rocks with small recrystallized grains may have been deformed at faster strain rates than those with larger recrystallized grains, under otherwise equal conditions, but again the relationships are poorly understood. The variety of textures described above suggests that variable stress and strain-rate conditions may have been experienced by rocks within this suite.

Fluid pressure: Because ocean-floor basaltic magma is quite dry (Delaney and others, 1977; Delaney and Mathez, 1978), the partial pressure of water in these rocks may be very low until fracturing or other deformation opens conduits along which fluids may be introduced. Some

samples apparently remained closed to water until late in their cooling history, as evidenced by a lack of hydrous high-temperature minerals. Other samples became open to water while they were still hot. If we assume that water is by far the largest component of the fluid phase, a reasonable assumption in light of the geologic setting and the mineralogy of the samples, we can estimate the relative magnitudes of water pressure and confining pressure. Due to the fractured nature of the oceanic crust, it is reasonable to assume that in most instances water is a mobile component and therefore P_{H_2O} will be equal to hydrostatic pressure of the appropriate water column (Miyashiro, 1973). This hydrostatic pressure is always less than confining pressure, but approaches it in value as the rocks approach the sea floor. If (overburden decreases) the rock and water system becomes closed by mineral growth, P_{H_2O} may increase, due to thermal expansion, but is unlikely to exceed confining pressure for two reasons: 1) hydration reactions will occur, reducing the amount of unbound water, and 2) because the strength of the rock is reduced with increasing pore pressure and the tectonic environment is such that deviatoric stress is likely to exist, the rocks may be expected to fail before pore pressure exceeds confining pressure. Carbon dioxide is considered to have been a minimal component of the fluid phase with the exception of the few instances where calcite replaces olivine. In these cases carbon dioxide was significant late in the rock history and probably did not affect the response of the rock to stress.

Composition and mineralogy: Compositional differences among many samples in the Cayman suite are not very large, but nevertheless there are significant variations in mineralogy. The relative abundances of olivine, clinopyroxene, plagioclase and possibly amphibole should and

apparently do have an effect on the types of textures developed due to their different responses to stress (Nicolas and Poirier, 1976). Olivine and plagioclase are more likely to recrystallize rather than break under conditions that will break clinopyroxene and amphiboles. This may be the reason that cataclastic textures are apparently absent from olivine-rich gabbroic samples (including troctolites), yet are relatively common in clinopyroxene- or amphibole-bearing samples. Differences in responses to stress also explain the greater abundance of strain features in plagioclase than in the mafic minerals in almost all samples.

Time: The samples collected from Dive Area 1 and Dive Area 2 have a maximum age of 2.2 and 1.9 m.y., respectively, calculated on the basis of a half-spreading rate of 10 mm/yr (Macdonald and Holcombe, 1978) and distance from the axial singularity (chosen to be the deepest part of the axial valley). These ages, however, do not represent the time available for deformation. Most of the observed textures developed at high temperatures and therefore early in the cooling history of the rocks. We suggest that these textures were created within the first million years of the rocks' history, before the rocks left the floor of the axial valley.

Estimates of values for the above parameters for the conditions of strain allow us to evaluate the strain features observed in these rocks. Every sample has undergone some strain, and can be grouped according to the textures developed.

Those samples which contain recrystallized mafic minerals were strained under high-temperature and in the presence of a minor amount of water. Strain rates were usually slow enough to prevent brittle failure but in some instances recrystallization was preceded by such failure, such as in sample seen in Figure 11. Little water was available to form

hydrous secondary minerals, as primary mineralogy is preserved; however, in many cases some water was present to form hydrous phases along narrow zones. Often the total amount of deformation was quite limited, because foliation is either weakly developed or was not developed, grain size was not greatly reduced, and igneous grain shapes are preserved. Following recrystallization many of these rocks were cooled quickly and/or in the absence of much water, preventing further modification. Other samples were involved in continued deformation at high temperatures and with more water, leading to the development of amphibole replacing all mafics and sometimes the development of a strong foliation. Many samples were probably deformed rapidly, either with actual fracturing or with recrystallization into very small grains. The amount of strain varied from slight, creating a few fractures filled with hornblende or plagioclase to substantial, forming a mylonite rock. In all cases the amount of fluid present during deformation helped determine the extent to which primary mineralogy was preserved. High-temperature strain of all types varied not only from sample to sample, but sometimes within a single sample over distances of millimeters.

Superimposed on the various high-temperature textures may be lower-temperature strains; these strains may also be seen in rocks with no previous deformation. Continued deformation of plagioclase, which may create further internal strain in recrystallized grains; formation of crosscutting fractures and veins filled with lower-temperature amphiboles, chlorite or serpentine and, in a few cases, fracturing and alignment of blue-green amphiboles or sheet silicates in narrow strain zones are observed. Most of the low-temperature strain is not penetrative but localized, as strain becomes concentrated along very narrow zones. Thus, at high temperatures strain may be penetrative or localized, but at

lower temperature it is almost always localized. The fact that low-temperature strain appears to be less prevalent in the samples than is high-temperature deformation is probably the result of a sampling bias imposed by the localized, and therefore heterogeneously distributed nature of low-temperature strain.

All of the deformation textures described above were created within the MCR. Although our knowledge of the conditions that the MCR rocks have experienced is limited to maxima and minima for many of the variables controlling deformation mechanisms such as temperature, pressure, fluid pressure, stress and time, as outlined above; nevertheless we can postulate a scenario for the development of the deformation features in these rocks within the tectonic setting of a slowly spreading accreting plate boundary. The scenario developed will be restricted to the uppermost portion of the gabbroic complex because our understanding of the tectonics of this area indicates that the exposure of deep-seated rocks on the surface is unlikely and therefore speculation on processes at deeper levels are totally unconstrained by this data set. Under the axis of a spreading center the magma chamber continually cools, creating gabbroic rocks and therefore shrinks from the walls inward, but the roof is pulled apart so that new space is created at the center of the magma chamber. Fresh magma must be introduced into the magma chamber to fill the volume created by spreading. It has been documented by Dungan and Rhodes (1978) and Walker and others (1979) that magma mixing occurs at accreting plate boundaries, and the occurrence of olivine-free clinopyroxene gabbros among our samples supports the notion that this process operates at the MCR as well (see Chapter 1). Furthermore, the gabbro lining the magma chamber will be at or very close to solidus temperatures and therefore is likely to deform in a ductile manner under low stresses.

Taking these conditions into consideration, we suggest that the influx of new magma into the chamber may be fast enough and the magmatic fluid pressures great enough to produce sufficient deviatoric stress to fracture or shear the wall rock. The extent of fracture or shear of the wall rock will depend on the rate of flow of the magma, the depth of the rock, the fluid pressure of the magma, and the exact temperature and composition of the wall rock. Intrusion of small amounts of magma into crystallized gabbro may create features similar to the clinopyroxene + brown hornblende vein depicted in Figure 8. Bending, twinning and/or coarse penetrative recrystallization of plagioclase and recrystallization of clinopyroxene in rocks where no foliation is developed may have formed in response to ductile shear resulting from the flow of magma past the wall rock. We expect that features resulting from influx of new magma will not be very extensive nor generally very well developed. In addition, they are likely to be masked by subsequent, more intense deformation should it occur.

Foliated textures and narrow shear zones with extreme grain size reduction are probably not formed by this mechanism because the conditions required to create these will probably not be met by flow of magma, although the constraints on this statement are poor. We suggest that these foliations and shear zones are the result of differential movement within gabbro at temperatures somewhat below the solidus but still above 550°C because hornblende + plagioclase is the lowest-temperature assemblage involved. The zones of movement are thought to represent the subsurface continuation of normal faults that create the rift valley topography. These faults are well documented in the FAMOUS area (Ballard and van Andel, 1977); the topography of the upper valley walls in the MCR is also clearly created by normal faulting (CAYTROUGH, 1979).

Some normal faulting occurs over the roof of the magma chamber of the MCR, because there is no flat floor and the topography, similar to that further up the walls is unlikely to be purely constructional. The deformation along these faults is brittle near the surface, and as a result of increasing pressure and temperature becomes ductile at depth. The depth of the ductile/brittle transition along faults cannot be constrained in the MCR with the data available, but may be close to the gabbro/basalt boundary. Recrystallization is almost ubiquitous within the deformed zones observed in the hand specimens, and in many samples hydration of the mafic minerals is limited, suggesting that these zones are not open cracks through which any large amount of water circulates. The degree to which foliation is developed and the degree of hydration of the mafic minerals are in part controlled by the amount and speed of movement along the fault zone. Both processes are considered favored by more and/or faster movement. The degree of hydration will also decrease with increasing distance from the sea floor, because the water must travel further, temperatures are higher and fewer conduits will be available due to higher confining pressure. The orientation of these zones will be parallel to the steeply dipping faults near the surface and may flatten at depth as observed in rifts such as the Bay of Biscay (de Charpal and others, 1978). The amount of flattening of the fault surface will depend on the rheology and thickness of the crust at the time of the fault movement. At the axial singularity the base of the sheeted dikes (assumed to be less than 500 m below the sea floor on the basis of gabbroic exposures on the rift valley walls) represents the termination of faults. These dikes are considered to be vertical and parallel to the axis of the valley (as according to the models of Dewey and Kidd, 1978; Gass and Smewing, 1973; which are based on

ophiolites). If faulting occurs during or under the same conditions as dike emplacement, these faults will be vertical and have no change in dip. As the crust thickens, however, movement on previous faults and new, similarly oriented faults will result in propagation of these fault planes beyond the base of the sheeted dikes. If the rheological properties of the diabase and gabbro are sufficiently different, there may be a marked change in the orientation of the faults at this boundary. Whether or not there is a rheological contrast, the foliation produced by shear along these fault zones is not likely to be as steep as the faults at the surface due to temperature and pressure gradients. Shear zones in the gabbroic portions of the North Arm Mountain ophiolite, Bay of Islands, Newfoundland, cannot be followed into the overlying sheeted dikes (Rosencrantz and Casey, pers. comm., 1979), but if the zones in the gabbro and those in the sheeted dikes <u>are</u> related, the displacement on these faults is less than about 100 m, based on current exposure. Because faults with throws of less than 100 m are by far the most common on the rift valley walls, the evidence from North Arm Mountain does not negate the possibility of extension of these faults into the gabbroic layer, neither does it confirm the possibility. In the MCR, as in other rift valleys, many of the faults observed strike parallel to the rift valley axis (N-S in the MCR), and probably maintain this orientation with depth. The N-S trending faults observed face toward the axis, but the existence of outward-facing faults has been argued by White and Stroup (1979). The subhorizontal lineation observed in some outcrops, if correlative to foliation in the rock may represent intersection of the observed fault plane with an older shear zone formed along either an outward-facing fault or an inward-facing fault with a different dip. Oriented samples of the sheared rock might have permitted discrimination

between these two cases, but these are not available. There are numerous E-W-striking faults (CAYTROUGH, 1979; Stroup, 1979) in addition to the N-S-trending faults, which suggests that shear zones may also be oriented in this direction.

Movement along the faults discussed in the preceding paragraph is probably responsible for the foliated textures, most of the recrystallization textures and perhaps even some of the higher-temperature brittle textures such as fractures filled with strongly colored amphiboles. Although this deformation occurred at high temperatures and therefore presumably close to the axis, it is possible that there is further movement along these or similar zones at a later time. Because the rock is continuously cooling, this later movement will be brittle to greater depths than it was originally, although we see very little evidence of this later, brittle shearing deformation within our samples. The effects of very late cooler deformation we observed are predominantly randomly oriented fractures filled with pale amphiboles, chlorite, serpentine and other sheet silicates with little or no offset. As fractures of this type are found to varying degrees in most samples, this fracturing is likely to be pervasive. We suggest that it may be a result of decompression during uplift along the valley walls and/or contraction due to cooling. These cracks are open for long enough times for water to flow along them, because they are filled with hydrous phases not obviously formed by simple reaction of the host minerals. However, some of these cracks contain only a limited amount of water for a short time because alteration is often confined to within millimeters of the crack boundaries. Alteration associated with these fractures is affected only by lower-temperature fracturing. In rocks where alteration is quite extensive, some of the late fracturing may also be due to expansion of the

rock as a result of the hydration of the mafic phases.

IMPLICATIONS

The present study has shown that gabbroic rocks from a slowly accreting plate boundary exhibit heterogeneous strain features on thin section and much larger scales. Heterogeneity includes differences in grain size, degree of anisotropy and mineralogy as well as brittle and ductile structures. The Cayman gabbroic rocks deformed locally throughout their history, commencing during or shortly after crystallization and continuing until exposure at the seawater-rock interface. Individual zones of deformation were active at different periods in the rocks' cooling history. The rates at which these rocks cooled and moved upward and the extent to which water was introduced into the system were variable and were important in determining the variable nature of the textures developed.

The uniqueness of the setting from which these rocks were collected requires caution in extrapolating insights gained from this study to gabbroic rocks from other oceanic settings. The MCR rocks crystallized at depths considerably shallower than the 1.75 km depth of the Layer 2-Layer 3 transition in mean oceanic crust (Christensen, 1978), which is considered to represent the basalt/gabbro transition; the MCR basalts are probably less than 500 m thick (CAYTROUGH, 1979). (We choose not to discuss the validity of the concept of mean oceanic crust, but use it for the comparative purposes.) Shallow-level crystallization probably affects the textures that are developed in these gabbroic rocks in several ways. A lower confining pressure favors brittle fracturing over ductile flow, other conditions being equal. Conductive cooling is more rapid under a thinner insulating basaltic cover and convective

cooling may be increased as a result of fracturing. Water circulating through fractures will cool the rocks unevenly and the distribution of water within the rocks is likely to be heterogeneous. Rocks under the same stress conditions will deform differently under the variable water and temperature conditions. All these influences resulting from shallow-level emplacement will lead to a very heterogeneous rock body.

If our analysis of the heterogeneity within the MCR suite is correct, rock suites similar to this collection should exist where plutonic rocks are intruded at shallow levels within the oceanic crust and subsequently exposed at the sea floor. Although there is little seismic evidence to support his view (and seismic layering is not necessarily equivalent to lithologic layering), Fox (1978) suggests that the basaltic cap thins toward ridge/transform intersections will be subjected to conditions similar to those experienced by the MCR rocks and therefore are likely to exhibit similar heterogeneities in texture. Bonatti and others (1970) describe cataclastic to mylonitic gabbros, norites, olivine gabbros and nepheline gabbros from fracture zones of the equatorial Mid-Atlantic Ridge. They also note that these rocks contain numerous veins of prehnite, analcite, talc and antigorite. These rocks are apparently not as heterogeneous with respect to deformation as the MCR rocks, but this appearance may be due to the preliminary nature of the descriptions rather than the nature of the rocks. Bogdanov and Ploshko (1967) and Ploshko and others (1970) have described various gabbros and gabbro-amphibolites from the Romanche Fracture Zone. The textures in these rocks are ophitic to mylonitic. Some of the amphibolites are granoblastic or porphyroblastic, and banded. Engel and Fisher (1969) and Chernysheva (1970) have described gabbroic rocks from the Mid-Indian Ocean Ridge that are also variably altered and range

from undeformed to gneissically banded. Chernysheva notes crystallization and cataclasis in some of his samples. Miyashiro and others (1971) report metagabbros that are cataclastically deformed after metamorphic recrystallization occur in a fracture zone and within the median valley of the Mid-Atlantic Ridge near 24°N. All of these descriptions of gabbroic rocks from fracture zones indicate that deformation textures equivalent to some of those observed in the MCR suite indeed occur in the fracture zone setting, but insufficient data are available to compare the degree of heterogeneity of the deformation textures in the MCR and in fracture zones. Bonatti and others (1975) describe fractures, and veined metagabbros as well as banded amphibolitic metagabbros collected from the MAR at 06°N; these rocks are apparent equivalent to the MCR rocks in texture although some of the accessory and secondary phases (such as zircon, epidote and quartz) observed in the MAR rocks are not as abundant in the MCR rocks. The similarities of gabbros from the MCR and from other oceanic settings suggest that similar temperature, confining pressure, fluid pressure, stress and strain-rate conditions prevailed during the deformation of all these rocks. On the basis of the similarity of the rocks from these environments we suggest that fracture zones may expose gabbros that crystallized under thin basalt caps.

Descriptions of deformation in oceanic gabbros is limited to descriptions of rocks from slowly spreading ridges and fracture zones. No detailed descriptions are available for gabbros from fast spreading ridges. In view of the substantial evidence that ophiolites represent displaced oceanic crust, these bodies should provide additional information on the nature of ocean-floor deformation in gabbros, provided a reasonable distinction can be made between features related to ocean-

floor processes and those related to the tectonic emplacement of the ophiolite and/or subsequent tectonic events. Unfortunately, many of the descriptions of the gabbroic sections and more specifically the non-layered portions of these sections, of various ophiolites in the journal literature are very brief and therefore inadequate for a detailed evaluation of the similarity or differences in style, degree and distribution of deformation (e.g., Reinhardt, 1969; Saleeby, 1978; Karson and Dewey, 1978; Davies, 1971). Some of the ophiolitic gabbros, however, apparently exhibit no deformation textures whatsoever, for example, those of Mings Bight (Kidd and others, 1978), Costa Rica (Galli-Oliver, 1979), and Troodos (George, 1978). These totally undeformed gabbros may differ from both the ocean-floor gabbros and from the other ophiolitic gabbros and may therefore have formed in a distinctly different environment, one in which vertical and lateral tectonic movements do not disrupt the gabbroic section. Alternatively, the descriptions of these may reflect reconnaissance mapping, unstated disregard for features assumed to be related to emplacement, and/or insufficient exposure that masks narrow, widely spaced zones of deformation. The latter alternatives are considered more likely because other portions of these same ophiolites are described as deformed and it seems highly unlikely that a middle layer would remain undeformed while units above and below are deformed. In the Semail, Kings River and western Lewis Hills gabbros, there are narrow zones of highly sheared rocks (Reinhardt, 1969; Saleeby, 1978; and Karson and Dewey, 1978, respectively); these zones are widely spaced and steeply dipping in the Lewis Hills area (Karson and Dewey, 1978). Davies (1971) notes partially recrystallized textures in some of the gabbros of the Papuan ophiolite and Reinhardt (1969) mentions the existence of fractured and sheared gabbros in the

Semail ophiolite, but neither of these authors discusses the distribution of these deformed rocks.

On the basis of this information, then, sheared and recrystallized gabbroic rocks are observed in both ocean-floor and ophiolitic settings but the finely fractured and veined rocks are apparently only seen in samples from the oceanfloor environment. This difference may exist because the fractures result from the deformation directly involved in exposing the gabbroic rocks on the oceanfloor, in which case this deformation might only be expected in those ophiolitic gabbros juxtaposed with pelagic sediments prior to emplacement. This difference is also possibly a function of disregard for presumably very late features by the geologists studying the ophiolitic gabbros. The latter possibility is preferred by the author. Until more detailed descriptions of ophiolitic gabbros are available and the distribution of sampling of gabbros from the ocean floor is improved, our understanding of the deformation of the upper part of the gabbroic layer of oceanic crust will be limited. Results of studies to date suggest that a variety of textures are developed and that this indicates variable conditions of deformation on a small scale, at least within shallow-emplacement environments and in the vicinity of fracture zones, but the extent of deformation within the upper gabbros and the nature of deformation away from transform domains is unknown.

Bibliography - Chapter II

Ballard, R.D. and van Andel, Tj.H., 1977. Morphology and tectonics of the inner rift valley at lat. 36°50'N on the Mid-Atlantic Ridge, Geol. Soc. America Bull., v. 88, p. 507-530.

Bell, T.H. and Etheridge, M.A., 1973. Microstructure of mylonites and their descriptive terminology, Lithos, v. 6, p. 337-348.

Bogdanov, Yu.A. and Ploshko, V.V., 1967. Igneous and metamorphic rocks from the abyssal Romanche Depression, Dokl. Akad. Nauk. SSSR., v. 177, p. 173-176.

Bonatti, E., Honnorez, J. and Ferrara, G., 1970. Equatorial Mid-Atlantic Ridge: petrologic and Sr-isotopic evidence for an alpine-type assemblage, Earth Planet. Sci. Lett., v. 9, p. 242-256.

Bonatti, E., Honnorez, J., Kirst, P. and Radicati, F., 1975. Metagabbros from the Mid-Atlantic Ridge at 06°N: contact-hydrothermal-dynamic metamorphism beneath the axial valley, Jour. Geology, v. 83, p. 61-78.

Borg, I.Y. and Heard, H.C., 1970. Experimental deformation of plagioclases in Paulitsch, P., ed., Experimental and Natural Rock Deformation, Springer-Verlag, Berlin, p. 375-403.

CAYTROUGH, 1979. Geological and geophysical investigation of the Mid-Cayman Rise spreading center: initial results and observations, in Talwani, M., Harrison, C.G. and Hayes, D., eds., Deep drilling results in Atlantic Ocean: Ocean Crust, Maurice Ewing Ser., v. 2.

Chernysheva, V.I., 1970. Greenstone-altered rocks of rift zones in meridian ridges of the Indian Ocean, Internat. Geol. Rev., v. 13, p. 903.

Christensen, N.I., 1978. Ophiolites, seismic velocities and oceanic crustal structures, Tectonophys., v. 47, p. 131-157.

Davies, H.L., 1971. Peridotite-gabbro-basalt complex in eastern Papua: an overthrust plate of oceanic mantle and crust, Bureau of Min. Resources, Geology and Geophysics, Dept. of National Development Australia; Bull. No. 128.

Davis, K.E., deBoer, J., Fox, P.J. and Spydell, R., 1978. Magnetic properties of oceanic layer 3 (abs.) Trans. Amer. Geophys. Union, v. 59, p. 1056.

de Charpal, O., Guennoc, P., Montadert, L. and Roberts, D.G., 1978. Rifting, crustal attenuation and subsidence in the Bay of Biscay, Nature, v. 275, p. 706-711.

Delaney, J.R. and Mathez, E.A., 1978. Interpretation of volatile contents of glass-vapor inclusions in crystalline phases of submarine basalt glasses (abs.), Trans. Amer. Geophys. Union, v. 59, p. 409.

Delaney, J.R., Muenow, D., Ganguly, J. and Royce, D., 1977. Anhydrous glass-vapor inclusions from phenocrysts in oceanic tholeiitic pillow basalts (abs.) Trans. Amer. Geophys. Union, v. 58, p. 530.

Dewey, J.F. and Kidd, W.S.F., 1978. Geometry of plate accretion, Geol. Soc. America Bull., v. 88, p. 960-968.

Dungan, M.A. and Rhodes, J.M., 1978. Residual glasses and melt inclusions in basalts from DSDP Legs 45 and 46: evidence for magma mixing, Contrib. Mineral. Petrol., v. 67, p. 417-431.

Engel, C.G. and Fisher, R.L., 1969. Lherzolite, anorthosite, gabbro and basalt dredged from the Mid-Indian Ocean Ridge, Science, v. 166, p. 1136-1141.

Engel, C.G. and Fisher, R.L., 1975. Granitic to ultramafic rock complexes of the Indian Ocean ridge system, Western Indian Ocean, Geol. Soc. America Bull., v. 86, p. 1553-1578.

Fawcett, J.J. and Yoder, H.S., 1966. Phase relationships of chlorites in the system $MgO-Al_2O_3-SiO_2-H_2O$, Am. Mineral., v. 51, p. 353-380.

Fox, P.J., 1978. The effect of transform faults on the character of the oceanic crust, Geol. Soc. America Abs. with Program., v. 10, p. 403.

Galli-Olivier, C., 1979. Ophiolite and island-arc volcanism in Costa Rica, Geol. Soc. America Bull., Part I, v. 90, p. 444-452.

Gass, I.G. and Smewing, J.D., 1973. Intrusion, extrusion and metamorphism at constructive margins: evidence from the Troodos massif, Cyprus, Nature, v. 242, p. 26-29.

George, R.P., Jr., 1978. Structural petrology of the Olympus ultramafic complex in the Troodos ophiolite, Cyprus, Geol. Soc. America Bull., v. 89, p. 845-865.

Helmstaedt, H. and Allen, J.M., 1977. Metagabbronorite from DSDP hole 334: an example of high-temperature deformation and recrystallization near the Mid-Atlantic Ridge, Canadian Jour. Earth Sci., v. 14, p. 886-898.

Higgins, M.W., 1971. Cataclastic rocks, U.S. Geological Survey Professional Paper 687, 97 pp.

Holcombe, T.L., Vogt, P.R., Matthews, J.E. and Murchison, R.R., 1973. Evidence for sea-floor spreading in the Cayman Trough, Earth Planet. Sci. Lett., v. 20, p. 357-371.

Karson, J. and Dewey, J.F., 1978. Coastal complex, western Newfoundland: an early Ordovician oceanic fracture zone, Geol. Soc. America Bull., v. 89, p. 1037-1049.

Kidd, W.S.F., Dewey, J.F. and Bird, J.M., 1978. The Mings Bight ophiolite complex, Newfoundland: Appalachian oceanic crust and mantle, Canadian Jour. Earth Sci., v. 15, p. 781-804.

Liou, J.G., Kuniyoski, S. and Ito, K., 1974. Experimental studies of the phase relations between greenschist and amphibolite in a basaltic system, Am. Jour. Sci., v. 274, p. 613-632.

Macdonald, K.C. and Holcombe, T.L., 1978. Inversion of magnetic anomalies and sea-floor spreading in the Cayman Trough, Earth Planet. Sci. Lett., v. 40, p. 407-414.

Malcolm, F.L., 1978. Mineral chemistry of plutonic rocks from the Cayman Trough, Caribbean Sea (abs.), Trans. Amer. Geophys. Union, v. 59, p. 405.

Melson, W.G., Thompson, G. and van Andel, T.H., 1968. Volcanism and metamorphism in the Mid-Atlantic Ridge, 22°N, Jour. Geophys. Research, v. 73, p. 5925-5941.

Mercier, J.-C.C., Anderson, D.A. and Carter, N.L., 1977. Stress in the lithosphere: inferences from steady state flow of rocks, Pageoph., v. 115, p. 199-226.

Miyashiro, A., 1973. Metamorphism and Metamorphic Belts, John Wiley and Sons, New York, 492 pp.

Miyashiro, A., Shido, F. and Ewing, M., 1971. Metamorphism in the Mid-Atlantic Ridge near 24° and 30°N, Philos. Trans. Roy. Soc. London, Ser. A, v. 268, p. 589-603.

Nicolas, A. and Poirier, J.P., 1976. Crystalline Plasticity and Solid State Flow in Metamorphic Rocks, Wiley, London, 444 pp.

Ploshko, V.V., Bogdanov, Y.A. and Knyazuva, D.N., 1970. Gabbro-amphibolite from the abyssal Romanche Trench, Atlantic region, Dokl. Akad. Nauk. SSSR, v. 192, p. 615-618.

Ramsay, J.G. and Graham, R.H., 1970. Strain variation in shear belts, Canadian Jour. Earth Sci., v. 7, p. 786-813.

Reinhardt, B.M., 1969. On the genesis and emplacement of ophiolites in the Oman Mountains geosyncline, Schweitz. Mineral. Petrog. Mitt. v. 49, p. 1-30.

Saleeby, J., 1978. Kings River ophiolite, southwest Sierra Nevada foothills, California, Geol. Soc. America Bull., v. 89, p. 617-636.

Stroup, J.B., 1979. Geologic investigations of the Mid-Cayman Rise spreading center, Caribbean, State University of New York at Albany, master's thesis.

Twiss, R.J., 1977. Theory and applicability of a recrystallized grain size paleopiezometer, Pageoph., v. 115, p. 227-244.

Walker, D., Shibata, T. and DeLong, S.E., 1979. Abyssal tholeiites from the Oceanographer Fracture Zone: II. Phase equilibria and mixing (in review).

White, G.W. and Stroup, J.B., 1979. Distribution of rock types in the Mid-Cayman Rise, Caribbean Sea, as evidence for conjugate normal faulting in slowly spreading ridges, Geology, v. 7, p. 32-36.

White, S.H., 1979. Difficulties associated with paleo-stress estimates, Bull. Mineral., v. 102, p. 210-215.

Winkler, H.G.F., 1976. Petrogenesis of Metamorphic Rocks, 4th ed., Springer-Verlag, New York, 334 pp.

Yoder, H.S. and Tilley, C.E., 1962. Origin of basalt magmas, Jour. Petrology, v. 3, p. 342.

Zeck, H.P., 1974. Cataclastites, hemiclastites, holoclastites, blasto-ditto and myloblastites-cataclastic rocks, Am. Jour. Sci., v. 274, p. 1064-1073.